ULTRASONOGRAPHIC MEDIAN NERVE CHARACTERISTICS RELATED TO RISK FACTORS AND SYMPTOMS OF CARPAL TUNNEL SYNDROME IN MANUAL WHEELCHAIR USERS

by

Bradley G. Impink

BS, Bioengineering, University of Pittsburgh, 2002

Submitted to the Graduate Faculty of

The Swanson School of Engineering in partial fulfillment

of the requirements for the degree of

Doctor of Philosophy

University of Pittsburgh

2010

UNIVERSITY OF PITTSBURGH

SWANSON SCHOOL OF ENGINEERING

This dissertation was presented

by

Bradley G. Impink

It was defended on

May 27, 2010

and approved by

George Stetten, MD, PhD, Professor, Department of Bioengineering

Rakié Cham, PhD, Associate Professor, Department of Bioengineering

Alicia Koontz, PhD, Assistant Professor, Department of Rehabilitation Science and Technology

Dissertation Director: Michael L. Boninger, MD, Chair, Department of Physical Medicine and Rehabilitation

ULTRASONOGRAPHIC MEDIAN NERVE CHARACTERISTICS RELATED TO RISK FACTORS AND SYMPTOMS OF CARPAL TUNNEL SYNDROME IN MANUAL WHEELCHAIR USERS

Bradley G. Impink, PhD

University of Pittsburgh, 2010

Carpal tunnel syndrome (CTS) is a common problem among manual wheelchair users (MWU), which is no surprise given the high force, high repetition nature of wheelchair propulsion. Since MWU rely heavily on the upper extremities for mobility, a greater focus should be placed on prevention of this overuse syndrome rather than treatment. In order to achieve this, there needs to be a better understanding of the pathophysiology of CTS, specifically median nerve characteristics related to wheelchair propulsion. Ultrasonography provides the means necessary to study the median nerve characteristics and physiologic changes associated with wheelchair propulsion. In this research, we used ultrasound and image analysis techniques to quantify median nerve shape and size characteristics. We developed a standardized imaging protocol to reliably assess median nerve changes in response to manual wheelchair propulsion. We also developed methodology for assessing dynamic characteristics of median nerve entrapment and compression during finger movements. Participants underwent ultrasound examinations of the wrist before and after a strenuous wheelchair propulsion task. Comparing individuals with and without symptoms of CTS, we found no significant differences at baseline, but did see significantly different and opposite median nerve changes in response to propulsion. Specifically, the three most common ultrasound characteristics previously related to CTS,

including median nerve cross-sectional area at the pisiform level, flattening ratio at the hamate level, and swelling ratio, were significantly different between symptom groups. We were unable to determine any significant relationships between median nerve changes and propulsion biomechanics variables, including resultant force, stroke frequency, and wrist joint angles. In a subsample of subjects, we found dynamic signs of median nerve entrapment and compression in individuals with symptoms of CTS. While making a loose fist, symptomatic participants showed significantly less median nerve displacement within the carpal tunnel and significantly greater compression of the median nerve compared to asymptomatic participants. In conclusion, quantitative ultrasound measures of the median nerve are useful for studying CTS and assessing the nerve response to activity. The techniques presented here may be useful in developing interventions to prevent or reduce the likelihood of median nerve damage among both MWU and other populations affected by CTS.

TABLE OF CONTENTS

LIST OF TABLES

LIST OF FIGURES

1.0 INTRODUCTION

Ergonomics literature identifies force, repetition, and posture as three primary biomechanical risk factors for developing musculoskeletal disorders. High force, high repetition tasks involving large joint excursions can result in strain among nerves and tendons which over time can ultimately lead to a repetitive strain injury.[1-5] A common overuse disorder is carpal tunnel syndrome (CTS). CTS is a disorder that affects the median nerve at the wrist resulting in numbness, tingling, and weakness in the hands. It is the most common entrapment neuropathy with a prevalence ranging from 1.5-2.7% in the general population.[6-10] It is estimated that CTS costs two billion dollars per year in surgery alone.[11] According to the National Institute of Neurological Disorders and Stroke, in the workplace it is estimated that CTS has lifetime costs of approximately $30,000 per afflicted worker. In manual wheelchair users (MWU) the prevalence of signs and symptoms of CTS has been shown to range from 49-74%, which is no surprise given the high force, high repetition nature of wheelchair propulsion.[12-19] Furthermore, the incidence of CTS has been shown to increase with a greater duration of wheelchair use.[12,15,17,19] Previous research has shown a direct link between the way an individual propels a manual wheelchair and injury to the median nerve.[20,21] Since manual wheelchair users rely heavily on the upper extremities for mobility, a repetitive strain injury such as CTS, could be detrimental to their ability to perform daily activities.

Initial treatment of CTS typically involves immobilizing and resting the affected hand and wrist for several weeks. If symptoms persist over several months, most often the next option

is surgery, which may require months for full recovery. Neither of these treatments is well tolerated by MWU as their upper extremities are necessary for their daily mobility and independence. To maintain independence and quality of life, it is important to minimize the pain and prevalence of repetitive upper extremity injuries (e.g. CTS) associated with everyday wheelchair propulsion. For MWU, a greater focus should be placed on prevention of this overuse syndrome rather than treatment, however there needs to be a better understanding of the pathophysiology of CTS in relation to wheelchair propulsion. Understanding the underlying physiological changes in the carpal tunnel and pathologies associated with pain may be beneficial in reducing and preventing pain in MWU and may provide some insight as to why the prevalence of CTS and other repetitive strain injury is so high in this population.

Ultrasonography has been shown to be a reliable method of displaying carpal tunnel anatomy and useful in diagnosing CTS by measuring nerve characteristics. The most common finding associated with CTS is an increased cross sectional area (CSA) at the pisiform level.[22-39] Ultrasound has also been used to study the acute response of the median nerve to activity including repetitive gripping, squeezing, and twisting with the hands[40,41] as well as manual wheelchair propulsion.[42] One of the benefits of ultrasound is its ability to visualize movement. As the term entrapment suggests, the median nerve movement is limited which in turn may increase strain and compression of nerves[43-47] and thus contribute to symptoms of CTS. Median nerve movement during various wrist and finger activities has been quantified using ultrasound.[48-51]

Obtaining a better understanding of the pathophysiology of CTS and the acute median nerve response to wheelchair propulsion may be helpful in the development of new technology and

techniques to prevent and/or reduce the likelihood of a developing a chronic repetitive strain injury and improve overall quality of life. In this study we used ultrasound to investigate the acute response of the median nerve after intense wheelchair propulsion and compared these changes to wheelchair propulsion biomechanics. In addition we quantified median nerve movement and deformation during grip and examined the relationship between movement, deformation and CTS risk factors.

1.1 BACKGROUND LITERATURE

1.1.1 Carpal Tunnel Syndrome

Carpal tunnel syndrome is the most common entrapment neuropathy and is a major public health problem. Studies have shown the prevalence to range between 1.5-2.7% in the general population.[6-10] It has been estimated that CTS costs over 1.9 billion dollars a year.[11,52] The medical costs and production loss due to CTS has been estimated to average about $30,000 per injured worker. CTS is a chronic pathology resulting from compression of the median nerve and typically results in pain, numbness, tingling, and weakness in the wrists, hands, and fingers.[53] When the median nerve is compressed within the carpal tunnel it often results in enlargement of the nerve just proximal to the point of compression at the tunnel inlet.[37,54] The actual cause of this compression is not fully understood, but it is believed that overuse of the hands and fingers leads to inflammation in the tendons within the tunnel and produces nerve compression.[55,56] CTS is commonly diagnosed by clinical examination and electrodiagnostic tests. Common treatments include immobilization (via splinting), medication, and carpal tunnel release surgery.

1.1.2 Carpal Tunnel Syndrome Pathophysiology

There are several theories regarding the cause of CTS. A common one is compression of the median nerve within the carpal tunnel.[57,58] Studies have shown that increased intracarpal canal pressures are a causal factor in the development of median mononeuropathy at the wrist.[17,59-63] Increased canal pressures can affect median nerve perfusion leading to the numbness, tingling, and weakness associated with CTS. Compared with individuals without CTS, research shows that those with CTS have higher intracarpal canal pressures.[56,61,62,64] Research has also shown that active gripping with the hands increases the carpal canal and intraneural median nerve pressures.[61,65-69] Okutsu et al found that carpal canal pressures nearly tripled when comparing a resting position to an active power grip.[66] Werner studied the changes in carpal tunnel pressures between relaxed hand, closed fist, and pinch grip and found increased pressures during closed fist and pinching compared to a relaxed hand posture.[65] Seradge et al. and Luchetti et al. both studied carpal tunnel pressures in individuals with CTS and controls for various hand and wrist postures and found greater pressures in CTS patients and increased pressures when making a fist.[68,69]

Previous research suggests that repetitive hand activities may lead to increased carpal canal pressures due to synovial thickening[56] which has been found in cadaver studies at the entrance and exit regions of the carpal tunnel.[70] In addition to ischemic factors, direct mechanical trauma to the median nerve plays a role in the pathophysiology of CTS.[55] During extremity movement, gliding between peripheral nerves and neighboring tissues is necessary to minimize traction and reduce compression on nerves.[71] Fibrosis or edema in the connective tissues surrounding the nerve may hinder nerve gliding and result in strain or compression of the nerve ultimately leading to dysfunction.[72-75]

1.1.3 Ergonomic Factors and Carpal Tunnel Syndrome

Some believe that CTS is a result of injury to the median nerve with high repetition, high-force actions of the wrist, as well as large joint excursions.[3,5,76] Ergonomics literature states force, repetition (or cadence of an activity), and posture as the primary risk factors for musculoskeletal disorders. In a report of musculoskeletal disorders in the workplace, NIOSH (National Institute for Occupational Safety and Health) defined repetitive hand and wrist activities as those involving repeated hand/finger or wrist movements such as gripping or cyclical flexion/extension, ulnar/radial deviation, and supination/pronation.[2] Wheelchair propulsion, while not an occupational task, fits this definition.[77] The effects of repetition can be magnified when combined with awkward postures or loading of the upper extremity such as occurs in wheelchair propulsion.[2] Work related CTS has been associated with high force and high repetition tasks, with a cadence greater than 2 cycles per minute and forces ranging from 10-40 N.[3] Wheelchair propulsion, with a stroke occurring approximately once per second and peak forces around 45-110 N, would exceed what the majority of studies consider a high force high repetition task.[20] With a cycle time of 1 second, if a wheelchair user propels for as little as 16 minutes, they would exceed the number of repetitions a factory worker in a high cycle task would complete in an 8 hour day. Research has also shown that the carpal tunnel pressure increases with increased external loads applied to the wrist and palm.[78,79] Cobb studied the changes in carpal tunnel pressure when an external force was applied to 16 different locations on the palm. All locations resulted in an increase in carpal tunnel pressure with the greatest increases occurring when forces were applied near the base of the palm.[78] A study by Goodman, investigating the effects of wheelchair propulsion on carpal canal pressures, found increased pressures present during propulsion.[79]

1.1.4 Carpal Tunnel Syndrome in Manual Wheelchair Users

Given the high forces and cadences associated with wheelchair propulsion, it is no surprise that the prevalence of CTS among MWU is much greater than the general population with a prevalence ranging between 49% and 73%.[14,15,17,19,80-82] In a study by Gellman of 77 individuals with paraplegia, 49% had signs and symptoms of CTS.[17] A study by Sie interviewed 103 subjects with paraplegia and found 66% had historical or physical examination evidence of CTS.[15] These studies also found the incidence of CTS increased with increased duration of wheelchair use. A number of investigators have performed nerve conduction studies (NCS) on wheelchair users. Aljure studied 47 patients with a spinal cord injury (SCI) below the T2 level and found 63% had electrodiagnostic evidence of CTS and 40% had clinical evidence of CTS.[18] This study also found an increased prevalence of CTS with duration of paralysis. A study by Tun on individuals with paraplegia below the T1 level, found slowed motor conduction of the median nerve at the wrist in 50% of the participants.[16] Another study of 31 patients with paraplegia below the T1 level found 55% of patients had electrodiagnostic evidence of CTS and 74% had symptoms of numbness or tingling in the hand.[13] Yang et al. studied 126 MWU with paraplegia and found that 57% reported symptoms of CTS, 60% had physical examination findings indicative of CTS, and 78% showed electrophysiological evidence of median mononeuropathy.[19] Most of the studies found a greater prevalence of abnormalities on NCS than actual clinical symptoms. This may signify that sub-clinical nerve damage exists in a number of these individuals. In all of these studies, wheelchair propulsion has been implicated as contributing to injury. From these studies, it is apparent that CTS is a common problem among manual wheelchair users. In addition to these studies on the prevalence of CTS among MWU, research has shown a direct link between wheelchair propulsion and pathology in the

wrist.[20,21,83,84] The primary results of these studies show median and ulnar nerve function are significantly correlated with cadence of propulsion, magnitude and rate of rise of forces used for propulsion. Specifically, higher cadences and higher forces were correlated with worse median nerve function. Clearly, high force, high repetition tasks need to be addressed in order to maintain upper extremity function in MWU.

1.1.5 Wheelchair Propulsion Biomechanics and Carpal Tunnel Syndrome

Methods have been previously developed for analyzing pushrim forces critical to assessing injury mechanisms through the use of the Smartwheel.[85-87] Research has found stable pushrim force and moment measures that are statistically valid metrics.[77] Using the Smartwheel, several studies have related injury to wheelchair propulsion variables.[20,21,88] With respect to CTS, our previous research has found that wheelchair pushrim forces are related to nerve conduction study variables.[20,21] We found that, when controlling for weight, there were correlations between median nerve function and the cadence of propulsion and rate and rise of the resultant force. In another study on median nerve conduction studies and biomechanics, we found an inverse relationship between median nerve health and range of motions at the wrist.[20] Greater range of motion was associated with better median nerve function. Further analysis found that greater wrist range of motion was associated with greater push angles, lower forces and cadence. By taking long strokes, wheelchair users are able to generate work without high peak forces. As a follow up to this study, an analysis of longitudinal data was completed. The longitudinal analysis showed that risk of injury to the median nerve could be predicted by wheelchair propulsion biomechanics.[88] Individuals who used greater force and cadence at their initial visit had greater progression in median nerve damage approximately three years later at a second

visit. Once again, peak resultant force was a predictor of progression of nerve conduction study abnormalities. Based on these findings it appears that force and cadence may be the more critical variables to investigate rather than posture and range of motion.

1.1.6 Carpal Tunnel Syndrome and Ultrasound

While NCS are a widely accepted method for diagnosing CTS, ultrasonography has become a popular diagnostic tool because of its non-invasiveness, shorter examination time, and lower cost. Ultrasound has been shown to be a very precise method of viewing musculoskeletal anatomy. In a study by Kamolz, the cross-sectional areas of the median nerves of 20 cadavers were measured both anatomically and using ultrasonography. There were no significant differences found between these measurements and they concluded that ultrasound is a very precise method to display the anatomy of the carpal tunnel and median nerve.[32] In order to validate the diagnostic usefulness of ultrasound, researchers have compared ultrasound findings with electrodiagnostic findings. In general ultrasound was found to be comparable to electrophysiology and in some cases could provide more information about possible anatomic causes of CTS where NCS could not.[24,29,30] Studies have shown ultrasound to be useful in the diagnosis of CTS, specifically by measuring the median nerve cross-sectional area.[22-24,28-36] Buchberger et al. was the first to report three common findings associated with CTS: (1) increased cross sectional area (CSA) at the pisiform level; (2) increased swelling ratio (SR); and (3) increased flattening ratio (FR) at hamate level.[22,23] The SR is defined as the ratio of the CSA at pisiform with respect to the CSA at the distal radius. The FR is defined as the ratio of the long axis of nerve with respect to the short axis when viewing the median nerve transversely. Other

researchers have confirmed these findings with the most common finding being increased CSA at the pisiform level.[24-39]

1.1.7 Ultrasound and the Acute Median Nerve Response to Activity

Much of the research using ultrasound to investigate the median nerve in individuals with CTS is focused on determining the typical CSA that is correlated with CTS. We are interested in using ultrasound to investigate changes in median nerve CSA after an activity, specifically wheelchair propulsion, and attempting to relate these changes to variables known to be involved in the cause of CTS. Two studies using ultrasound to investigate changes in the median nerve after activity found increases in CSA post activity.[40,41] Altinok investigated the effects of forceful bidirectional squeezing and twisting with the hands. They compared individuals with CTS to asymptomatic controls. They found significant increases in CSA at the pisiform and SR after these activities in both groups. The increases in participants with CTS were greater than that of control subjects.[40] A study by Massy-Westropp investigated the changes in the median nerve after performing a cutting task repeatedly for five minutes. They studied individuals without CTS or symptoms of CTS and found that the CSA of the median nerve increased immediately after activity at both the distal wrist crease and pisiform levels. Within 10 minutes post-activity, they found the median nerve returned to a size not significantly different than pre-activity. At the hamate level they found an increase in the anterior-posterior diameter (i.e. less flattening) of the nerve after activity.[41] An investigation of changes in the median nerve before and after a wheelchair sporting event found a significant decrease in CSA at the distal radius after activity. This study also found that participants with physical examination findings indicative of CTS showed significantly different and opposite changes in the SR after activity.[42] Understanding the

anatomical changes of the median nerve as a result of a high impact, high repetition task may improve the understanding of causes of CTS and lead to better preventative measures ultimately resulting in a significant decrease in the costs associated with CTS.

1.1.8 Ultrasound and Median Nerve Movement

Research on the displacement of the median nerve and tendons of the carpal tunnel has shown that hand, wrist, and finger movements affect median nerve strain. These studies suggested that repetitive wrist and finger activities may lead to pathological changes in the nerve (e.g. CTS).[48-50,89,90] Nakamichi used ultrasound to measure the transverse sliding of the median nerve during passive flexion and extension of the fingers in individuals with CTS and controls. They found less nerve movement present in individuals with CTS compared to unaffected controls.[49] A study by Erel investigated both longitudinal and transverse nerve sliding during passive finger extension in individuals with CTS and controls. They used a cross-correlation algorithm for determining longitudinal sliding, while transverse measurements were done by simply comparing the pre-extension and post-extension images. They also found less transverse nerve sliding in individuals with CTS.[48] At the time this research study was conducted, investigating how the median nerve both moves and deforms during a gripping task, to our knowledge, had not been studied. Recently, we found two studies with objectives similar ours. Yoshii et al. studied the relative median nerve displacement as well as changes in CSA, aspect ratio (similar to the FR), perimeter (PERIM), and circularity (CIRC) by comparing the median nerve at a starting, resting position to a posture with the fingers fully flexed, or a fist position. [51] Van Doesburg et al. investigated the same variables as Yoshii, but compared full extension to full flexion of both the index finger and the thumb.[91]

1.2 RESEARCH OBJECTIVES

The overall goal of this research was to quantify ultrasonographic median nerve characteristics in a population at high risk for developing CTS. Our target population was MWU and we were interested in studying the effects of wheelchair propulsion on the acute response of the median nerve to loading. In order to confidently assess changes, we needed to be sure that we could reliably measure the median nerve. In Chapter 2 we conducted a repeatability analysis of key median nerve measures which have been previously related to CTS and developed an ideal study design for accurately assessing median response. Once an appropriate protocol was determined, Chapter 3 was focused on quantifying median nerve characteristics before and after wheelchair propulsion and related these findings to the presence of symptoms of CTS. In Chapter 4, we sought to relate specific characteristics of propulsion (force, repetition, posture) to the nerve responses calculated in Chapter 3. In addition to these static median nerve measures, we developed new methods for assessing the dynamic characteristics of the median nerve during simple finger movements in this high risk population. Chapter 5 focuses on the development of several algorithms for quantifying deformation and displacement of the median nerve during grip. Finally, Chapter 6 presents the findings from applying one of these algorithms to assess differences in deformation and displacement among symptomatic and asymptomatic participants.

2.0 RELIABILITY OF ULTRASONOGRAPHIC MEDIAN NERVE MEASURES

Published in Muscle & Nerve (in press)

2.1 INTRODUCTION

Carpal tunnel syndrome (CTS) is the most common entrapment neuropathy affecting the median nerve.[10] The most accepted theory for the pathophysiology of CTS is compression of the median nerve in the carpal tunnel which typically results in pain, numbness, tingling, and weakness in the hands and fingers.[57,58] When the median nerve is compressed within the carpal tunnel it typically results in enlargement of the nerve just proximal to the point of compression at the tunnel inlet.[37,54] The actual cause of this compression is not fully understood, but it is believed that overuse of the hands and fingers leads to inflammation in the tendons within the tunnel and produces nerve compression.[55,56]

CTS is commonly diagnosed by clinical examination and electrodiagnostic tests. Recently, ultrasound has become a popular diagnostic tool for CTS due to its low cost, noninvasiveness, and short examination times. Ultrasonography can be used to accurately measure the shape and size of the median nerve at various levels of the wrist.[32] Many studies have compared these ultrasound measures of the median nerve with electrodiagnostic and clinical examinations and found that individuals with CTS most commonly have increased

median nerve cross sectional area (CSA) at the level of the pisiform bone, increased flattening ratio (FR) at the level of the hook of the hamate, increased palmar bowing of the flexor retinaculum, and an increased swelling ratio (SR), defined as the ratio of the median nerve CSA at the pisiform level with respect to the distal radius level.[22,23,25-27,31,33-39]

In addition to diagnostic uses, ultrasound has been used as a research tool for assessing the acute response of the median nerve to repetitive activity.[40-42] The magnitude of change in median nerve variables in these three studies ranged from ~4-20%, and a majority were rather small changes of less than 10%. Measuring acute median nerve changes may be useful in predicting the likelihood of developing CTS and assessing the risks involved with certain tasks. It may also allow for the testing of interventions that may reduce acute trauma to the nerve and ultimately delay or prevent the onset of CTS. In order to confidently detect these small changes and attribute them to activity, it must be shown that the nerve can be reliably measured when no changes have occurred. Based on our literature search we found little research on the repeatability of median nerve ultrasound measures and minimum detectable change (MDC). Two studies investigated median nerve CSA repeatability and found test and retest measurements were highly correlated, but neither assessed the standard error of measurement (SEM) or MDC.[92,93]

In this study we sought to expand upon the limited reliability literature and investigated the repeatability of several median nerve ultrasound measures (CSA, FR, SR, mean grayscale). We also evaluated the effects of several protocol designs on the dependability coefficient and standard error of measurement. We hypothesized that reliability measures would help us to determine a reliable protocol that could be used in future research focused on quantifying median nerve changes in response to activity.

2.2 METHODS

2.2.1 Participants

Twenty participants volunteered for this study. Fifteen able bodied individuals (12 male, 3 female, mean age 43.8±13.1 years) and five manual wheelchair users (5 male, mean age 43.5±15.5 years) provided informed consent before enrolling in the study. All manual wheelchair users had a spinal cord injury. We included wheelchair users in this study because they are at high risk for CTS,[13,16-18,82] and we plan to conduct future research in this target population. Participants were required to be between the ages of 18 and 75 years and available to attend multiple ultrasound examinations.

2.2.2 Data Collection

Images were collected at three levels of the wrist while participants maintained a seated posture with upper arm relaxed, fully adducted with no internal/external rotation and elbow flexed at 90 degrees with the forearm supported. The forearm was supinated with the wrist at neutral and fingers relaxed. Images were collected using a Philips HD11 XE system with a 5-12 MHz linear array transducer (Philips Medical Systems, Bothell, WA). All machine settings (gain, focus, etc.) were held constant across all participants and evaluators. While scanning, the probe was rested on the skin while minimal pressure was applied as necessary to obtain quality images. Transverse images of the median nerve were collected at the distal radius, the pisiform, and the hook of the hamate levels. The level of the radius was at the most distal ridge of the radius. It was found by moving the ultrasound probe distally along the wrist until the radius dropped out of

view, at which time the probe was slid proximally until the bony landmark reappeared. This corresponds to the point at which the distal ridge of the radius is closest to the skin. The pisiform level was found by scanning distally until the pisiform first appeared in the image. The level of the hook of the hamate was found by scanning further distally into the palm of the hand until the hook of the hamate first appeared in the image. Figure 1 shows sample images collected with the bony landmarks and median nerve labeled. These image levels are easily viewed using ultrasound, and nerve characteristics at these locations have been linked to CTS. [22-39]

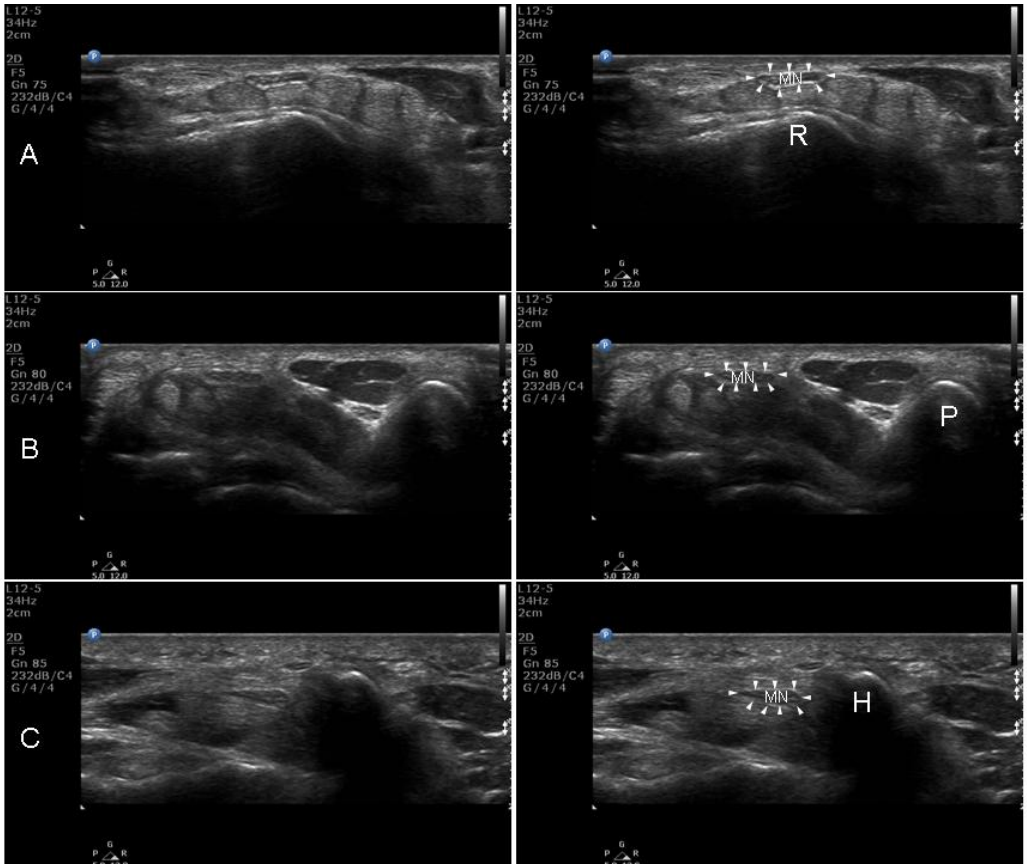

Figure 1. Sample ultrasound images at each image level

Unlabeled (left) and labeled (right) cross sectional images of the median nerve (MN) at the A) distal radius (R), B) pisiform (P), and C) hook of the hamate (H).

Two examiners collected the ultrasound images on each participant. Both examiners were trained on the same protocol and had approximately 3 years of experience imaging soft tissues of the upper extremity including muscles, tendons, and peripheral nerves. One investigator collected two images at each level followed by 15-30 minutes of rest. After the rest, another set of two images at each level was collected. Next, a second investigator repeated the same image collection protocol. Each image was saved for later analysis, as described below.

2.2.3 Data Analysis

We measured three median nerve variables (CSA, FR, mean grayscale) at each image level and calculated the SR based on the distal radius and pisiform CSAs, for a total of 10 variables. A single investigator, blinded to occasion and image number, analyzed each image, performing a boundary trace to calculate CSA and measuring the major and minor axes of the nerve in order to calculate the FR (major axis / minor axis). The boundary trace was performed along the circumference of the nerve excluding the hyperechoic epineurium. Figure 2 shows an example of the boundary trace and major and minor axis selections. The grayscale values of each pixel within the selected area were averaged together to calculate the mean grayscale of the nerve. The SR was calculated by dividing the CSA at the level of the pisiform by the CSA at the distal radius. This method is in line with previous research relating the SR to CTS. [23,39,40,94]For inter-rater reliability a single reading was used for each image from each evaluator for a total of eight measures per variable per subject (two evaluators x two occasions x two images x one reading). For intra-rater reliability, each image collected by evaluator one was analyzed twice (readings one and two) resulting in eight measures per variable per subject (one evaluator x two occasions

x two images x two readings). The eight measures for inter- and intra-rater reliability were analyzed using generalizability theory as described in the statistical analysis section.

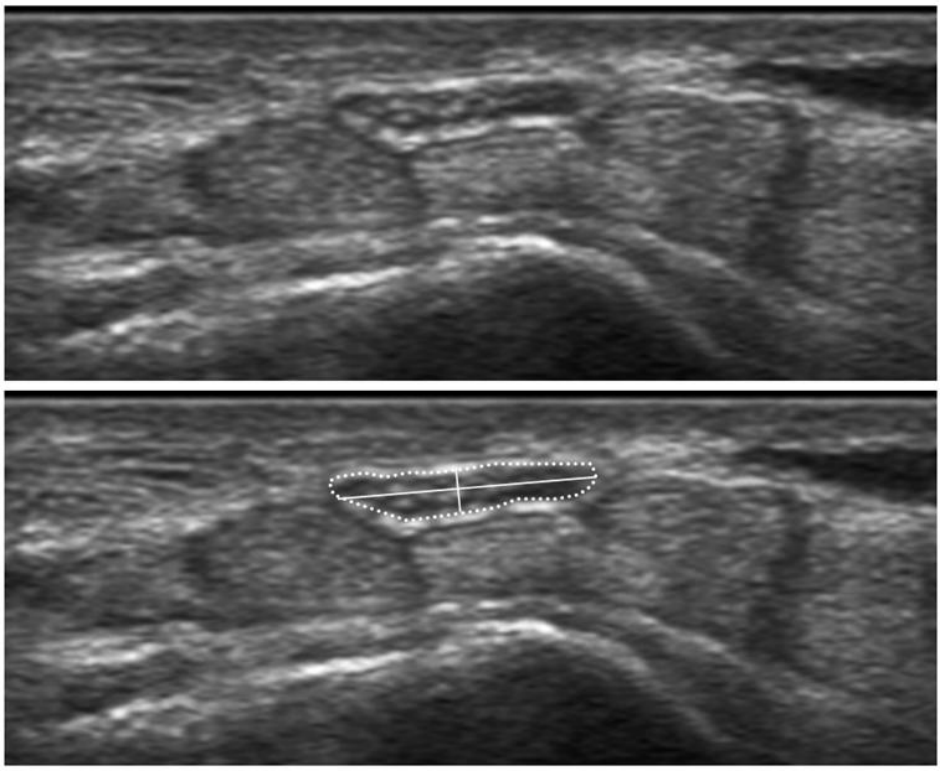

Figure 2. Example of the image analysis selections

The images show a close up of the median nerve (top) and the same image with the boundary trace (dotted line) and the major and minor axes (solid lines) selected during the image analysis (bottom).

2.2.4 Statistical Analysis

Generalizabiltiy theory is a reliability analysis technique similar to the intra-class correlation coefficient, except that it determines the magnitude of each source of variance (generalizability or G-study) and uses this information to evaluate the effects of different study designs (dependability or D-study).[95] We used a random D-study model which allows for all sources of variance to contribute to measurement error. The two measures we used are the dependability

coefficient (Φ) and the normalized standard error of measurement (SEM_{NORM}). The dependability coefficient (Φ) is defined as a ratio of variance of interest over the sum of the variance of interest and the error variance. The dependability coefficient which ranges from 0 to 1 is typically interpreted as follows: $\Phi>0.75$ signifies good reliability, $0.50<\Phi<0.75$ represents moderate reliability, and $\Phi<0.50$ represents poor reliability. [96] In other words, when the observed measure represents the hypothetical true value at least 75% of the time, the measure is said to have good reliability. The standard error of measurement (SEM) is calculated by taking the square root of the error variance and is expressed in the same units as the variable from which it is calculated. Theoretically, the SEM assumes that a subject will obtain an observed score within 1 SEM of their hypothetical true score about 68% of the time and within 2 SEM of their hypothetical true score 95% of the time when data are normally distributed (within-subject standard deviation). To allow for easier interpretation, we calculated SEM_{NORM}, a unitless normalized percentage defined as (SEM/overall mean)*100, where overall mean is the mean of all eight measures of a particular variable. These measures provide an estimation of the amount of uncertainty of an observed measurement in reference to a hypothetical true score, assuming that all testing conditions remain stable. A lower SEM_{NORM} suggests that the observed measure is closer to the hypothetical true value.

Lastly, we calculated the MDC which is the 95% confidence interval of the SEM and is calculated as $SEM*1.96*\sqrt{2}$. The MDC can be interpreted as the magnitude of absolute change necessary to detect a difference that represents a true median nerve change, significantly exceeding the measurement error associated with each measure. To facilitate interpretation and make the MDC independent of the units of measurement, it was also expressed as a normalized percentage (MDC_{NORM}) which was calculated as (MDC/overall mean)*100. When investigating

changes within a single subject, a change that is greater than this MDC_{NORM} can be considered significant while changes less than the MDC_{NORM} cannot be differentiated from measurement error. No hypotheses were made regarding the MDC. It is presented as it may be useful for future applications using ultrasound to assess changes in median nerve characteristics over time.

Using the G-study we determined the magnitudes of the different sources of variance for both inter-rater and intra-rater measures. The inter-rater design included the single sources of participant, evaluator (E), occasion (O), and image (I), and all possible combinations of these, while the intra-rater study included the single sources of participant, occasion (O), image (I), and reading (R), and all combinations of these. The random D-study model was then used to evaluate different protocol designs, varying the number of occasions, images and readings and their effect on the dependability coefficient (Φ), SEM_{NORM}, and MDC_{NORM}.

2.3 RESULTS

2.3.1 Inter-rater Reliability

The inter-rater findings are presented in Table 1. Using the simplest design, with either evaluator capturing a single image at a single occasion (E=1,O=1,I=1), CSA at the distal radius showed good inter-rater reliability (Φ=0.928), however other reliability measures were moderate to poor ($0.038<\Phi<0.737$). Measurement error (SEM_{NORM}) ranged from ~5-21% depending on image level and variable. CSA at the radius and the pisiform, the SR, and mean grayscale at the radius had the least error, all less than 10%, while all other measures had error greater than ~17%.

Table 1. The effect of various study designs on the inter-rater reliability measures

Nerve Measure	Image Level	Reliability Measure	E = 1 O = 1 I = 1	E = 1 O = 1 I = 2	E = 1 O = 2 I = 1	E = 1 O = 2 I = 2
Cross Sectional Area	Radius	Φ	0.928	0.934	0.933	0.937
		SEM_{NORM} (%)	4.825	4.612	4.651	4.515
		MDC_{NORM} (%)	13.374	12.783	12.892	12.516
	Pisiform	Φ	0.632	0.651	0.650	0.662
		SEM_{NORM} (%)	8.558	8.216	8.223	8.019
		MDC_{NORM} (%)	23.720	22.773	22.794	22.227
	Hamate	Φ	0.332	0.333	0.334	0.334
		SEM_{NORM} (%)	19.772	19.721	19.696	19.667
		MDC_{NORM} (%)	54.804	54.665	54.594	54.515
Flattening Ratio	Radius	Φ	0.529	0.583	0.582	0.619
		SEM_{NORM} (%)	20.546	18.429	18.451	17.072
		MDC_{NORM} (%)	56.951	51.084	51.144	47.321
	Pisiform	Φ	0.427	0.452	0.502	0.521
		SEM_{NORM} (%)	18.249	17.337	15.668	15.087
		MDC_{NORM} (%)	50.583	48.055	43.431	41.819
	Hamate	Φ	0.691	0.752	0.777	0.814
		SEM_{NORM} (%)	19.932	17.102	15.969	14.234
		MDC_{NORM} (%)	55.250	47.404	44.264	39.453
Mean Grayscale	Radius	Φ	0.575	0.668	0.670	0.732
		SEM_{NORM} (%)	9.130	7.495	7.458	6.422
		MDC_{NORM} (%)	25.308	20.775	20.674	17.802
	Pisiform	Φ	0.308	0.334	0.376	0.396
		SEM_{NORM} (%)	16.967	15.976	14.576	13.980
		MDC_{NORM} (%)	47.031	44.284	40.403	38.750
	Hamate	Φ	0.038	0.044	0.048	0.053
		SEM_{NORM} (%)	21.626	20.122	19.195	18.195
		MDC_{NORM} (%)	59.945	55.775	53.207	50.433
Swelling Ratio	Pisiform Radius	Φ	0.737	0.766	0.764	0.783
		SEM_{NORM} (%)	8.323	7.708	7.751	7.345
		MDC_{NORM} (%)	23.069	21.365	21.485	20.360

The dependability coefficient (Φ) normalized standard error of measurement (SEM_{NORM}), and minimum detectable change (MDC_{NORM}) are presented for each median nerve measure. The column headers represent the number of evaluators (E), occasions (O), and images (I) which were used in determining the reliability measures.

2.3.2 Intra-rater Reliability

Intra-rater reliability was better than inter-rater reliability for all variables. All intra-rater reliability findings are presented in Table 2. With the simplest design of a single image and reading at either occasion (O=1,I=1,R=1), intra-rater measures were moderate to good ($0.575<\Phi<0.995$) with most (6 of 10) measures having dependability coefficients greater than 0.876. The most reliable measure was CSA ($\Phi>0.982$), followed by SR ($\Phi=0.975$), then FR ($0.662<\Phi<0.887$) and lastly grayscale ($0.575<\Phi<0.674$). For all variables, measurement error (SEM_{NORM}) was lower than the inter-rater measures and ranged from ~1-14% depending on image level and variable. CSA and SR had the least error; all were less than 2.3%, while flattening ratio and mean grayscale were mostly (5 out of 6 measures) greater than 10% error.

2.3.3 Minimum Detectable Change

The MDC varied greatly depending on the variable and image level. The MDC_{NORM} for inter-rater measures were all greater than 13%, and many (n=5) were greater than 50%. Intra-rater was much lower with MDC_{NORM} ranging from 3.8-6.2% for all CSA measures and SR, while all flattening ratio and mean grayscale measures ranged from ~16-40%.

Table 2. The effect of various study designs on the intra-rater reliability measures

Nerve Measure	Image Level	Reliability Measure	O = 1 I = 1 R = 1	O = 1 I = 1 R = 2	O = 1 I = 2 R = 1	O = 1 I = 2 R = 2
Cross Sectional Area	Radius	Φ	0.995	0.996	0.997	0.998
		SEM_{NORM} (%)	1.371	1.198	1.087	0.916
		MDC_{NORM} (%)	3.800	3.319	3.014	2.538
	Pisiform	Φ	0.982	0.985	0.989	0.992
		SEM_{NORM} (%)	1.992	1.834	1.535	1.367
		MDC_{NORM} (%)	5.521	5.083	4.255	3.788
	Hamate	Φ	0.994	0.995	0.996	0.996
		SEM_{NORM} (%)	2.235	2.102	1.872	1.768
		MDC_{NORM} (%)	6.196	5.827	5.190	4.900
Flattening Ratio	Radius	Φ	0.876	0.889	0.922	0.930
		SEM_{NORM} (%)	10.360	9.735	8.046	7.592
		MDC_{NORM} (%)	28.716	26.983	22.303	21.044
	Pisiform	Φ	0.662	0.671	0.683	0.688
		SEM_{NORM} (%)	14.242	13.943	13.554	13.396
		MDC_{NORM} (%)	39.476	38.649	37.568	37.132
	Hamate	Φ	0.887	0.890	0.917	0.919
		SEM_{NORM} (%)	12.287	12.122	10.343	10.237
		MDC_{NORM} (%)	34.057	33.600	28.668	28.376
Mean Grayscale	Radius	Φ	0.674	0.677	0.764	0.767
		SEM_{NORM} (%)	5.753	5.707	4.592	4.562
		MDC_{NORM} (%)	15.946	15.818	12.728	12.645
	Pisiform	Φ	0.575	0.577	0.612	0.613
		SEM_{NORM} (%)	12.649	12.609	11.738	11.714
		MDC_{NORM} (%)	35.062	34.950	32.536	32.469
	Hamate	Φ	0.613	0.617	0.675	0.678
		SEM_{NORM} (%)	12.833	12.729	11.210	11.132
		MDC_{NORM} (%)	35.570	35.284	31.073	30.856
Swelling Ratio	Pisiform Radius	Φ	0.975	0.977	0.988	0.989
		SEM_{NORM} (%)	2.222	2.127	1.571	1.504
		MDC_{NORM} (%)	6.159	5.896	4.355	4.169

The dependability coefficient (Φ) normalized standard error of measurement (SEM_{NORM}), and minimum detectable change (MDC_{NORM}) are presented for each median nerve measure. The column headers represent the number of occasions (O), images (I), and readings (R) which were used in determining the reliability measures.

2.3.4 Effect of Various Study Designs

Tables 1 and 2 also show the effects of different study designs on the inter- and intra-rater dependability coefficient (Φ) normalized standard error of measurement (SEM_{NORM}), and minimum detectable change (MDC_{NORM}) for each median nerve measure. Table 1 shows the improvements that can be obtained in inter-rater measures by averaging the readings of: two images at one occasion (E=1,O=1,I=2), a single image at two occasions (E=1,O=2,I=1), or two images at two occasions (E=1,O=2,I=2). Table 2 shows the improvements that can be obtained in intra-rater measures by averaging the results of: two readings of a single image (O=1,I=1,R=2), a single reading of two images (O=1,I=2,R=1), or two readings of two images (O=1,I=2,R=2). When comparing the simplest design using no averaging (first data column in the tables) with the most complex design averaging multiple measures (last data column in the tables), it is apparent that averaging measurements obtained from repeat images and/or readings, whether performed at the same or different occasions, did not appreciably improve the reliability of any measures.

2.4 DISCUSSION

In this study we assessed the reliability, measurement error, and MDC associated with quantifying median nerve ultrasound characteristics. We also evaluated the effects of different protocol designs so that an efficient and reliable protocol can be used for future assessment of the acute median nerve response to activity. Intra-rater reliability was better than inter-rater reliability, which is in line with previous research.[93,97] CSA at the distal radius level showed

good inter-rater reliability while other inter-rater reliability measures were moderate to poor. Inter-rater reliability of CSA and mean grayscale value were greatly affected by the location of measurement. The reliability measures decreased substantially as the image level moved distally from the radius to the pisiform to the hamate level. This could be due to difficulty keeping the probe perpendicular to the nerve as it dives further from the skin at the more distal two levels. While it may have been possible to improve our ability to visualize the median nerve and thus the reliability of the CSA measures by adjusting the gain and focus settings, we would have introduced more variability into the grayscale measures. In order to characterize median nerve size and grayscale characteristics in a time efficient manner, we chose to hold the gain and focus constant. Given the suboptimal inter-rater reliability findings, research seeking to identify small changes in the median nerve would be best performed by a single investigator doing all the ultrasound imaging.

While inter-rater measures of median nerve ultrasound characteristics were only moderately reliable, intra-rater measures showed mostly good dependability. Cross sectional area is the variable of greatest interest, since it is the most common measure linked to CTS and showed very high intra-rater reliability. Other measures commonly associated with CTS are the swelling ratio and flattening ratio. The swelling ratio also had very high reliability, and the flattening ratio showed good dependability for two of the three imaging levels. Given these three variables show good reliability when no change is present, they will likely be useful for detecting small differences when changes do occur. The mean grayscale value of the median nerve on the other hand was only moderately reliable. Mean grayscale may still be a useful measure, but a different imaging protocol may be necessary to insure high reproducibility of this variable. The mean grayscale value of a structure is highly dependent on probe orientation, as minor changes

in probe tilt can greatly affect anisotropy and result in a darker appearance. A protocol focused on obtaining an image where the probe is perpendicular to both the nerve and the tendons near the nerve may improve the reliability of the mean grayscale measure. Furthermore, as ultrasound technology advances, there will be higher frequency probes and improved signal processing techniques which will in turn improve image quality and likely the reliability of median nerve measures.

The results of this study show the MDC varies greatly, with CSA and SR to ranging from 3.8% to 6.2% while FR and grayscale ranged from 15.9% to 39.5% if a single investigator performs the ultrasound scanning. These values may be helpful for determining median nerve changes within a single patient at different time points (either acutely or chronically). This has clinical implications if trying to determine the progression of nerve pathology over several visits. If the patient's nerve changes by a value greater than the MDC then the clinician can be confident that there is a true change in the nerve and not just error in their measurement. The MDC presented here has some limitations in that it was only calculated based on a small number of volunteers (n=20). A larger study may be necessary to better assess the MDC. Given this, the values presented here should only be used as a rough guideline.

Based on the results of the intra-rater D-study we found very little improvement in reliability and measurement error when capturing and analyzing images multiple times. Comparing a protocol using a single image and reading (see O=1, I=1, R=1 in Table 2) to a protocol of two images and readings (see O=1, I=2, R=2 in Table 2), the greatest decrease in SEM_{NORM} was less than 3% and on average was only 1.18%. Given the limited benefit associated with using multiple images and readings we suggest using a single image and reading for future studies that quantify changes in median nerve variables. If time is an issue, we suggest

that at each time point, a single investigator collects a single image at the pisiform level and analyzes each image once. Following this protocol should result in highly reliable images collected at the site where swelling is most commonly seen in individuals with CTS. If time permits collecting an additional image at the distal radius would give another reference point with good reliability.

2.5 CONCLUSION

In conclusion, ultrasound is a reliable tool for measuring the median nerve and therefore may be useful for assessing changes in median nerve measures and CTS. As long as a standard imaging protocol is followed, in which a single investigator performs the imaging, CSA, FR, and SR, the measures most commonly related to CTS, are highly reproducible. In a clinical setting, measuring acute change of the median nerve to activity may also be helpful from a diagnostic perspective. By testing the median nerve response to different interventions or activities in individuals with and without CTS we may be able to better understand the pathophysiology of CTS.

3.0 MEDIAN NERVE CHARACTERISTICS BEFORE AND AFTER WHEELCHAIR PROPULSION RELATED TO SUBJECT CHARACTERISTIC RISK FACTORS AND SYMPTOMS OF CARPAL TUNNEL SYNDROME

3.1 INTRODUCTION

Carpal tunnel syndrome (CTS) is the most common entrapment neuropathy and is a major public health problem. Studies have shown the prevalence to range between 1.5-2.7% in the general population.[6-9] There are several theories regarding the cause of CTS, a common one being compression of the median nerve within the carpal tunnel.[57,58] Ergonomics literature states force, repetition (or cadence of an activity), and posture as the primary risk factors for musculoskeletal disorders.[2] Given the high forces and cadences associated with wheelchair propulsion, it is no surprise that the prevalence of CTS among MWU is much greater than the general population with a prevalence ranging between 49% and 73%.[12-19] Several of these studies also found the incidence of CTS increased with greater duration of wheelchair use. In all of these studies, wheelchair propulsion has been implicated as contributing to injury.

While NCS are a widely accepted method for diagnosing CTS, ultrasonography has become a popular diagnostic tool because of its non-invasiveness, shorter examination time, and lower cost. Ultrasound has been shown to be a very precise method of viewing musculoskeletal anatomy.[32] In order to validate the diagnostic usefulness of ultrasound, researchers have

compared ultrasound findings with electrodiagnostic findings. In general ultrasound was found to be comparable to electrophysiology and in some cases could provide more information about possible anatomic causes of CTS where NCS could not.[24,29,30] Studies have shown ultrasound to be useful in the diagnosis of CTS, specifically by measuring the median nerve cross-sectional area. [22-24,28-36] Buchberger et al. were some of the first to investigate CTS using ultrasound and found that subjects with CTS had a significant increase in the median nerve cross-sectional area (CSA) at the pisiform level, an increase in the flattening ratio (FR) at the hamate level, and an increased swelling ratio (SR). The FR is defined as the ratio of long axis of nerve with respect to the short axis when looking at the nerve in cross-section and the SR is defined as the ratio of CSA at pisiform level with respect to the CSA at the distal radius.[22,23] Other researchers have confirmed these findings with the most common finding being increased CSA at the pisiform level.[24,28-36] Measurement of median nerve characteristics using ultrasound has been shown to be reliable when following a consistent imaging protocol.[35,41,93,97,98]

We are interested in using ultrasound to quantify median nerve characteristics before and after an activity, specifically wheelchair propulsion, and attempting to relate median nerve changes to variables associated with CTS. Two studies using ultrasound to investigate changes in the median nerve after activity found increases in CSA post activity.[40,41] Altinok investigated the effects of forceful bidirectional squeezing and twisting with the hands. They found significant increases in CSA at the pisiform and SR after activity and the increases in participants with CTS were greater than that of control subjects.[40] A study by Massy-Westropp investigated the changes in the median nerve after performing a cutting task repeatedly for five minutes. They studied individuals without CTS or symptoms of CTS and found that the CSA of the median nerve increased immediately after activity at both the distal wrist crease and pisiform

levels. Within 10 minutes post-activity, they found the median nerve returned to a size not significantly different than pre-activity. At the hamate level they found an increase in the anterior-posterior diameter of the nerve after activity.[41] Our investigation of changes in the median nerve before and after a wheelchair sporting event found a significant decrease in CSA at the distal radius after activity. We also found that participants with physical examination findings indicative of CTS showed significantly different and opposite changes in the SR after activity.[42] There were several limitations associated with our previous study which led to the design of the current study. These limitations included varying durations of wheelchair propulsion at unknown velocities and different time between cessation of activity and follow up ultrasound examinations.

These three previous studies on median nerve response to activity only focused on the immediate response of the median nerve within 10 minutes of cessation of activity. It is possible that there is a post-acute response that could be seen by imaging the nerve for a greater duration post activity. No previous literature was found that tracked the post-acute nerve response and we believe this may provide a better understanding of the pathophysiology in the median nerve associated with micro trauma resulting from high-repetition, high force activities.

The objective of this study was to quantify median nerve characteristics at baseline and after strenuous wheelchair propulsion and relate them to subject characteristics and symptoms of CTS. We determined both the acute (immediately after activity) and post-acute (over 30 minutes) response of the median nerve to wheelchair propulsion. We expected subject characteristics previously related to CTS including BMI, duration of wheelchair use, and age[15,17,18,54,63,99] to be related to baseline, acute, and post-acute median nerve measures. Specifically we expected greater BMI, duration of wheelchair use, and age to correlate with

greater baseline CSA, FR, and SR, and greater acute changes in these variables both acutely and post-acutely. To investigate the effect of symptoms of CTS on median nerve characteristics we split the population into asymptomatic and symptomatic groups. We hypothesized that the symptom groups would have different baseline median nerve characteristics and different median nerve responses both immediately after propulsion and over time. Specifically, we expected the symptomatic individuals would have evidence of CTS in baseline median nerve characteristics indicated by a larger CSA, FR, and SR compared to the asymptomatic population. Upon investigating median nerve changes we hypothesized that symptomatic participants would show greater immediate changes in median nerve characteristics and that these changes would take longer to subside. We further hypothesized that the amount of change would correlate with symptom scores.

3.2 METHODS

3.2.1 Participants

Fifty-four participants (50 males, 4 females) provided written informed consent for this institutional review board approved study before enrolling. The participants were a convenience sample recruited in response to fliers and direct contact at the 2007 and 2008 National Veterans Wheelchair Games (NVWG) and through registries at the Human Engineering Research Laboratories (HERL). All participants were between ages 18 and 65 and had a non-progressive or non-degenerative disability which did not directly affect their upper extremity function. Participants were required to use a manual wheelchair beginning after the age of 18 as their

primary means of mobility. Individuals were excluded if they reported traumatic injury to the wrist or a history of cardiovascular disease or another condition which could be exacerbated by intense physical activity.

3.2.2 Data Collection

Participants completed questionnaires about subject demographics and the presence and severity of symptoms of CTS including the Boston Carpal Tunnel Questionnaire (BCTQ), which includes the Symptom Severity Scale (SSS) and Functional Status Scale (FSS) developed by Levine. We chose to use this questionnaire because it is the most commonly used outcome measure for assessing CTS patients[100] and was shown to have high reproducibility (Pearson's correlation of 0.90), internal consistency (Cronbach's alpha of 0.89), validity, and sensitivity to clinical change.[52] Furthermore the BCTQ has been used to assess severity of symptoms in MWU[19] and related to ultrasound measures of the median nerve.[101]

The ultrasound images were collected as described in our previous research[98], with imaging of the median nerve at three levels of the wrist (distal radius, pisiform, and hamate). Briefly, images were collected while participants maintained a seated posture with upper arm relaxed, fully adducted with no internal/external rotation and elbow flexed at 90 degrees with the forearm supported. The forearm was supinated with the wrist at neutral and fingers relaxed. Images were collected using a Philips HD11 XE system with a 5-12 MHz linear array transducer (Philips Medical Systems, Bothell, WA). All machine settings (gain, focus, etc.) were held constant across all participants. A single investigator with approximately three years of experience imaging soft tissues of the upper extremity including muscles, tendons, and peripheral nerves performed all ultrasound imaging. Figure 1 (in Chapter 2) shows sample

images collected with the bony landmarks and median nerve labeled. The image levels collected are easily viewed using ultrasound, and nerve characteristics at these locations have been linked to CTS. [22-39] For some participants we were not able to obtain images at the level of the hamate due to difficulty viewing the nerve. At this level of the wrist the nerve is sometimes deep and oblique, not allowing a clear, analyzable image to be obtained.[35,40,101] Based on the findings of our previous research, we determined that a protocol capturing a single image at each level would be the most efficient design for this study while still maintaining a high degree of reliability.[98]

After the baseline ultrasound examination, individuals completed a wheelchair propulsion task which was designed to stress the upper extremities to induce a physiological response which would be observed in the post ultrasound examinations. This propulsion task was a figure-eight course (see Figure 3) as described in our previous research.[102] A brief description is provided here. The propulsion consisted of individuals propelling their wheelchairs over a hard, smooth surface (i.e. tile floor) at a self selected maximum speed for a total of 12 minutes and included starting, stopping, straight propulsion, and left and right turns. We chose a self selected maximum speed in order to stress each individual to the maximum of their capabilities. The protocol included three 4-minute propulsion periods separated by 90 seconds of rest. Immediately after the third propulsion period was completed, individuals underwent a follow-up ultrasound examination during which images were collected every 5 minutes for 30 minutes.

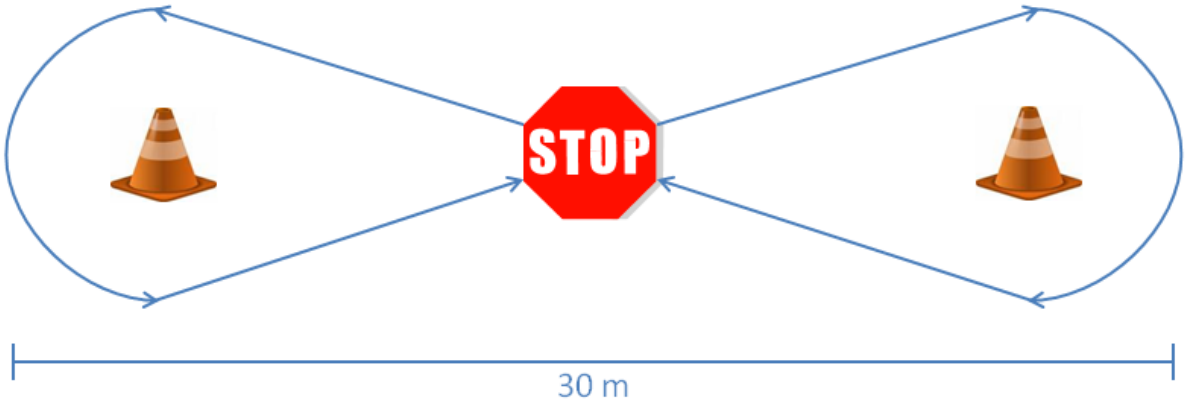

Figure 3. Schematic of over ground figure-eight propulsion course

3.2.3 Data Analysis

Since females comprised such a small portion of our population and comparisons between genders would not be valid, they were excluded from the analysis. We also excluded individuals with CTS (n=6) due to the unknown effects of surgery and other treatments on the median nerve response to activity, leaving us with a total of 44 participants. Because of difficulty imaging at the level of the hamate only 30 subjects were included in the analysis of median nerve characteristics at this level. Each ultrasound image was analyzed as described in our previous research.[98] In summary, we measured CSA and FR at each image level and calculated the SR based on the distal radius and pisiform CSAs, for a total of 7 variables. Based on previous work, we determined that a single investigator, analyzing each image once would be best suited for this study.[98] We analyzed each image by performing a boundary trace to calculate CSA and measuring the major and minor axes of the nerve in order to calculate the FR (major axis / minor axis). Figure 2 (in Chapter 2) shows an example of the boundary trace and major and minor axis selections. The investigator was blinded to the image time point, subject characteristics, and

presence of CTS symptoms. For all variables, percent change with respect to baseline was calculated at each time point.

3.2.4 Statistical Analysis

The data were first analyzed for normality and to appropriately address outliers. To evaluate the relationships between subject characteristics and baseline and acute change in median nerve variables we used Pearson's and Spearman's correlations where appropriate. Bonferroni correction was used to control for multiple comparisons. A repeated measures ANOVA was used to determine the effects of different subject characteristics on the post-acute median nerve response. To relate median nerve characteristics to symptoms of CTS, the BCTQ was used to dichotomize the population into two groups: asymptomatic (reporting no symptoms) and symptomatic (reporting any degree of symptoms). Based on previous research, we expected individuals signs and symptoms of CTS to show different median nerve responses to activity compared to asymptomatic, healthy individuals.[40,42] This dichotomization was also partly due to the nature of the questionnaire and the fact that many of the participants are asymptomatic. Performing any correlation analysis on the whole group using the BCTQ scores would be weakened by the many zero scores reported by the asymptomatic individuals. Differences between symptom groups with respect to baseline and immediate percent change in median nerve variables were assessed using independent samples and Mann Whitney t-tests where applicable. Using a mixed model, repeated measures ANOVA, we investigated the effects of symptoms and time post activity on median nerve characteristics. For each median nerve measure, the post activity percent change values at each time point were entered as the within-subjects factors and the presence/absence of symptoms was entered as the between-subjects

factor. Spearman's correlations were done in the symptomatic group to relate BCTQ scores to baseline and percent change in median nerve variables. The Holm-Bonferroni method was used to control for multiple comparisons.

As a secondary analysis we wanted to investigate the extremes of the acute change data, looking both at the distribution and the relationship to subject characteristics and symptoms of CTS. To categorize change groups we used the minimum detectable change (MDC_{NORM}) calculations which were developed from our reliability analysis of ultrasonographic median nerve characteristics (see Chapter 2).[98] This MDC would provide us with a 95% confidence interval of the standard error of measurement (SEM). Using this we could categorize participants who we were confident showed a change greater than the error associated with our measurements and those who we could not confidently detect changes in. We compared the two extreme groups, those showing either increases after activity or those showing decreases. This categorization was only done on the median nerve CSA variable as only 5 participants showed changes in FR outside of this 95% confidence interval. In theory, if the changes were due to random chance, we would have expected to see an even split between the groups. To determine if the distributions were significantly different from random chance, we performed a single sample chi-square analysis. We then used independent samples and Mann Whitney t-tests where applicable to investigate differences in age, BMI, duration of wheelchair use, and symptom scores between these groups. A significance level of $p<0.050$ was used for all statistical tests. All statistical analysis was performed using SPSS (SPSS Inc., Chicago, IL).

3.3 RESULTS

3.3.1 Participants

Forty-four participants were included in the analysis of this study. The reasons for using a manual wheelchair as the primary means of mobility included paraplegia (n=39), lower limb amputation (n=2), and other conditions (n=3). The average age, duration of wheelchair use, and BMI were 43.0 ± 11.5 years, 12.1 ± 10.7 years, and 25.6 ± 5.8, respectively. The dichotomization based on symptoms resulted in 18 subjects in the asymptomatic group and 26 in the symptomatic group.

3.3.2 Baseline Median Nerve Characteristics

Relationship to Subject Characteristics

There was a significant positive correlation between BMI and CSA at the radius ($r = 0.426$, $p = 0.004$) and between age and FR at the hamate ($r = 0.498$, $p = 0.004$). There were no significant correlations between duration of wheelchair use and baseline median nerve variables.

Relationship to Symptoms of CTS

There were no significant differences in baseline median nerve measures when comparing symptom groups (see Table 3). There were no significant correlations between symptom scores and baseline median nerve variables in the symptomatic group.

Table 3. Comparison of baseline median nerve characteristics between symptom groups

Nerve Measure	Image Level	Baseline Value Mean (SD)		P-value
		Asymptomatic	Symptomatic	
Cross Sectional Area	Radius	11.52 (3.47)	12.09 (2.75)	0.549
	Pisiform	11.59 (3.18)	11.76 (2.64)	0.738
	Hamate	13.22 (3.85)	13.98 (2.40)	0.506
Swelling Ratio	Pisiform / Radius	1.02 (0.14)	0.99 (0.18)	0.526
Flattening Ratio	Radius	3.92 (1.36)	3.38 (1.86)	0.268
	Pisiform	3.74 (1.56)	3.44 (1.28)	0.431
	Hamate	5.27 (1.35)	5.37 (1.10)	0.823

3.3.3 Acute Median Nerve Changes

Relationship to Subject Characteristics

The immediate changes in median nerve characteristics were not significantly correlated with BMI, age, or duration of wheelchair use.

Relationship to Symptoms of CTS

Individuals with symptoms of CTS showed significantly different percent change compared to the asymptomatic participants in our key variables of CSA at pisiform ($p=0.014$), FR at hamate ($p=0.022$), and a very strong trend towards a difference in SR ($p=0.0502$). For each of these variables, the change in the symptomatic group was in the opposite direction of the change in the asymptomatic group. Symptomatic participants showed a mean increase in CSA at the pisiform

and SR and a mean decrease in FR at the hamate while the asymptomatic group showed a mean decrease in CSA at the pisiform and SR and a mean increase in FR at the hamate. No other significant differences were found. Table 4 summarizes the differences between symptom groups with respect to mean percent change of each median nerve variable.

Table 4. Comparison of acute changes in median nerve variables between symptom groups

Nerve Measure	Image Level	Percent Change Mean (SD) Asymptomatic		Symptomatic		P-value
Cross Sectional Area	Radius	-1.93	(6.56)	-1.45	(8.48)	0.843
	Pisiform	-5.76	(8.81)	0.94	(7.88)	0.012*
	Hamate	4.34	(11.91)	-1.59	(10.58)	0.164
Swelling Ratio	Pisiform / Radius	-3.54	(10.76)	3.90	(13.66)	0.050†
Flattening Ratio	Radius	-3.11	(15.52)	1.96	(17.82)	0.331
	Pisiform	-6.30	(22.52)	-3.84	(24.46)	0.737
	Hamate	4.30	(16.69)	-10.18	(17.20)	0.029*

*Indicates a significant difference between symptom groups

†Indicates a trend towards a difference between symptom groups

3.3.4 Categorizing Acute Median Nerve Change

The chi-square analysis showed that the distribution between groups was not significantly different from an even distribution, although a mild trend may be appreciated at the radius and pisiform. Table 5 summarizes the distribution within each change group as well as the results of

the chi-square analysis. Comparison of subject characteristics and symptom scores between these two groups found no significant differences.

Table 5. Distribution of participants based on categorization of acute change in CSA

Image Level	Increase in CSA	Decrease in CSA	Chi Square p-value
Radius	**6**	**12**	**0.157**
Pisiform	**6**	**13**	**0.108**
Hamate	**6**	**7**	**0.782**

3.3.5 Post Acute Median Nerve Response

Relationship to Subject Characteristics

There were no significant trends over 30 minutes following propulsion or significant effects of subject characteristics on the post-acute median nerve response.

Relationship to Symptoms of CTS

There were no significant trends over time or significant effects of symptom group on the post-acute median nerve changes.

3.4 DISCUSSION

In this study we expected that subject characteristics which have been previously identified as risk factors for CTS (age, duration of wheelchair use, and BMI) would be significantly related to several of the baseline median nerve variables. While we found two significant relationships which were in the directions we expected, the overall association between median nerve characteristics and subject characteristic risk factors of CTS was rather limited. Upon investigating symptoms, we expected to find evidence of CTS in the baseline ultrasound images in the symptomatic group, but not in the asymptomatic group. Surprisingly, we found that both groups had very similar baseline characteristics.

Looking at acute median nerve changes we were unable to determine any significant relationship between change variables and subject characteristics. We did, however, find that the three most common median nerve ultrasound variables associated with CTS showed different and opposite immediate change in response to wheelchair propulsion when comparing symptomatic and asymptomatic participants. The fact that different symptom groups showed no baseline differences, but did have different median nerve changes after activity has interesting implications when using ultrasound as a diagnostic tool. When looking at individuals who are in the developing stages of CTS, they may not show typical ultrasound characteristics of CTS when imaging the median nerve at a single time point. Since CTS is a chronic condition, the median nerve may have begun to undergo minor physiologic changes resulting in symptoms, but has not changed enough to show ultrasonographic evidence of CTS. Adding a component to the examination which assesses the median nerve changes in response to a provocative activity may improve the diagnostic capabilities. This has also been suggested by previous research.[40]

From previous research we know that individuals with CTS typically have a larger pisiform CSA and larger SR and we found these variables increased in the corresponding direction after activity in participants with symptoms of CTS. It should be noted that while there was a significant difference in percent change in median nerve CSA at the pisiform between groups, the symptomatic group showed an increase just over 1% while the asymptomatic group showed a decrease of almost 6%. It could be that the normal nerve response to wheelchair propulsion is a decrease in size, due to the high compressive forces on the palm of the hand resulting in increased carpal tunnel pressures[78,79], while the nerves of individuals with CTS have begun to undergo minor physiologic changes such as ischemia and fibrosis[72-75] which prevented any decrease in size. Another possible explanation for the different responses between groups is that the symptomatic group altered their propulsion biomechanics due to the pain or other symptoms of CTS and these altered biomechanics resulted in a different median nerve response than the asymptomatic participants. Therefore, further investigation of wheelchair biomechanics and their effect on the median nerve response is necessary.

Several of the changes we found in this study are similar to previous studies assessing median nerve change after activity. Our symptomatic group showed the same direction of change in both CSA at the pisiform level and SR as the group with CTS in the study by Altinok et al., who investigated the acute median nerve response to bidirectional squeezing and twisting.[40] In this current study, both the symptomatic and asymptomatic groups responded in the same manner as our previous work looking at changes after a wheelchair sporting event, where we saw an increase in SR in individuals with physical examination signs of CTS and a decrease in those without. There were also some differences between our findings and the previous research, namely the asymptomatic group showing decreases in CSA at the pisiform

and radius levels, while Altinok and Massy both found increases in control subjects after activity. We believe that the higher impact associated with wheelchair propulsion compared to the lower impact activities of these other studies may account for the differences in the direction of CSA change in the asymptomatic and control groups.

The categorization of acute change resulted in what appeared to be an uneven distribution at the pisiform and radius levels, but the chi-square analysis showed that it was not statistically significant. Since there was a small number of participants ($n<20$) included in this portion of the analysis and the p-values were approaching a trend, more research is necessary to further investigate the distribution within these acute change groups. Future research may need to look at how the direction of acute change relates to the development of CTS over time or relates to wheelchair propulsion biomechanics.

We expected that after the initial response, subject characteristic risk factors for CTS and symptoms of CTS would affect the median nerve response over time following intense wheelchair propulsion. We were unable to find any significant trends beyond the initial median nerve response and found no significant effects of subject characteristics or symptoms on the post-acute median nerve response. It may be that a greater post-acute response does not occur until hours after the activity rather than minutes. Based on our findings and others who have studied the nerve response to activity, more research is necessary to determine the extended effects (over several hours) of wheelchair propulsion or other activities on the median nerve.

In this study we attempted to relate the baseline and acute median nerve change variables to the severity of symptoms of which the latter has not been done before. Baseline median nerve characteristics were not significantly related to symptom scores which is in line with previous research.[101] In addition, we were not able to determine any significant relationships between the

amount of change and the degree of symptoms. It is possible that a greater change is not associated with greater severity of symptoms, but that simply looking at the direction of median nerve response is necessary for determining the likelihood of symptoms. Further research is necessary to determine if there are other factors which may affect the amount of change that occurs in response to activity such as forces and postures. Investigation of the acute median nerve changes may be useful in identifying risk factors for CTS such as propulsion biomechanics, wheelchair setup, or investigating interventions such as ergonomic pushrims or propulsion training.

3.5 CONCLUSION

Studying a population at high risk for CTS, including individuals who may be in the developing stages of CTS, but not yet diagnosed with CTS, we found no baseline differences between symptom groups, but did find that the immediate median nerve response to activity visualized using ultrasound is related to the presence/absence of symptoms. Based on this study and previous research it appears that focusing on the immediate nerve response to activity may provide useful insight into the effects of an activity on the development of CTS. We have shown that there are several median nerve responses to wheelchair propulsion associated with symptoms of CTS. The next step is to determine if there are any characteristics of propulsion (i.e. force, repetition, posture) that may affect the median nerve response in a manner which has been associated with CTS.

4.0 MEDIAN NERVE CHARACTERISTICS BEFORE AND AFTER ACTIVITY RELATED TO WHEELCHAIR PROPULSION BIOMECHANICS

4.1 INTRODUCTION

Ergonomics literature states force, repetition (or cadence of an activity), and posture as the primary risk factors for musculoskeletal disorders. In a report of musculoskeletal disorders in the workplace, NIOSH (National Institute for Occupational Safety and Health) defined repetitive hand and wrist activities as those involving repeated hand/finger or wrist movements such as gripping or cyclical flexion/extension, ulnar/radial deviation, and supination/pronation. The effects of repetition can be magnified when combined with awkward postures or loading of the upper extremity such as occurs in wheelchair propulsion.[2] Work related CTS has been associated with high force and high repetition tasks, with a cadence greater than 2 cycles per minute and forces ranging from 10-40 N.[3] Wheelchair propulsion, with a stroke occurring approximately once per second and peak forces ranging from approximately 45-110 N, would exceed what the majority of studies consider a high force high repetition task.[20] With a cycle time of 1 second, if a wheelchair user propels for as little as 16 minutes, they would exceed the number of repetitions a factory worker in a high cycle task would complete in an 8 hour day.

Several studies have related upper extremity pathologies to wheelchair propulsion variables.[20,21,88] With respect to CTS, our previous research has found that wheelchair pushrim

forces are related to nerve conduction study variables.[20,21] We found that, when controlling for weight, there were correlations between median nerve function and the cadence of propulsion and rate and rise of the resultant force. We also found that a greater range of motion was associated with better median nerve function. Further analysis found that greater wrist range of motion was associated with greater pushrim contact angles, lower forces and lower cadence. By taking long strokes, wheelchair users are able to generate work without high peak forces. Longitudinal analysis of median nerve injury related wheelchair propulsion biomechanics, found that individuals who used greater force and cadence at their initial visit had greater progression in median nerve damage approximately three years later at a second visit. Once again, peak resultant force was a predictor of progression of nerve conduction study abnormalities.[88] Based on these studies it appears that forces may be more important contributors to median nerve health than wrist posture or range of motion.

We know from previous research (including Chapter 3) that the amount and direction of median nerve change in response to activity differs in individuals with CTS or symptoms of CTS compared to healthy controls.[40-42] Neither these studies nor other previous research, to our knowledge, has attempted to relate specific characteristics (such as force or posture) of an activity to acute changes in the median nerve. Understanding how the acute median nerve response relates to the characteristics of a task may be useful in determining the likelihood of developing CTS. In addition, modifying a task to reduce possible detrimental acute nerve changes may delay or prevent the onset of chronic nerve pathology such as CTS. Ultrasound provides the means necessary to assess this acute response because it can easily and quickly be used to gather information about median nerve characteristics before and immediately after an

activity. In this study we sought to relate both baseline and median nerve change variables to wheelchair propulsion characteristics including both kinetics and kinematics.

This study involved two parts: investigating pushrim propulsion kinetics during an over ground task and their relation to median nerve characteristics (Part I) and an investigation of wrist propulsion kinetics and kinematics at a steady state speed during dynamometer propulsion (Part II).

Part I - The analysis was focused on resultant force, cadence, and contact angle based on our previous research suggesting that long, smooth propulsive strokes are less detrimental to nerve health than short, high impact strokes.[20,21] We hypothesized that larger peak and rate of rise of resultant force, greater cadence, and smaller contact angle would correlate with a larger baseline CSA, SR, and FR. We also expected propulsion kinetics to relate to median nerve changes. Specifically, we expected greater peak and rate of rise of resultant force, higher cadence, and lower contact angle, to positively correlate with median nerve change in CSA at pisiform, SR, and FR at hamate. We further hypothesized that linear regression models combining resultant force, cadence, and contact angle would successfully predict baseline and median nerve change variables.

Part II - In this analysis, we expected wrist joint reaction force and wrist postures to be related to baseline and changes in median nerve characteristics. We hypothesized that greater peak wrist resultant force and greater peak joint angles would positively correlate with higher baseline and greater changes in median nerve CSA, SR, and FR.

4.2 METHODS

4.2.1 Participants

Forty-four participants that were evaluated before and after the figure-eight protocol described in Chapter 3 were included in Part I of this study. They were recruited at the 2007 and 2008 NVWG as well as through registries at HERL and provided written informed consent prior to participation. Part II included a subset (n=15) of these participants who propelled on a dynamometer at HERL. All participants were between ages 18 and 65 and had a non-progressive or non-degenerative disability which did not directly affect their upper extremity function. Participants were required to use a manual wheelchair beginning after the age of 18 as their primary means of mobility. Individuals were excluded if they reported traumatic injury to the wrist or a history of cardiovascular disease or another condition which could be exacerbated by intense physical activity.

4.2.2 Data Collection

Ultrasound images were obtained following previously described methods[98] (see also Chapter 2), both before and immediately after the figure-eight wheelchair propulsion task. For Part I, the Smartwheels (Three Rivers Holdings LLC, Mesa, AZ) were used to collect propulsion forces, velocity, and contact angle during the first full lap of each 4-minute trial of the figure-eight propulsion. For Part II, Smartwheels were used to collect forces while the Optotrak (Northern Digital Inc., Ontario, Canada) was used to collect three dimensional position of the non-dominant arm with markers placed on the third metacarpophalangeal joint, the ulnar and radial

styloids, the olecranon and the lateral epicondyle. Kinetic and kinematic data were collected for twenty seconds while participants propelled at a steady state, self-selected, comfortable velocity.

4.2.3 Data Analysis

The ultrasound variables used in this study included both baseline and percent change in CSA at pisiform, FR at hamate, and SR and were calculated as previously described.[98] For Part I, we chose to use the propulsion variables from the second 4-minute trial to eliminate the effects of learning which may have been present in the first trial and to eliminate the effects of fatigue which may have occurred during the third trial. We calculated pushrim biomechanics using only the straight propulsion segments excluding the acceleration and deceleration components associated with turns, starts and stops. The primary propulsion variables of interest included stroke frequency (or cadence), contact angle, and peak and rate of rise of resultant force. Since propulsion forces were highly correlated with both weight and velocity, all forces were normalized to these two variables. Previous research has shown that weight and propulsion forces are highly correlated and therefore controlling for weight is necessary.[21] Since individuals all propelled at a self-selected maximum velocity it was necessary to account for this in the analysis.

For Part II, participants propelled at a self-selected velocity as this would represent the way they typically propel their wheelchair on a daily basis. Using this information we could potentially identify any propulsion characteristics which may have lead to any baseline median nerve characteristics indicative of CTS. The kinetics and kinematics collected during the dynamometer propulsion were combined using inverse dynamics to determine the peak wrist

joint angles and peak wrist joint reaction force (again normalized to force and velocity).[103,104] We calculated peak wrist flexion/extension, ulnar/radial deviation and pronation/supination.

4.2.4 Statistical Analysis

The data were analyzed for normality and to appropriately address outliers. To determine if any of the key biomechanics variables were directly related to baseline or percent change in median nerve characteristics, Pearson's and Spearman rho correlations were used. For Part I the linear regression models included baseline and percent change in median nerve characteristics as the dependent variables, and peak resultant force, cadence, and contact angle as the independent variables. Peak rate of rise of resultant force was not included as it was highly correlated with peak resultant force. As a secondary analysis we wanted to investigate the extremes of the acute change data and the relationship to propulsion biomechanics. We categorized the change groups as previously discussed in Chapter 3, based on the minimum detectable change (MDC_{NORM}) from our reliability analysis of ultrasonographic median nerve characteristics (see Chapter 2).[98] We compared the two extreme groups, those showing either increases after activity or those showing decreases. This categorization was only done on the median nerve CSA variable as only 5 participants showed changes in FR greater than the MDC. We used independent samples and Mann Whitney t-tests where applicable to investigate differences in both kinetic and kinematics variables between these groups. A significance level of $p<0.05$ was used for all statistical tests. All statistical analysis was performed using SPSS (SPSS Inc., Chicago, IL).

4.3 RESULTS

4.3.1 Baseline and Acute Changes Related to Biomechanics

Part I - No significant correlations were observed between baseline or change in CSA at pisiform, FR at hamate, or SR with peak or rate of rise of resultant force, cadence, or contact angle. There was a strong negative trend (r=-0.361, p=0.0502) between baseline FR at hamate and contact angle (see Figure 4). None of the linear regression models significantly predicted baseline or percent change in median nerve variables.

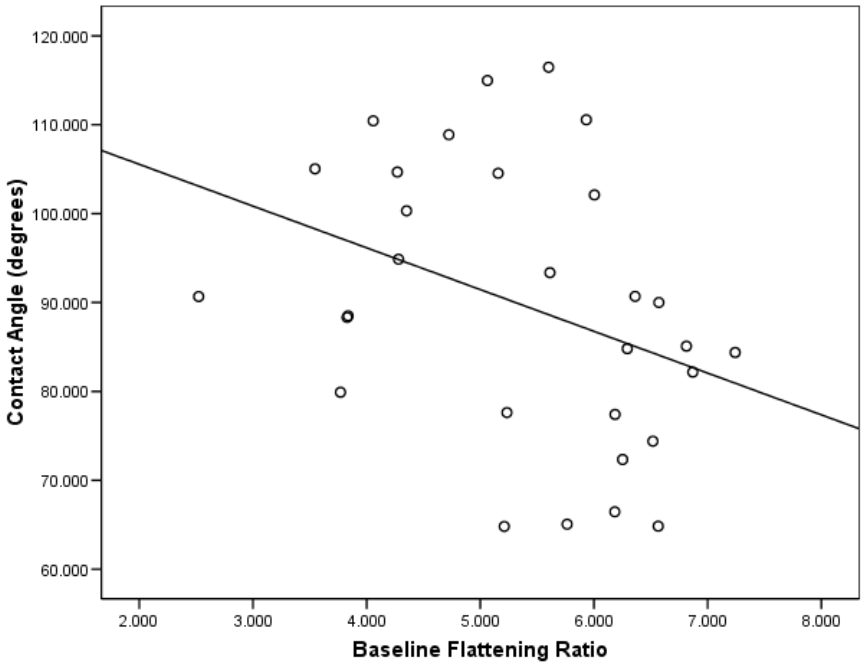

Figure 4. Scatter plot of pushrim contact angle vs. baseline FR at the hamate

Part II - No significant correlations were observed between baseline or change in CSA at pisiform, FR at hamate, or SR with peak or rate of rise of resultant force or peak joint angles.

4.3.2 Categorization of Acute Median Nerve Changes

Comparing biomechanics variables between the different acute change groups resulted in no significant findings.

4.4 DISCUSSION

Individuals who use a manual wheelchair as their primary means of mobility are at high risk for developing CTS. Given the nature of everyday wheelchair use and ergonomics literature suggesting that high-force, high-repetition activities lead to CTS, we expected that wheelchair propulsion characteristics such as force, repetition, and posture would be correlated with baseline median nerve characteristics previously related to CTS. We also expected the median nerve response to activity to be related to propulsion characteristics.

To our knowledge this was the first attempt to relate median nerve ultrasound characteristics before and after a provocative activity to specific characteristics of that activity. Based on our previous research[20,21] we hypothesized that greater forces, cadences, contact angle, and peak joint angles would correlate with baseline and median nerve changes more indicative of CTS, but this was not the case. We were unable to determine any significant relationships between propulsion variables and baseline median nerve variables or median nerve response to activity. We did however see a strong trend between baseline FR at the hamate and contact angle. The direction of this relationship is what we would expect based on our previous research suggesting that short, high impact strokes are more detrimental to nerve health[20] and research linking increased FR at the hamate to CTS.[22,23,35,39] An increased CSA at the pisiform is the

most common median nerve ultrasound characteristic related to CTS. Furthermore, in individuals with CTS or symptoms of CTS the CSA at the pisiform has been shown to increase after provocative activities[40,41] including wheelchair propulsion as seen in Chapter 3. Surprisingly there was no relationship between baseline or change in CSA at the pisiform and propulsion kinetics and kinematics. Even through categorization of the extremes of change we were unable to determine any significant findings between median nerve changes and propulsion biomechanics. More research is needed to determine the exact cause of the acute median nerve response and if other characteristics of wheelchair propulsion may contribute to the response.

It should be noted that, based on our previous research suggesting that kinetics variables may be of greater significance than kinematics[20], our top priority in this study was the assessment of propulsion kinetics related to median nerve characteristics. Therefore we only placed a small emphasis on the collection of kinematics in this research. One possible explanation for the lack of significant findings regarding the kinematics is that this portion of this study occurred on a dynamometer at a self selected, comfortable velocity, and therefore the kinematics may have been different from those used during the provocative wheelchair propulsion task. Previous research has shown that wrist biomechanics differ between different propulsion speeds[105] and the mean velocities in this study were 0.47 m/s on the dynamometer compared to 1.59 m/s during the over-ground figure-eight propulsion task. Furthermore, due to limitations in subject recruitment the kinematic data in this study only included 15 subjects. Additionally, due to limitations in kinematic equipment and the impracticality of collecting kinematics data at the NVWG our ability to fully assess kinematics during provocative wheelchair propulsion and relate this to median nerve changes after activity was hindered. Since pushrim kinetics variables did not result in any significant findings, it may be of interest to

elaborate on the research protocols used here and fully assess the kinematics used during a wheelchair propulsion task and relate them to median nerve changes.

There are several possible explanations for the lack of significant findings in this study. First of all, the relatively small sample size could result in greater variability in the data. Future studies with larger sample sizes are needed to reduce this potential variability. In addition, it is possible that the greatest changes in the median nerve occur chronically rather than acutely and studying ultrasound characteristics of the median nerve over months or years related to propulsion biomechanics may lead to some significant findings. Another possible explanation for the lack of significant findings could be the nature of the figure-eight course. Since we asked participants to propel at their maximum self selected velocity, the propulsion kinetics that were measured may have been different than the way they typically propel during everyday propulsion. Since the everyday propulsion is likely a contributor to the development of CTS, future research could focus on the biomechanics of a provocative propulsion task more similar to everyday propulsion and their effects on median nerve response. It may also be possible that forces applied to the pushrim during propulsion are not the critical variables affecting the median nerve response. Future studies may need to investigate other features related to everyday wheelchair use and their effect on median nerve health such as wheelchair setup or transfer biomechanics or other genetic or physiology factors. Research has shown that changes can be made to the wheelchair that will impact biomechanics and offer the potential for intervention.[106] It may be of interest to study how various interventions such as different wheelchair setups, ergonomic pushrims, and/or propulsion training alter both biomechanics and the acute median nerve response.

4.5 CONCLUSION

In this study we were unable to relate the common biomechanical risk factors for CTS including force, repetition, and posture to median nerve characteristics before and after strenuous wheelchair propulsion. More research is needed to determine the specific characteristics of wheelchair propulsion and other activities on the acute median nerve response.

5.0 DEVELOPMENT AND ASSESSMENT OF ALGORITHMS FOR DETERMINING MEDIAN NERVE DISPLACEMENT AND DEFORMATION DURING FINGER MOVEMENT

5.1 INTRODUCTION

Ultrasound is commonly used in the diagnosis of CTS by assessing static images of the median nerve and carpal tunnel anatomy.[22-24,28-36] In addition to capturing static images, ultrasound has the capability to capture real time anatomical motion. Research on the displacement of the median nerve and tendons of the carpal tunnel has shown that hand, wrist, and finger movements affect median nerve strain and suggest that repetitive wrist and finger activities over time may lead to pathological changes in the nerve (e.g. CTS).[48-50,89,90] Nakamichi used ultrasound to measure the transverse sliding of the median nerve during passive flexion and extension of the fingers in individuals with CTS and controls. They found less nerve movement present in individuals with CTS compared to unaffected controls.[49] A study by Erel investigated both longitudinal and transverse nerve sliding during passive finger extension in individuals with CTS and controls. They used a cross-correlation algorithm for determining longitudinal sliding, while transverse measurements were done by simply comparing the pre-extension and post-extension images. They also found less transverse nerve sliding in individuals with CTS.[48]

At the time this research study was conducted, we were unable to find any research on how the median nerve both moves and deforms during an active gripping task. Determining how the median nerve moves and deforms at the wrist may be useful in understanding the pathophysiology of CTS and may also be useful diagnostically. The objective of our study was to obtain a dynamic measure of median nerve entrapment and compression using the capabilities of ultrasound in that it can capture real-time, in vivo, anatomical motions within the carpal tunnel resulting from finger movements. While it may be possible to simply watch an ultrasound movie and determine where the extremes of displacement occur, it would be rather difficult to visually determine where the peaks of deformation occur, thus the need for a method to analyze videos that minimizes analysis time while still providing accurate measures.

In this paper, we compared three algorithms in order to determine which one would provide the best balance between accuracy and analysis time. These algorithms included a semi-automated algorithm and two interpolation algorithms. This chapter will describe the methodology behind each of these algorithms as well as a comparison of each with the results of a manual trace which will serve as the "gold standard".

5.2 METHODS

5.2.1 Development of Algorithms

A video was loaded into Matlab and the first frame was analyzed to determine the median nerve location and shape characteristics which would be used as the reference point for all deformation and displacement calculations. In order to accurately quantify nerve displacement, it had to be

calculated with respect to a rigid structure. To accomplish this, we drew a rectangle around a bony landmark which remained visible for the duration of the video. The coordinates of the bottom right point of the rectangle were used as the reference point for calculating median nerve displacement. After the bony landmark was identified in the first frame of the video, the median nerve was traced using a series of twelve vertices. Using twelve points we could easily outline the typical nerve shapes ranging from an elongated ellipse to a more circular shape. The basic configuration consisted of three points defining each side of the nerve (ulnar, radial, palmar, and dorsal) with each having a vertex at the approximate center and the other two points varying based on the nerve shape. For a circular shaped nerve, the vertices would be more evenly spaced all around the nerve, while in an ellipse, the sharply curved ulnar/radial edges would have three vertices close together and vertices along the palmar/dorsal sides would be spaced further apart. Figure 5 shows circular, and normal and elongated elliptical examples of how the median nerve was outlined using twelve points.

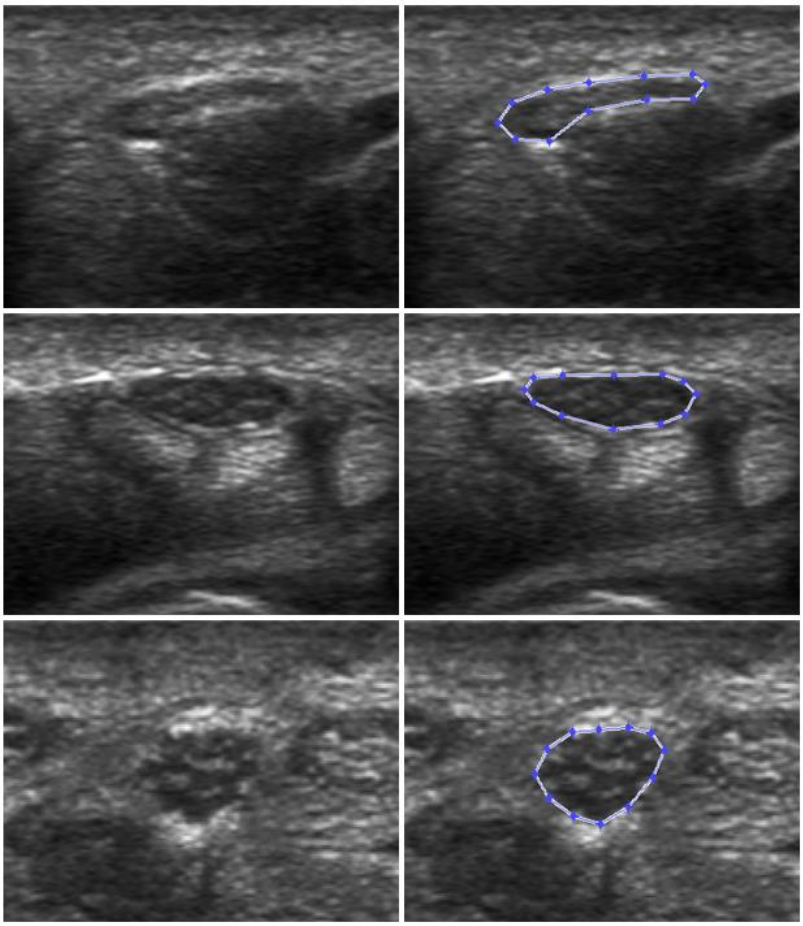

Figure 5. Examples of the twelve point boundary traces for common median nerve shapes

After analyzing the first frame of each video, every tenth frame of the video was analyzed by selecting both the bony landmark and the twelve vertices outlining the median nerve. Using a cubic spline interpolation we estimated the coordinates of the bony landmark and median nerve vertices for each frame of the video in between those that were analyzed manually. The interpolation algorithm was done two ways: (1) using each of the analyzed frames (i.e. every tenth frame of the video) and (2) using every other analyzed frame (i.e. every twentieth frame of the video). These two algorithms will be referred to as INTERP-10 and INTERP-20, respectively throughout the remainder of this paper. The third algorithm we used was a semi-

automated algorithm which took the output from analyzing the first frame of the video and attempted to automatically track the median nerve using a combination of cross-correlation and techniques designed to detect the borders of the nerve. The following is a detailed description of this algorithm.

The bony landmark selection and median nerve selection from the first frame were independently cross-correlated with the second frame of the video to find the most probable coordinates of the bone and nerve in the second frame. The first step in the cross-correlation process was to store the pixel grayscale values of the second frame of the video in the matrix *I* which has *x* rows and *y* columns. The grayscale values of the template (either the bony landmark or the median nerve selection from the first frame) are stored in matrix *T,* which is *M* rows by *N* columns. To calculate the position of the template, *T*, in the image, *I*, the normalized cross-correlation, *C*, is calculated at each point (*i, j*) for *I* and *T* (which is shifted by *i* steps in the *x* direction and *j* steps in the *y* direction). This is represented mathematically as:

$$C(i,j) = \frac{\sum_{x,y}\left(I(x,y) - \bar{I}(i,j)\right)\left(T(x-i,y-j) - \bar{T}\right)}{\sqrt{\sum_{x,y}\left(I(x,y) - \bar{I}(i,j)\right)^2 \sum_{x,y}\left(T(x-i,y-j) - \bar{T}\right)^2}}$$

The term $\bar{I}(i,j)$ represents the mean value of $I(x,y)$ within the area of the template shifted to (i,j) and is calculated

$$\bar{I}(i,j) = \frac{\sum_{x=i}^{i+M-1}\sum_{y=j}^{j+N-1} I(x,y)}{M \cdot N}$$

The maximum value of the normalized cross-correlation matrix will occur where the template best aligns with the next frame of the video. In order to decrease computation time, the template is not cross-correlated with the entire image, but rather a smaller region of interest which is determined by pre-screening each video to determine the approximate extents of bony landmark and nerve movement. In addition, the frame to frame movement was constrained to a realistic range. This not only decreases computation time, but also improves accuracy as the algorithm will not falsely detect structures similar to the nerve, which are outside the carpal tunnel.

The cross-correlation results were used to create a new bony landmark from frame two, using the same size rectangle as in frame one since the bone is rigid and does not change shape or size. Because the median nerve can change shape and size the new median nerve selection was more complicated and required application of techniques to automatically identify the borders of the nerve. To do this we first found five key points, which we will refer to as foci, within the borders of the nerve based on the twelve vertices outlining the nerve (see Figure 6), panel 1). The far ulnar/radial foci (A and E) were determined by averaging coordinates of the three points defining the radial (8, 9, 10) or ulnar (2, 3, 4) nerve border. Each of the middle three foci (B, C, D) was determined by averaging the coordinates of the two points (7 and 11, 6 and 12, or 1 and 5, respectively) on the palmar and dorsal sides. The coordinates of these points were then shifted based on the results of the cross-correlation algorithm. Figure 7, Step 1 shows a schematic demonstration of an exaggerated shift of these points from one frame to the next. From these new points, we searched outward for the borders of the nerve (see Figure 6, panel 2 and Figure 7, Step 2).

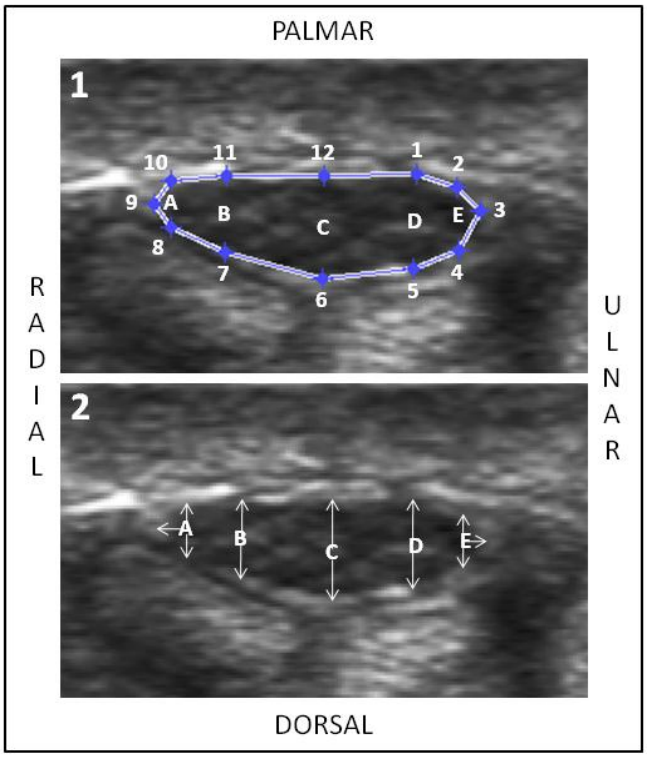

Figure 6. Example images showing the key points used to identify the median nerve borders

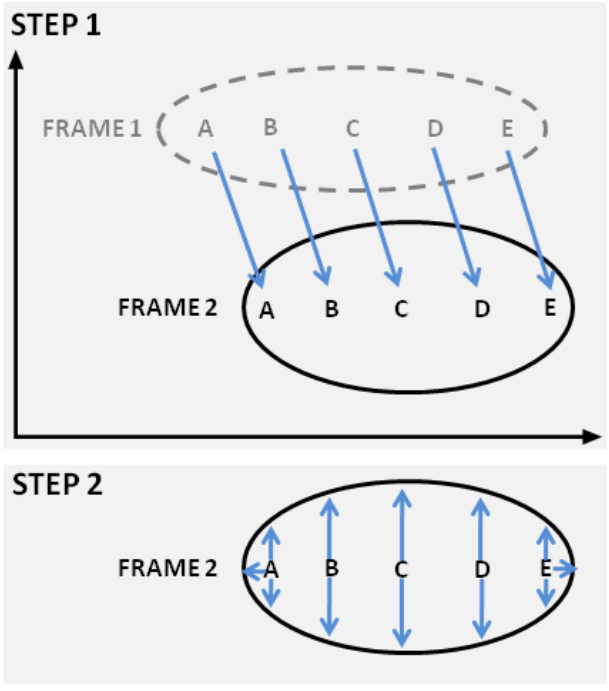

Figure 7. Schematic examples of an exaggerated median nerve shift between two video frames (step 1) and boundary identification techniques (step 2)

When searching for the borders of a nerve we used a band of pixels which was centered at one of the foci and moved outward along one dimension (either ulnar/radial or palmar/dorsal) towards one of the borders of the nerve. Using twelve bands, we identified twelve new vertices outlining the nerve. Foci E and A were used to determine the far ulnar/radial vertices, respectively, and each foci was used to determine the palmar/dorsal vertices directly above or below itself. Each band varied in length and contained eleven one-pixel wide vectors. Each band began at a focus and continued outward ten pixels beyond the location of the previous vertex, thus the varying length of each band (see Figure 8, panel 1). Within each vector, a three pixel blur was applied to reduce false edges by averaging each pixel with the two neighboring pixels. Since the nerve is darker inside and has a brighter hyperechoic border we searched outward for the peak pixel intensity within each vector (see Figure 8, panel 2). Combining the results from each vector we determined the most likely border of the nerve and thus the location of the new vertex. This process was repeated for each of the remaining twelve vertices, creating a new median nerve selection.

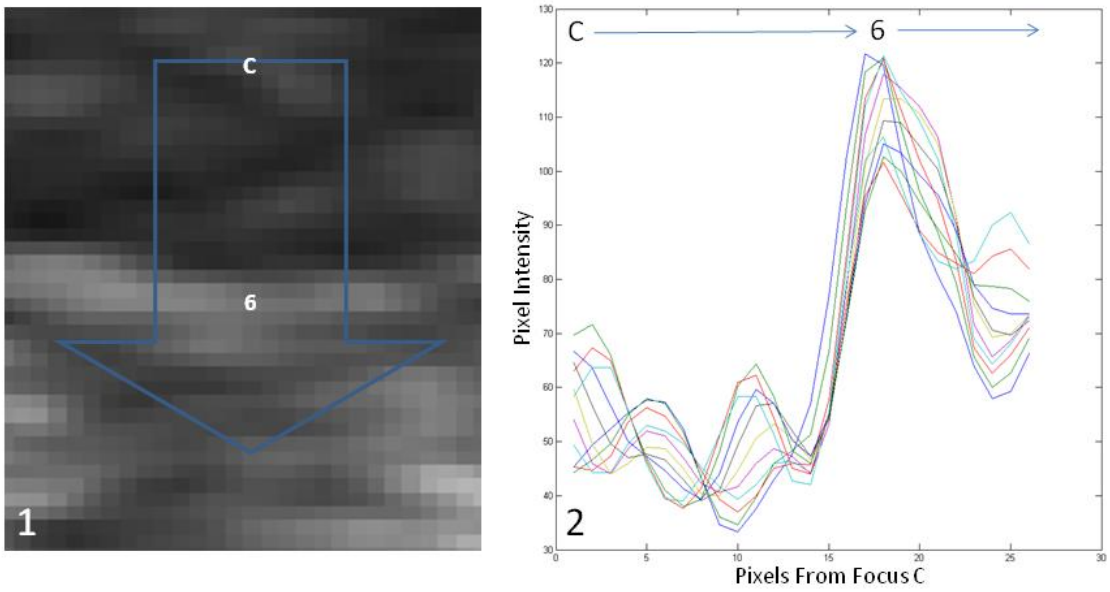

Figure 8. Magnified image and graphical representation of the edge of a nerve

Using the new median nerve and bony landmark selections, the process was repeated beginning by cross-correlating the new selections with the next frame of the video. This process continued for each successive frame of the video. Given the nature of our videos, specifically the constantly changing median nerve, it was not easily feasible to create a fully automated algorithm and therefore an investigator was required to check the algorithm periodically to confirm that the program was accurately tracking the nerve and correct it when necessary, thus making it semi-automated. At every tenth frame the user was prompted with a display of the current video frame, and the current median nerve and bony landmark selections. The investigator was prompted to confirm that the current selections were correct and on track, or manually update the selections if necessary. Once all frames of the video were processed, a weighted, smoothing filter was applied so that the confirmed/corrected frames were weighted higher than the automatically evaluated frames in between every tenth frame.

5.2.2 Data Collection

Five participants with no history of carpal tunnel syndrome, who provided IRB approved consent, underwent dynamic ultrasound examination at two levels of the wrist: the distal radius and pisiform levels. Using the Philips HD11 XE ultrasound machine (Philips Medical Systems, Bothell, WA), equipped with a 5-12 MHz linear array transducer, videos of transverse movement of the median nerve were captured at each wrist level. Participants began with the hand open and fingers relaxed while the video capture began. Participants were then instructed to fully flex the fingers forming a loose fist and then fully extend the fingers returning to an open hand posture. While capturing the videos, focus was placed on limiting probe movement and ensuring

that the bony landmark of interest remained visible. Videos were captured at a frame rate of 33 Hz.

5.2.3 Data Analysis

Each video was processed using the three different algorithms in order to determine the vertices outlining the nerve for the first 100 frames of the video. Using these vertices we calculated the median nerve CSA, FR, and centroid coordinates for each frame. In order to assess accuracy, each algorithm was compared to a manual trace at several time points throughout the video. At every fifth frame of the video a manual analysis of the video was done to determine the location, size and shape of the nerve. A difference variable was calculated between the manual trace and each of the different algorithms at this frame. For deformation variables (CSA and FR) we calculated a percent difference while displacement difference was calculated in millimeters. This was repeated at every fifth frame for the first one hundred frames of the 10 videos. We calculated the difference in pixels for the ulnar/radial, palmar/dorsal, and resultant offsets of each algorithm with respect to the manual trace. Additionally, we calculated the percent difference in CSA and FR between the manual trace and each algorithm. Figure 9 shows a graphical representation of the CSA and ulnar/radial displacement curves of the three different algorithms and the manual trace plotted with respect to video frame number.

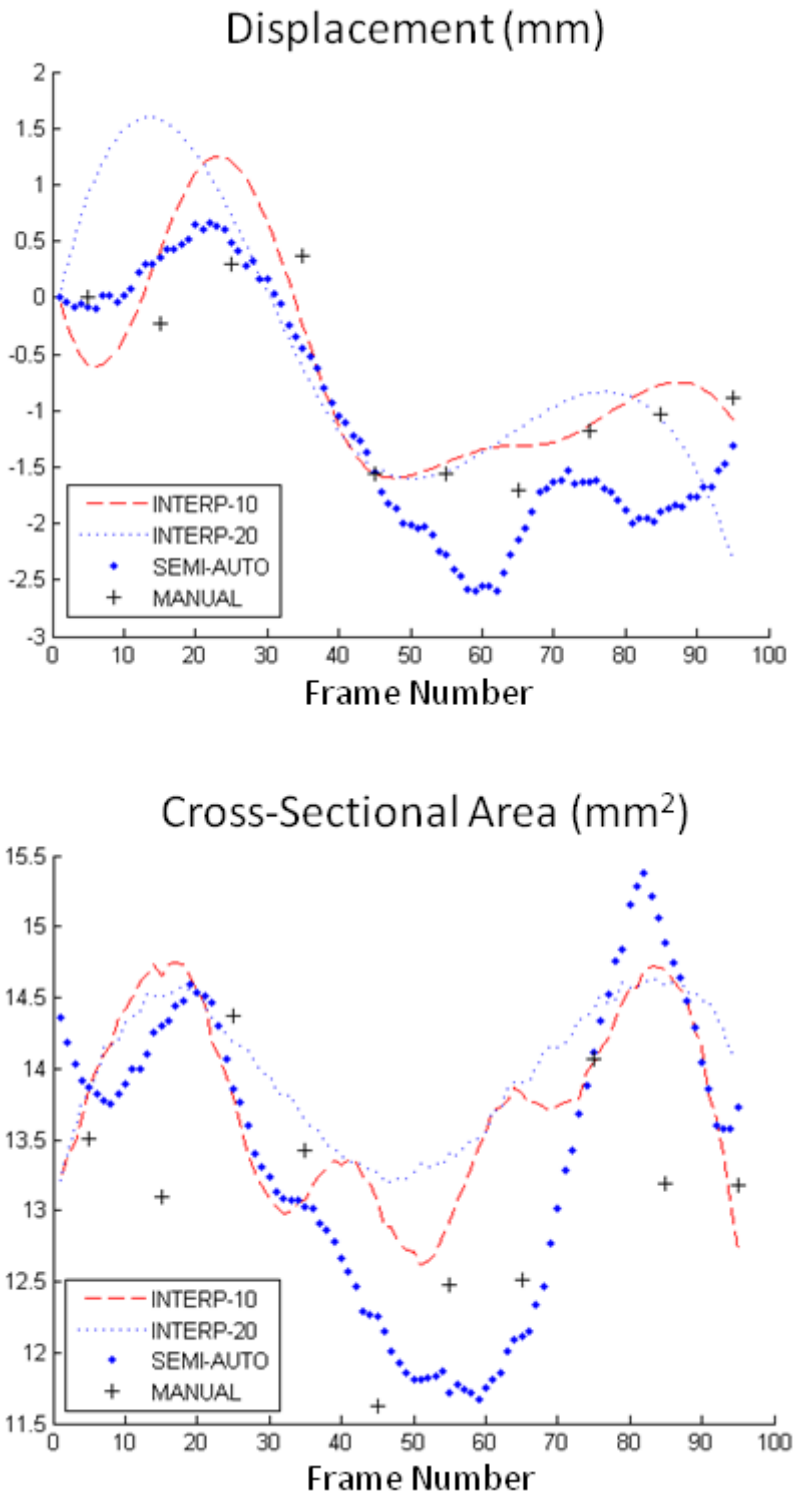

Figure 9. Graphical representation of the cross-sectional area and displacement curves for the three different algorithms and the manual trace

5.3 RESULTS

Compared to a manual trace, we found that the INTERP-10 algorithm resulted in the least percent difference in displacement variables, while the INTERP-20 and semi-automated showed the least percent difference in deformation variables of CSA and FR, respectively. Table 6 summarizes the mean findings at each level as well as the total averages of all ten videos.

Table 6. Displacement and deformation differences between a manual trace and three different algorithms

Wrist Level	Variable		Semi-Automated	INTERP-10	INTERP-20
Radius	Displacement Difference (mm)	Ulnar/Radial	0.57	0.30	0.41
		Palmar/Dorsal	0.17	0.15	0.24
		Resultant	0.56	0.31	0.45
	Deformation Difference (%)	CSA	16.49	11.14	11.4
		FR	7.68	7.76	9.97
Pisiform	Displacement Difference (mm)	Ulnar/Radial	0.43	0.36	0.75
		Palmar/Dorsal	0.13	0.12	0.23
		Resultant	0.46	0.40	0.48
	Deformation Difference (%)	CSA	15.68	14.34	13.45
		FR	7.32	9.50	7.88
Total	Displacement Difference (mm)	Ulnar/Radial	0.50	0.33	0.58
		Palmar/Dorsal	0.15	0.14	0.23
		Resultant	0.51	0.36	0.46
	Deformation Difference (%)	CSA	16.09	12.74	12.42
		FR	7.50	8.63	16.09

5.4 DISCUSSION

Overall, INTERP-10 showed the best accuracy, followed by the semi-automated algorithm and lastly INTERP-20. While INTERP-10 was slightly more accurate overall it also required the most user input/time to analyze a video. Analyzing every tenth frame (i.e. 10% of the total video frames) required twice as much user input as analyzing every twentieth frame (i.e. 5% of the total frames) which required slightly more time than the semi-automated algorithm. Based on the number of times the semi-automated algorithm needed to be corrected/updated in this accuracy assessment, only 4.7% of the total frames needed to be analyzed. Given this reduction in user input coupled with only a marginal improvement in accuracy when using INTERP-10, we feel the semi-automated approach would be best suited for our future endeavors in assessing median nerve deformation and displacements in larger populations. Compared to INTERP-10, the semi-automated algorithm could significantly reduce the total number of frames that need to be analyzed over the course of all the videos analyzed in a larger study population. Unfortunately we did not measure processing time as a part of this study, but this would be something to consider for future applications of these or similar methods

It should be noted that some of the differences between the algorithms and the manual trace are fairly large (approximately 15%). One possible explanation for this is that the algorithms have information about the future movement and deformation of the nerve and the anticipation of these changes could lead to differences between the manual trace and the algorithms. Furthermore, because the semi-automated algorithm works on a pixel to pixel basis it may actually be more accurate than a visual manual trace which is not conducted under the magnification where you can compare two adjacent pixels. Thus a visual trace slightly "blurs" the edges and the trace may select a vertex that is a few pixels different from the algorithm. If

each vertex is different by a few pixels this could result in rather different CSA, and FR measurements.

Some limitations of this study include a small number of subjects and rather basic image processing techniques. Including more subjects would reduce data variability and provide better insight into the accuracy of these algorithms. Regarding image processing, we had originally planned to approximate the derivative of the pixel intensity curves (see Figure 8, panel 2), but simply using the peak pixel intensity provided a simple and accurate determination of the nerve edge. Adding an approximate derivative component and combining this with the peak pixel intensity may improve accuracy in detecting the nerve borders by reducing false edges associated with spikes in the pixel intensity as a result of non-uniformity of the median nerve and its surroundings.

5.5 CONCLUSION

In conclusion we have developed algorithms which are capable of obtaining valuable information from an ultrasound movie of median nerve motion without having to manually analyze every frame of each movie. While an interpolation algorithm was the most accurate in this study, the semi-automated algorithm provided the best balance between accuracy and user input. These algorithms can be applied to future research hoping to assess median nerve deformation and displacement within the carpal tunnel while performing various hand, wrist and finger activities.

6.0 MEDIAN NERVE DISPLACEMENT AND DEFORMATION DURING FINGER MOVEMENT RELATED TO SUBJECT CHARACTERISTIC RISK FACTORS AND SYMPTOMS OF CARPAL TUNNEL SYNDROME

6.1 INTRODUCTION

Carpal tunnel syndrome is the most common entrapment neuropathy, resulting in pain, numbness and weakness in the hands and fingers. There are several theories regarding the cause of CTS. A common one is compression of the median nerve within the carpal tunnel.[57,58] Studies have shown that increased intracarpal canal pressures are a causal factor in the development of median mononeuropathy at the wrist.[17,59-63] Increased canal pressures can affect median nerve perfusion leading to the numbness, tingling, and weakness associated with CTS. Compared with individuals without CTS, research shows that those with CTS have higher intracarpal canal pressures.[56,61,62,64] Research has also shown that active gripping with the hands increases the carpal canal and intraneural median nerve pressures.[61,65-69] Okutsu et al found that carpal canal pressures nearly tripled when comparing a resting position to an active power grip.[66] Werner studied the changes in carpal tunnel pressures between relaxed hand, closed fist, and pinch grip and found increased pressures during closed fist and pinching compared to a relaxed hand posture.[65] Seradge et al. and Luchetti et al. both studied carpal tunnel pressures in individuals with CTS and controls for various hand and wrist postures and found greater pressures in CTS

patients and increased pressures when making a fist.[68,69] Repetitive hand activities may lead to increased carpal canal pressures due to synovial thickening[56] which has been found in cadaver studies at the entrance and exit regions of the carpal tunnel.[70] In addition to ischemic factors, direct mechanical trauma to the median nerve plays a role in the pathophysiology of CTS.[55] During extremity movement, gliding between peripheral nerves and neighboring tissues is necessary to minimize traction and reduce compression on nerves.[71] Fibrosis or edema in the connective tissues surrounding the nerve may hinder nerve gliding and result strain or compression of the nerve ultimately leading to dysfunction.[72-75]

Ultrasound has been shown to be a very precise method of viewing the anatomy of the carpal tunnel and median nerve.[32] By capturing static images and primarily measuring the median nerve CSA,[22-39] ultrasonography has become a popular diagnostic tool due to its non-invasiveness, shorter examination time, and lower cost. In addition to these features, ultrasound has the capability to capture real time anatomical motion. Research on the displacement of the median nerve and tendons of the carpal tunnel has shown that hand, wrist, and finger movements affect median nerve strain and suggest that repetitive wrist and finger activities over time may lead to pathological changes in the nerve (e.g. CTS).[48-50,89,90] Nakamichi used ultrasound to measure the transverse sliding of the median nerve during passive flexion and extension of the fingers in individuals with CTS and controls. They found less nerve movement present in individuals with CTS compared to unaffected controls.[49] A study by Erel investigated both longitudinal and transverse nerve sliding during passive finger extension in individuals with CTS and controls. They used a cross-correlation algorithm for determining longitudinal sliding, while transverse measurements were done by simply comparing the pre-extension and post-extension images. They also found less transverse nerve sliding in individuals with CTS.[48]

At the time this research study was conducted, we were unable to find any research on how the median nerve both moves and deforms during an active gripping task. Recently, we found two studies with objectives similar ours. Yoshii et al. studied the relative median nerve displacement as well as changes in CSA, aspect ratio (similar to the FR), perimeter (PERIM), and circularity (CIRC) by comparing the median nerve at a starting, resting position to a posture with the fingers fully flexed, or a fist position.[51] Van Doesburg et al. investigated the same variables as Yoshii, but compared full extension to full flexion of both the index finger and the thumb.[91] Determining how the median nerve moves and deforms at the wrist may be useful in understanding the pathophysiology of CTS and may also be useful diagnostically. The objective of our study was to obtain a dynamic measure of median nerve entrapment and compression by taking full advantage of the capabilities of ultrasound in that it can capture real-time, in vivo, anatomical motions within the carpal tunnel resulting from finger movements. In order to quantify displacement and deformation, we developed a novel method, combining a cross-correlation algorithm and techniques for identifying the borders of the nerve, to analyze transverse median nerve movement and morphology changes throughout the duration of a video, rather than comparing two static images captured at different postures.

This study consisted of a subsample of the participants in our previous work (Chapter 3) so our first step was to determine if same findings with respect to subject characteristics and baseline median nerve characteristics held true in this smaller subsample. Based on the findings in Chapter 3, we hypothesized that there would be a significant positive correlation between CSA at the radius and BMI and between FR at the hamate and age. We also examined all other median nerve variables (CSA and FR at each level and SR) to determine any other potential relationships with subject characteristics including age, BMI, and duration of wheelchair use.

We also reexamined the effect of symptoms on baseline median nerve characteristics, by comparing symptom groups. Based on the the results of Chapter 3, we did not expect to see any significant differences between groups at baseline. Next, we anticipated that adding a dynamic component to the baseline examination might detect differences amongst symptom groups where static images could not. We hypothesized that individuals with symptoms of CTS would show decreased movement and increased peak deformation indicative of compression during finger movements compared to asymptomatic individuals. Specifically, we hypothesized that individuals with symptoms would show less displacement, a greater decrease in CSA and a greater increase in FR. In addition, we expected that displacement and compression (deformation) of the median nerve would be related to BMI, age, and duration of wheelchair use, and greater severity of symptoms in the symptomatic group. Specifically, we hypothesized that BMI, age, duration of wheelchair use, and symptoms scores would negatively correlate with median nerve displacement, and positively correlate with peak decrease in CSA and peak increase in FR.

6.2 METHODS

6.2.1 Participants

Twenty-eight participants (a subset of the 44 presented in Chapter 3) participated in this study. They were recruited at the 2008 NVWG as well as through registries at HERL and provided written informed IRB approved consent prior to participation. All participants were between ages 18 and 65 and had a non-progressive or non-degenerative disability which did not

directly affect their upper extremity function. Participants were required to use a manual wheelchair beginning after the age of 18 as their primary means of mobility. We chose to study wheelchair users as they are a population at high risk for developing CTS.[13,16-18,82] Individuals were excluded if they reported traumatic injury or surgery to the wrist which may have altered the wrist anatomy or dynamics of the carpal tunnel contents during activity of the hands and fingers.

6.2.2 Data Collection

Using the Philips HD11 XE ultrasound machine (Philips Medical Systems, Bothell, WA), equipped with a 5-12 MHz linear array transducer, static images of the median nerve were captured as described in our previous research[98], with imaging of the median nerve at three levels of the wrist (distal radius, pisiform, and hamate). Briefly, images were collected while participants maintained a seated posture with upper arm relaxed, fully adducted with no internal/external rotation and elbow flexed at 90 degrees with the forearm supported. The forearm was supinated with the wrist at neutral and fingers relaxed. The image levels collected are easily viewed using ultrasound, and nerve characteristics at these locations have been linked to CTS.[22-39] After the static images were collected, videos of transverse movement of the median nerve were captured at two levels of the wrist (the distal radius, and the pisiform). Participants began with the hand open and fingers relaxed while the video capture began. Participants were then instructed to fully flex the fingers forming a loose fist and then fully extend the fingers returning to an open hand posture. While capturing the videos, focus was placed on limiting probe movement and ensuring that the bony landmark of interest remained visible. Videos were

captured at a frame rate of 33 Hz. A single investigator performed all ultrasound data collection to reduce variability.[98]

In addition to the ultrasound examination, participants provided subject demographics information and completed the Boston Carpal Tunnel Questionnaire (BCTQ) developed by Levine. We chose to use this questionnaire because it is the most commonly used outcome measure for assessing CTS patients[100] and was shown to have high reproducibility (Pearson's correlation of 0.90), internal consistency (Cronbach's alpha of 0.89), validity, and sensitivity to clinical change.[52] Furthermore the BCTQ has been used to assess severity of symptoms in MWU[19] and related to ultrasound measures of the median nerve.[101]

6.2.3 Data Analysis

Each static ultrasound image was analyzed as described in our previous research.[98] In summary, we measured CSA and FR at each image level and calculated the SR based on the distal radius and pisiform CSAs, for a total of 7 static median nerve variables. Based on previous work, we determined that having a single investigator analyze all ultrasound data would be best suited for this study.[98] Videos were loaded into Matlab and analyzed using a specially designed program to quantify the dynamic median nerve characteristics of displacement and deformation. While it may be possible to simply watch a video and determine where the extremes of displacement occur, it would be rather difficult to visually determine where the peaks of deformation occur, thus the need for a method to analyze videos that minimizes analysis time while still providing accurate measures. In addition, simply comparing images at two different postures may miss the extremes which could occur in between the two endpoints of a movement. Figure 10 provides an example of this taken from a single video. It shows the curves

of displacement and CSA throughout a full fist cycle, starting with relaxed fingers, followed by flexion to make a loose fist and then extension, returning to a relaxed posture. It can be clearly seen that the peaks of the CSA and displacement occur outside of the relaxed or closed fist postures.

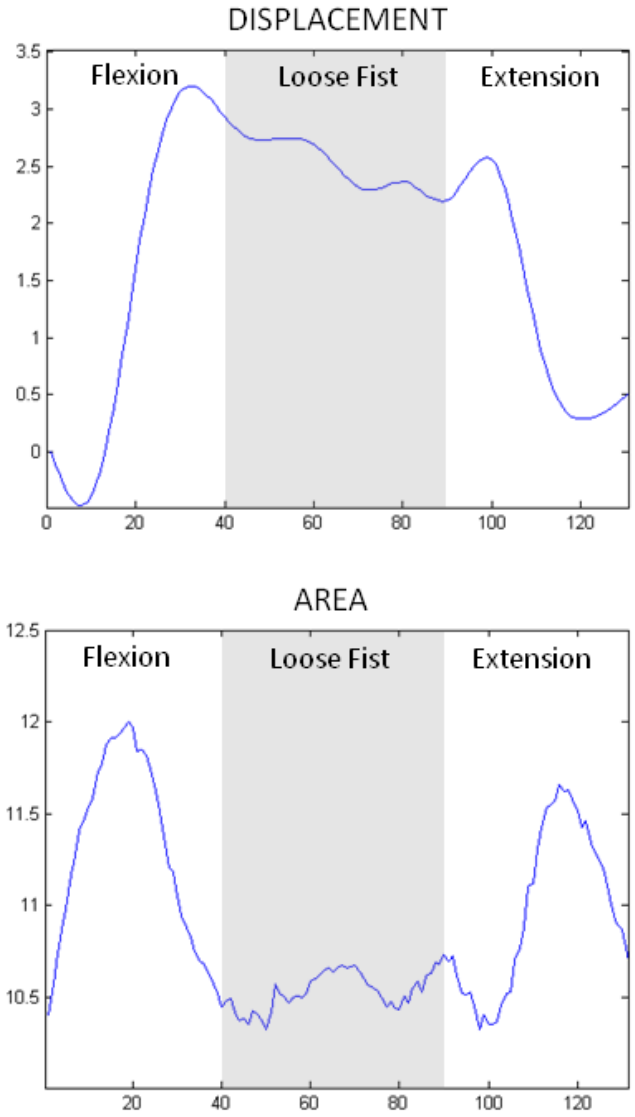

Figure 10. Sample curves of the displacement and CSA measures starting from relaxed fingers, through finger flexion, maintaining a loose fist, and finger extension

We have previously developed several algorithms (including semi-automated and interpolation techniques) for evaluating median nerve displacement and deformation during finger movements (see Chapter 4). We chose to use a semi-automated method over the interpolation methods because it provided the best balance between accuracy and time required for analysis. This semi-automated algorithm utilized cross-correlation combined with techniques for identifying the borders of the nerve to automatically track the location and changes in shape and size of the nerve. Given the nature of our videos, it was not easily feasible to create a fully automated algorithm and therefore an investigator was required to check the algorithm periodically to confirm that the program was accurately tracking the nerve and correct it when necessary, thus making it semi-automated.

The median nerve characteristics and centroid coordinates were determined for each frame of the video. For assessing deformation we investigated the median nerve CSA, FR, perimeter (PERIM), and circularity (CIRC). Using the first frame of each video, representing the starting, relaxed hand position as the reference point, we calculated the maximum percent change increase and decrease for each median nerve variable and determined the net ulnar/radial, palmar/dorsal, and resultant displacements. In order to accurately quantify nerve displacement, it was calculated with respect to a rigid structure, which for this study was a bony landmark that was also tracked using cross-correlation. Any movement of the bony landmark was subtracted from the median nerve displacement in order to provide a more accurate measurement of nerve movement.

6.2.4 Statistical Analysis

The data were analyzed for normality and to appropriately address outliers. We correlated both static (CSA, FR, SR) and dynamic (deformation, displacement) median nerve characteristics to subject characteristics (age, years of wheelchair use, BMI) using Pearson's and Spearman's correlations where appropriate and a Bonferroni correction to control for multiple comparisons. The primary dynamic variables of interest in this study included the net ulnar/radial, palmar/dorsal, and resultant displacements, maximum percent decrease in area (representative of nerve compression), and maximum percent increase in FR. No hypotheses were made regarding maximum area change, minimum FR change, and maximum and minimum CIRC and PERIM. However, since there is little research on this topic, these secondary variables were investigated for exploratory purposes. To investigate the effect of symptoms on median nerve characteristics, we split the group into asymptomatic (reporting no symptoms) and symptomatic (reporting any degree of symptoms) individuals based on their responses on BCTQ. Comparisons of static and dynamic median nerve variables between symptom groups were completed using Independent Samples t-tests and Mann-Whitney tests where appropriate. The Holm-Bonferroni method was used to correct for multiple statistical comparisons. In the symptomatic group, Pearson's and Spearman's correlations were used to investigate the relationship between symptom severity scores and static and dynamic median nerve characteristics. A significance value of $p<0.050$ was used for all statistical tests. All statistical analysis was performed using SPSS (SPSS Inc., Chicago, IL).

6.3 RESULTS

6.3.1 Participants

Twenty-eight participants were included in the analysis of this study. The reasons for using a manual wheelchair as the primary means of mobility included paraplegia (n=24), lower limb amputation (n=1), and other conditions (n=3). The average age, duration of wheelchair use, and BMI were 41.6 ± 12.2 years, 13.8 ± 11.6 years, and 25.8 ± 6.9, respectively. The dichotomization based on symptoms resulted in 12 subjects in the asymptomatic group and 16 in the symptomatic group.

6.3.2 Static Median Nerve Characteristics

Relationship to Subject Characteristics

The only significant correlation was between BMI and the CSA at the radius ($r=0.531$, $p=0.004$). All other static median nerve variables were not significantly related to subject characteristics.

Relationship to Symptoms of CTS

There were no significant differences between symptom groups when comparing static median nerve characteristics. There were no significant correlations between symptom scores and static median nerve variables in the symptomatic group.

6.3.3 Dynamic Median Nerve Characteristics

Relationship to Subject Characteristics

There were no significant correlations between subject characteristics and median nerve deformation or displacement variables at either level.

Relationship to Symptoms of CTS

Displacement - At the level of the distal radius, there were no significant differences between groups. At the level of the pisiform, we found individuals with symptoms of CTS showed significantly less displacement of the median nerve in both the ulnar/radial (p=0.031) and palmar/dorsal (p=0.035) directions. There was a trend (p=0.064) towards a difference in resultant displacement between the groups with the symptomatic group again experiencing less displacement. Table 7 summarizes the displacement findings at each level.

Table 7. Comparison of median nerve displacement between symptom groups

Image Level	Displacement Variable	Displacement in mm Mean (SD)		P-value
		Asymptomatic	Symptomatic	
Radius	Ulnar/Radial	5.01 (2.90)	4.13 (2.58)	0.329
	Palmar/Dorsal	1.30 (0.73)	1.10 (0.48)	0.696
	Resultant	4.25 (2.53)	3.59 (2.26)	0.558
Pisiform	Ulnar/Radial	4.16 (1.70)	2.89 (0.79)	0.031*
	Palmar/Dorsal	1.71 (1.01)	0.97 (0.50)	0.035*
	Resultant	3.32 (1.04)	2.61 (0.82)	0.064

*Indicates a significant difference between groups

Deformation - At the distal radius, no significant differences in deformation variables were observed. At the level of the pisiform, the primary analysis showed a significant difference in maximum percent decrease in median nerve CSA with symptomatic participants experiencing a 20.7% decrease compared to an 11.9% decrease in the asymptomatic individuals. No significant difference in maximum percent increase in FR was noted. The secondary analysis resulted in several significant differences between symptomatic and asymptomatic groups. These included, the maximum percent increases in CSA, CIRC, and PERIM. Table 8 summarizes the deformation findings at each level.

Correlations to Symptom Scores - There were no significant correlations between symptom severity scores and median nerve displacement and deformation characteristics.

Table 8. Comparison of median nerve deformation between symptom groups

Image Level	Deformation Variable	Peak Percent Change Mean (SD)		P-value
		Asymptomatic	Symptomatic	
Radius	AREA increase	14.4 (8.6)	18.8 (12.1)	0.303
	AREA decrease	12.9 (7.3)	11.2 (6.9)	0.544
	FR increase	22.0 (11.8)	27.9 (19.8)	0.360
	FR decrease	24.8 (17.0)	15.2 (10.5)	0.094
	CIRC increase	27.6 (15.6)	20.3 (12.0)	0.187
	CIRC decrease	14.3 (13.0)	9.3 (6.2)	0.198
	PERIM increase	14.8 (9.6)	11.3 (8.2)	0.311
	PERIM decrease	8.5 (9.9)	5.6 (4.3)	0.922
Pisiform	AREA increase	18.1 (16.2)	6.2 (6.1)	0.038*
	AREA decrease	11.9 (7.0)	20.7 (10.5)	0.019*
	FR increase	17.3 (14.2)	11.3 (11.0)	0.240
	FR decrease	25.5 (16.4)	24.4 (19.9)	0.880
	CIRC increase	24.1 (15.8)	10.6 (10.3)	0.022*
	CIRC decrease	12.9 (11.0)	15.3 (9.3)	0.557
	PERIM increase	13.5 (11.5)	3.1 (4.2)	0.001*
	PERIM decrease	8.9 (8.0)	14.1 (7.1)	0.093

*Indicates a significant difference between groups

6.4 DISCUSSION

In this study we sought to assess static median nerve characteristics and relate them to subject characteristic risk factors and symptoms of CTS. There was only one significant relationship between subject characteristics and static median nerve characteristics. Upon comparing static median nerve variables between symptom groups, we did not see any significant differences which is line with our previous work. Given the limited findings in static median nerve variables, we hoped dynamic measures of median nerve characteristics (deformation and displacement) associated with finger movements and would be related to subject characteristic risk factors and symptoms of CTS.

This study provides a unique approach to examining median nerve entrapment and compression which are thought to lead to the development of CTS. We implemented a novel method for assessing transverse median nerve displacement and deformation at the wrist while making a loose fist. We used a semi-automated algorithm, which combined cross-correlation along with techniques for detecting the nerve borders, to successfully quantify nerve deformation and displacement. Other studies have used cross-correlation to determine longitudinal sliding in the median nerve[48,107], but it has not been used, to our knowledge, in tracking the median nerve transversely.

We assessed median nerve deformation and displacement at two levels of the wrist: the level of the distal radius and just slightly more distally at the level of the pisiform bone. Comparing these dynamic measures to subject characteristics, surprisingly, resulted in no significant relationships. While we did not find any differences in symptomatic and asymptomatic individuals at the level of the radius, we did detect several differences at the pisiform level. The difference in findings at each level may be due to anatomical characteristics.

At the distal radius, the nerve is likely less constrained and able to move more freely in response to finger movements. At the pisiform level, which is just proximal to the carpal tunnel, there is less space which may be further reduced by the physiologic changes (synovial thickening, fibrosis, etc.) in the symptomatic wrist, and therefore the median nerve is more affected by finger movements. Since there were no significant differences between groups at the radius, all future discussion will be focused on the findings at the pisiform level.

As we hypothesized, individuals with symptoms of CTS showed significantly less median nerve movement during finger flexion compared to asymptomatic participants, which is line with previous research. Nakamichi et al. compared flexed and extended index finger postures and saw significantly different displacements of 0.37 mm in CTS patients compared to 1.75 mm in controls.[49] Erel et al. compared median nerve displacement at the level of the pisiform between a posture with fingers fully extended to one with 90° of metacarpophalangeal joint flexion and found less movement in CTS patients (0.89 mm) compared to controls (1.55 mm).[48] A study by Chhaya et al. compared a posture with the fingers fully extended to a fist posture and saw reduced ulnar/radial movement in CTS patients (1.28 mm) compared to controls (2.65 mm).[108] We saw much larger displacements, in some cases double, triple, or more, depending on image location and symptom group. This could be due to the fact that we examined nerve displacements throughout the entire duration of finger flexion activity rather than just comparing endpoints. It could also be due to the activity performed. Only one of the studies mentioned looked a displacement with a full fist, while the other two examined smaller finger movements. However, Yoshii et al. studied displacement in healthy controls during long-finger and fist motions and reported similar displacements of 2.09 mm and 2.07 mm respectively.[51] Our measurements are also larger than Yoshii's findings, so it appears that there

may be some additional information to be gained by analyzing the nerve displacement in-between the two endpoints of a particular motion as we observed in the example in Figure 10.

At the time this research study was conducted, we were unaware of the research by Yoshii et al. and Van Doesburg et al. These two studies investigated the relative median nerve displacement as well as changes in CSA, aspect ratio (similar to the FR), perimeter (PERIM), and circularity (CIRC) by comparing static images at two different postures in healthy control subjects. They calculated deformation variables as the ratio between the group mean at flexion with respect to extension, rather than calculating a deformation for each subject and then determining the mean. These two calculations are not mathematically equivalent and we feel the latter is the better assessment of deformation. Given these considerations, comparisons between their findings and ours would not be valid.

Looking at median nerve deformation, as expected, we saw a greater decrease in CSA in symptomatic participants compared to asymptomatic, but saw no significant differences in FR increase between groups. This is partly in agreement with findings by Erel et al., who investigated aspect ratio (similar to FR) in CTS patients and controls at neutral and with 90° of metacarpophalangeal joint flexion. They found significant differences existed between groups at the neutral posture (aspect ratio of 2.00 in controls and 2.29 in CTS patients), but not at the flexed posture (aspect ratio of 2.48 in controls and 2.37 in CTS patients).[48] They did not report any findings related to CSA changes between posture and CTS group. In the secondary variables, the most interesting finding was a significant difference between groups in percent increase in CSA, with asymptomatic showing an increase of 18.1% versus 6.2% in the symptomatic participants. This finding further supports the relationship between median nerve compression and symptoms of CTS as the nerves of asymptomatic participants were able to

swell slightly and to a much greater extent than symptomatic participants in response to finger movement. The variables of circularity and perimeter are difficult to interpret as they do not provide information about the direction of shape change. For example, a nerve that starts as a perfect circle and becomes flat and elongated in the ulnar/radial direction would show the same percent change in circularity and perimeter as a nerve that flattened and elongated by the same amounts in the palmar/dorsal direction.

There are several limitations of this study. First of all, only 28 participants were included in the analysis. While this was enough to detect differences between symptom groups a larger study would be necessary if this dynamic measure were to be used in assisting with diagnosis of CTS. Also, the rate of flexion and extension differed between subjects. Future studies may want to control the speed of movements as these may have an impact on deformation and displacement characteristics. Given the design of this study, it was not practical to make comparisons between different postures. Future research could apply similar techniques to assess a variety of activities in more detail. For example synching the ultrasound movie with live video of the activity so that external postures can be evaluated at the same time internal anatomical movements are assessed to determine any relationships between posture and nerve deformation or displacement.

Another potential limitation of this study is that longitudinal movement of the nerve may have contributed to the deformation that was seen. It is possible that during the grip maneuver, the median nerve may have slid longitudinally along with the finger flexor tendons resulting in a smaller or larger portion of the nerve entering our field of view, giving a false appearance of deformation. Previous research has shown that the median nerve slides longitudinally with finger movements.[48,109] Future research may need to combine both longitudinal and transverse

assessments to better assess median nerve deformation characteristics. However, measuring the longitudinal movement of the nerve while it is also sliding transversely is a difficult procedure as the nerve constantly slides out of the longitudinal plane of view. There are also some limitations with the displacement measures in our study. While we saw differences between symptom groups as expected, we did not control for wrist size as a factor for the amount of movement possible. This was not something we considered until after all data had been collected. We attempted to measure the carpal canal, but the videos we captured were not optimized for measuring carpal canal dimensions, but rather on maintaining ideal focus on the median nerve. Future research may need to control for wrist size by using anthropometrics (e.g. measuring wrist circumference) or by recording ultrasound measurements of the carpal canal dimensions.

6.5 CONCLUSION

In conclusion, we obtained dynamic measures of median nerve entrapment and compression, by quantifying displacement and deformation of the median nerve while making a loose fist and related this information to the presence of CTS symptoms. Since static median nerve measures were not different between symptom groups, these dynamic measures may have some applications in a diagnostic setting as supplemental tests to the static measurements typically obtained. Future research could focus on how median nerve displacement and deformation vary with different grip force, speed and repetition of movements, and degrees CTS.

7.0 CONCLUSION

Ultrasound has been used as a research tool for assessing the acute response of the median nerve to repetitive activity. The magnitude of change in median nerve variables in this previous work ranged from approximately 4-20%, and a majority were rather small changes of less than 10%. In order to confidently detect these small changes and attribute them to activity, it must be shown that the nerve could be reliably measured when no changes have occurred. We found limited research on the repeatability of median nerve ultrasound measures and minimum detectable change (MDC). In this dissertation we expanded upon the limited reliability literature and investigated the repeatability of several median nerve ultrasound measures (CSA, FR, SR, mean grayscale). We also evaluated the effects of several protocol designs on the dependability coefficient and standard error of measurement. We found that ultrasound is a reliable tool for measuring the median nerve and therefore may be useful for assessing changes in median nerve measures and CTS. We used the repeatability measures determine a reliable protocol that could be used in future research focused on quantifying median nerve changes in response to activity. We also determined the MDC which can serve as a guideline for confidently assessing true differences in nerve characteristics within a single subject over multiple time points either acutely or chronically.

Based on the findings from the reliability analysis we applied an appropriate protocol to study the acute median nerve response to activity in a population at high risk for CTS. This

population was manual wheelchair users and included individuals who may be in the developing stages of CTS, but not yet diagnosed with CTS. We found no ultrasonographic evidence of CTS at baseline indicated by a lack of difference in median nerve characteristics in symptomatic and asymptomatic individuals. However, we did find that the immediate median nerve response to activity visualized using ultrasound was related to the presence/absence of symptoms. Specifically, the median nerves of asymptomatic and symptomatic individuals responded significantly differently and in opposite directions after a period of strenuous wheelchair propulsion. The variables that significantly differed have been previously related to electrodiagnostic evidence of CTS, suggesting that wheelchair propulsion may slightly damage the median nerve acutely which when compounded over time could ultimately lead to the development of CTS.

Given the nature of everyday wheelchair use and ergonomics literature suggesting that high-force, high-repetition activities may lead to CTS, individuals who use a manual wheelchair as their primary means of mobility are at high risk for developing CTS. We attempted to relate wheelchair propulsion characteristics such as force, repetition, and posture to baseline median nerve characteristics previously related to CTS. We also expected the median nerve response to activity to be related to propulsion characteristics. To our knowledge this was the first attempt to relate median nerve ultrasound characteristics before and after a provocative activity to specific characteristics of that activity. Unfortunately, we were unable to find any significant relationships between propulsion variables and baseline median nerve variables or median nerve response to activity. This does not necessarily mean that these variables do not play an important role in the development of CTS, but that more detailed research is necessary to better investigate the effects of force, repetition and posture on the acute median nerve response.

In addition to all the static median nerve characteristics discussed to this point, we were interested in obtaining dynamic measures of median nerve entrapment and compression. To do this however, we needed to develop a way to efficiently and accurately, analyze an ultrasound movie of the median nerve moving within the carpal tunnel. We developed several algorithms which are capable of obtaining valuable information from an ultrasound movie of median nerve motion without having to analyze every frame of each movie. The algorithms developed in this dissertation range from simple interpolation methods requiring more user input, to more complex semi-automated methods needing less user input. The semi-automated method combined image processing techniques in a basic fashion including registration via cross-correlation and a simplified edge detection process in order to quantify median nerve deformation and displacement with limited user interaction. While these algorithms could be improved, possibly to provide real time tracking, they provide a basis for future research hoping to assess median nerve and tendon deformation and displacement within the carpal tunnel while performing various hand, wrist and finger activities.

Through the application of the algorithms developed we obtained dynamic measures of median nerve entrapment and compression, by quantifying median nerve displacement and deformation of the median nerve while making a loose fist and related this information to the presence of CTS symptoms. We found significant differences in deformation and displacement characteristics in individuals with and without symptoms of CTS. These measures may have some applications in a diagnostic setting as possible supplemental tests to the static measurements typically attained. Understanding the anatomical details of median nerve and tendon movements within the carpal tunnel could provide invaluable information for understanding the pathophysiology of CTS, specifically relating it to certain detrimental hand

and wrist activities. Future research could focus on how median nerve displacement and deformation vary with different grip force, speed and repetition of movements, and degrees CTS.

In this study we assessed static, dynamic, and acute changes in median nerve variables in asymptomatic and symptomatic participants. Surprisingly we learned very little about median nerve characteristics by looking at subject characteristics risk factors, given the limited association between age, BMI, and duration of wheelchair use with median nerve variables. One of the key findings in this analysis was that static median nerve characteristics were not significantly different and actually quite similar when comparing symptom groups. However, both dynamic and acute changes in median nerve characteristics differed between symptom groups. Because these symptomatic participants have not been diagnosed with CTS and are likely in the developing stages, this provides an opportunity for intervention to prevent the full progression to CTS. This finding also suggests that adding a quick dynamic evaluation and acute response assessment to activity may improve the diagnostic capabilities of ultrasound.

Studying an individuals daily activities, which likely lead to the development of symptoms, could provide insight into which activity or combination of activities are the greatest contributors to their symptoms. By studying the acute median nerve response after several minutes of performing a given activity, one could quantify how detrimental that task is to an individual's median nerve. By testing the nerve response to various interventions, the task could be modified to a point where it is no longer damaging and likely will not continue to contribute to their symptoms or progression of CTS. In manual wheelchair users this could include wheelchair propulsion training, wheelchair setup, ergonomic pushrims, and improved transfer techniques, to learn their effects on the median nerve response. Studying the acute changes has many applications outside of wheelchair users as well. Studying the acute median nerve

response to keyboarding, in assembly lines, among construction workers, or anywhere individuals perform high repetition activities or use vibrating tools, may be useful for identifying interventions to reduce the likelihood of developing CTS.

By studying the dynamic aspects of median nerve movement and deformation during various hand and finger activities, future research could attempt to quantify the progression of CTS or determining various stages of CTS. For example, early dynamic signs could be diminished movement and increased deformation which may ultimately lead to what is most commonly seen, an increase in median nerve CSA. In a diagnostic setting, performing a quick dynamic evaluation, not necessarily applying one of the algorithms presented here, may assist a clinician with accurately diagnosing CTS. A clinician could either qualitatively evaluate movement or quantitatively make some approximate measurements. In addition, if a real time tracking algorithm were developed it could provide immediate feedback of the various dynamic characteristics of nerve movement and deformation.

One limitation of this study is that all analysis was done on either asymptomatic participants or individuals with symptoms who have not been diagnosed with CTS. Future work should focus on the static and dynamic characteristics of the median nerve before and after activity in asymptomatic healthy controls, individuals in the developing stages of CTS with varying degrees of symptoms, and those who have definitive evidence of CTS. This will provide a better understanding of median nerve characteristics in a healthy population, how the nerve gradually changes while in the developing stages of CTS and ultimately then end result of CTS on nerve characteristics. By better understanding this progression, clinicians should be able to intervene in order to delay or prevent the development of median mononeuropathy and improve quality of life for the many individuals affected by CTS. Another limitation of our study was

that we only tested four females. Since females are at a greater risk for developing CTS, more research is needed on the gender differences in static, dynamic, and acute changes in median nerve characteristics.

In this study study, we measured the nerve at three different levels of the wrist based on previous findings relating ultrasonographic median nerve characteristics to CTS. However, more recent research suggests that there may be some more sensitive means of measuring median nerve characteristics, by taking measurements at levels other than at the wrist. A study by Hobson-Webb et al. suggests that the wrist-to-forearm ratio of the median nerve CSA is more sensitive than solely measuring CSA at the wrist.[110] They also recommend that this be specifically used in milder cases of CTS. Another study by Klauser et al. compared measurements of the nerve at the wrist with those more proximally at the level of the pronator quadrates muscle and found increased accuracy when using the proximal measurements.[111] Future studies assessing static, dynamic and acute changes in the median nerve may benefit from including some proximal (forearm) measures in the analysis. In addition, as ultrasound technology advances, three dimensional volumes of the carpal tunnel may be useful in diagnosing CTS.

In attempting to relate wheelchair propulsion biomechanics to the median nerve response to activity, we were unable to find any significant relationships. Unfortunately, we only captured propulsion kinetics during the activity and not kinematics. To better assess propulsion biomechanics related to median nerve changes, both kinetics and kinematics should be collected during the activity to directly relate wrist joint reaction forces and joint angles to the median nerve response. Even this however, may not be sufficient given differences in the way individuals grasp the pushrim. Some may pinch the pushrim between the thumb and index finger

(key pinch), while some use a fist to grasp the pushrim (power grip), and others may hardly grasp the pushrim at all relying primarily on friction between the hand and the pushrim. These different propulsion styles may be interepreted very similarly by the Smartwheel as it does not differentiate between the forces applied about the pushrim, but rather records the forces applied about the hub of the wheel. These different grasping techniques would affect activity of the finger flexor tendons and the impact forces on the palm of the hand which could lead to different median nerve responses. Future research is necessary to evaluate both the biomechanics of different pushrim grasping techniques and the associated median nerve responses.

In summary, ultrasound is a reliable, useful, and convenient method for assessing static, dynamic and acute changes in median nerve characteristics and examining their relationship to risk factors and symptoms of CTS. Where static images cannot differentiate between symptomatic and asymptomatic individuals, dynamic measures or the acute response to activity can be used to identify differences. Future research is necessary to evaluate other risk factors (e.g. gender) and to relate specific biomechanical characteristics of an acitivity to ultrasonographic median nerve characteristics.

APPENDIX A

MATLAB CODE FOR ANALYZING STATIC MEDIAN NERVE IMAGES

```
function median_nerve
% This program is designed to load a grayscale ultrasound image and allow the
% user to calculate the several median nerve characteristics including cross
% sectional area, flattening ratio, and mean grayscale.
%clear workspace variables
clc;
close all;
clear all;
%variable declaration/initialization
repeat=1; first_time=3; area=0; length1=0; known_length=0; loop_again=1;
epineurium=1; i=1; how_many=0; headers=1; one_time = 0;
store = []; bottom=0; top=0; running_gray = [0 0 0 0];
running_area = [0 0 0 0]; area_sum = [0 0 0 0];
%--------------------------------------------------------------------------
%Begin main body of program
%--------------------------------------------------------------------------
%allow for repeated iterations
%while repeat==1
total_images=input('Enter number of images to run: ');
start = ['S:\Protocols\Boninger\Ultrasound\DATA'];
cd(start);
for image_num = 1:total_images
    message = ['Select image ',num2str(image_num)];
    [filename,pathname]=uigetfile('*.*',message);
    cd(pathname);
    temp_image= imread(filename);
    all_images(:,:,image_num) = temp_image(147:end,:,1);
    image_ids(:,:,image_num)=filename(1:8);
end
b=1;
%function allows user to trace selection using series of mouse clicks
%hit enter after zooming appropriatly
%(shift / double click to end selection)
image_num_rand=randperm(total_images);
for image_num = 1:total_images
    image=all_images(:,:,image_num_rand(image_num));
    [size_x1 size_y1] = size(image);
```

```
    [cord_values,cords] = get_selection(size_x1,size_y1,image);
    %calls function to calculate area
    [area,first_time,length1,known_length,conversion,num_pixels] =
calc_area(cords,first_time,image,length1,known_length,loop_again);
    %calculate area assuming ellipse - returns area and major and minor
    %axes for calculating flattenning ratio
    [ellipse_area, major_axis_length_mm,
minor_axis_length_mm]=calc_area_ellipse(image, conversion);
    flattening_ratio = major_axis_length_mm/minor_axis_length_mm;
    %function to get boundary points of reference box/median nerve
    [out_y, start_x, end_x,btm_y,top_y] = get_points;
    close;
    %function to store grayscale values of reference block
    [reference, start_y,x_length,y_length] = create_reference(out_y, start_x,
end_x, image,btm_y,top_y);
    %function to analyze reference block into 10x10 evenly distributed matrix
    [plot_me,rows,cols] = analyze(reference);
    %calls average calculation / display function
    [reference_average, selection_average] = calc_average(cord_values,
plot_me);
    %converts the major and minor axis lengths from pixels to mm
    %necessary for output
    ratio = selection_average/reference_average;
    %--------------------------------------------------------------------
image_id=image_ids(:,:,image_num_rand(image_num));%image_ids(:,:,image_num);
j = b+2;
k = b+1;
    %stores several global variables in single array for printing to file
median_nerve=[area,selection_average,horizontal,vertical,reference_average,ra
tio,ellipse_area,major_axis_length_mm,minor_axis_length_mm,flattening_ratio,e
pi_height(1),epi_height(2)];
median_nerve=[area,ellipse_area,major_axis_length_mm,minor_axis_length_mm,fla
ttening_ratio,selection_average,reference_average,ratio];
    % appends data to end of file
    cd('S:\Protocols\Boninger\Ultrasound\');
    fid=fopen('mediannervedata.txt','a');
    if one_time == 0
        %writes headers to file
        fprintf(fid,'%8s\t%8s\t%8s\t%8s\t%8s\t%8s\t%8s\t%8s\t%8s\n','image
id','area','ellipse_area','major_axis','minor_axis','flat_ratio','mean_graysc
ale_nerve','mean_grayscale_reference','grayscale_ratio_nerve/ref');%,'epi
bottom','epi top');
    end
    %reformats vectors to accommodate output
    [median_nerve]=median_nerve';
    %writes filename to file
    fprintf(fid,'%8s\t',image_id);
    %writes data to file
    fprintf(fid,'%5.3f\t%5.3f\t%5.3f\t%5.3f\t%5.3f\t%5.3f\t%5.3f\t%5.3f\n',
median_nerve);
    fclose(fid);
    cord_values_brad = double(cord_values);
    [selection]=remove_zeros(cord_values_brad);
    %--------------------------------------------------------------------
    %increments counter to only display header once
    one_time = one_time + 1;
    %prompts user to repeat program
```

```
   %repeat=menu('Would you like to analyze a new set of images?','Yes','No');
end
end
%-------------------------------------------------------------------------
function [pass_area,first_time,length1,known_length,conversion,num_pixels] =
calc_area(region,first_time,image,length1,known_length,loop_again)
%this loop forces the user to set the pixel scale the first time through
%program, but allows use of same scale for subsequent iterations
while loop_again == 1;
    delete(findobj('Margin',6))
    %set_scale = menu('Do you want to set the mm/pixel scale?','Yes','No');
    set_scale = 2;
    switch set_scale
        case 1
            imshow(image);
            title('Select a line on the image of a known length - Shift click
/ Double Click to end');
            %gets length of line
            [x y] = getline;
            size_y = size(y);
            length1 = y(size_y(1)) - y(1);
            delete(findobj('Margin',6))
%%%%%%%%%%%%%%%%%%%%%%%%%%%%%%%%%%%%%%%%%%%%%%%%%%%%%%%%%%%%%%%%%%%%%%%%%%%
            %to set scale, user must enter a known length of measure in image
            title('Enter known length in command window');
            known_length = input('Enter the known length of the line: ');
            first_time = 3;
            loop_again = 0;
            delete(findobj('Margin',6))
%%%%%%%%%%%%%%%%%%%%%%%%%%%%%%%%%%%%%%%%%%%%%%%%%%%%%%%%%%%%%%%%%%%%%%%%%%%
        case 2
            if (first_time == 1)
                title('Warning: See command Window');
                disp('You must set scale the first time through the program
to calculate the area');
                disp('Please select yes from the set scale menu');
                loop_again = 1;
            elseif (first_time == 3)
                loop_again = 3;
            end
    end
    if first_time==1 || first_time == 3
        %converts the selected region from previous function to double matrix
        temp1 = double(region);
        %regionprops stores values as structure array
        temp2 = regionprops(temp1,'area');
        [x y] = size(region);
        num_pixels = 0;
        %loops to count number of pixels in selection
        for n = 1:x
            for m = 1:y
                if region(n,m) == 1
                    num_pixels = num_pixels+1;
                end
            end
        end
        %conversion = 13.5;
```

```
        conversion = length1 / known_length
        %calculates the cross sectional area
        pass_area = num_pixels/((conversion)^2);
    end
end
end
%-------------------------------------------------------------------------

%-------------------------------------------------------------------------
function [cord_values,cords] = get_selection(x,y,image)
cord_values=[]; m=1; n=1; test=2;
while(test == 2)
    %displays image and allows user to zoom in before selection
    imshow(image);
    title('Median Nerve: Click to Zoom, Hit Enter to Continue');
    hold on;
    zoom on;
    %allows user to select an area of a figure
    %stores data as 1 if point is inside, 0 if outside selection
    title('Hit any key to use a series of points to select median nerve -
Shift click / Double click to end');
    pause
    zoom off;
    cords = roipoly(image);
    delete(findobj('Margin',6));
    %loop to generate a matrix of grayscale values within selection
    for n = 1:x
        for m = 1:y
            if cords(n,m) == 1
                cord_values(n,m) = image(n,m);
            end
        end
    end
    %releases current figure
    hold off
    test=1;
    %    test = menu('Are you happy with your selection?','Yes','No');
end
end
%-------------------------------------------------------------------------

%-------------------------------------------------------------------------
function [ellipse_area, major_axis_length_mm,
minor_axis_length_mm]=calc_area_ellipse(image, conversion)
imshow(image)
zoom on;
pause;
zoom off;
title('select major axis');
[maj_x maj_y] = getline;
title('select minor axis');
[min_x min_y] = getline;
%calculate length in pixels
major_axis_length = sqrt((maj_x(1)-maj_x(length(maj_x)))^2+(maj_y(1)-
maj_y(length(maj_y)))^2);
```

```
minor_axis_length = sqrt((min_x(1)-min_x(length(min_x)))^2+(min_y(1)-
min_y(length(min_y)))^2);
%convert pixels to millimeters
major_axis_length_mm = major_axis_length/conversion;
minor_axis_length_mm = minor_axis_length/conversion;
%calculate area in square millimeters
ellipse_area = pi*major_axis_length_mm*minor_axis_length_mm/4;
end
%--------------------------------------------------------------------------

%--------------------------------------------------------------------------
function [out_y, start_x, end_x,btm_y,top_y] = get_points
%allows user to input 4 mouse clicks
zoom on;
title('Click leftmost point of median nerve');
click_pts_1 = ginput(1);
start_x = round(click_pts_1(1,1));
title('Click rightmost point of median nerve');
click_pts_2 = ginput(1);
end_x = round(click_pts_2(1,1));
title('Click bottommost point of median nerve - Do not include epineurium
(click just inside epineurium)');
click_pts_3 = ginput(1);
btm_y = round(click_pts_3(1,2));
title('Click topmost point of median nerve - Do not include epineurium (click
just inside epineurium)');
click_pts_4 = ginput(1);
top_y = round(click_pts_4(1,2));
title('Click topmost point of median nerve outside epineurium (click just
outside epineurium)');
click_pts_5 = ginput(1);
out_y = round(click_pts_5(1,2));
end
%--------------------------------------------------------------------------

%--------------------------------------------------------------------------
function [new,rows,cols] = analyze(reference)
%dimension variables
dimensions = size(reference);
num_rows = dimensions(1,1);
num_cols = dimensions(1,2);
rows = floor(num_rows/10);
cols = floor(num_cols/10);
row_rem = rem(num_rows,10);
col_rem = rem(num_cols,10);
n = 1;
m = 1;
for i = 1:10
    m = 1;
    end_n = i*rows;
    %check if end row exceeds matrix dimensions
    if end_n > num_rows
        %readjust final row
        end_n = num_rows;
    end
    for j = 1:10
```

```
        end_m = j*cols;
        %check if end column exceeds matrix dimensions
        if end_m > num_cols
            %readjust final column
            end_m = num_cols;
        end
        %creates 10x10 matrix new with average values of reference
        temp = reference(n:(end_n),m:(end_m));
        new(i,j) = mean(mean(temp));
        m = m+cols;
    end
    n = n+rows;
end
clc
end
%--------------------------------------------------------------------------

%--------------------------------------------------------------------------
function [reference_average, selection_average] =
calc_average(cord_values,new,rows,cols)
%counter declaration
o=1;
p=1;
avgcounter = 0;
%calculates size of coordinate value matrix
[size_x2 size_y2] = size(cord_values);
%loop to count number of nonzero elements for use in mean grayscale
calculation
for o = 1:size_x2
    for p = 1:size_y2
        if cord_values(o,p) ~= 0
            avgcounter = avgcounter+1;
        end
    end
end
%sets the reference to the last 10 rows above the median nerve
temp = new(10,:);
reference_average = mean(temp); %calculates average
cord_sum = sum(sum(cord_values)); %calculates sum of total matrix
selection_average = cord_sum/avgcounter; %calculates average of selection
end
%--------------------------------------------------------------------------

%--------------------------------------------------------------------------
function [reference, start_y,x_length, y_length] = create_reference(out_y,
start_x, end_x,image,btm_y,top_y)
%declare counters
e = 1;
f = 1;
start_y = 1;
reset_value = start_x;
%calculates change in width
x_length = (end_x - start_x);
%calculates change in height
y_length = (btm_y - top_y);
%initializes waiting bar
```

```
h = waitbar(0,'Please wait...');
while start_y < out_y
    %increments waiting bar so user knows progress of program calculation
    waitbar(start_y/out_y)
    while start_x < end_x
        %creates reference box above median nerve based on user input
        temp = impixel(image,start_x,start_y);
        reference(e,f) = temp(1,1) ;
        %increments counters
        f = f+1;
        start_x = start_x + 1;
    end
    %increments external counters, resets internal counters
    f = 1;
    start_x = reset_value;
    start_y = start_y + 1;
    e = e+1;
end
close(h);
end
%-------------------------------------------------------------------------
function [selection]=remove_zeros(cord_values_brad)
%%this function will remove the uneeded zeros in the matrix
%%containing the selection.
clear selection;
[rows,cols]=size(cord_values_brad);
%first remove all the columns of zeros preceding the selection
col=1;
while mean(cord_values_brad(:,col)) == 0
    col=col+1;
end
startcol=col;
count=0;
for c = startcol:cols
    count=count+1;
    temp_selection(:,count) = cord_values_brad(:,c);
end
%next remove all the rows of zeros preceding the selection
row=1;
while mean(cord_values_brad(row,:))==0
    row=row+1;
end
startrow=row;
count=0;
for r=startrow:rows
    count=count+1;
    selection(count,:) = temp_selection(r,:);
end
end
%-------------------------------------------------------------------------

%-------------------------------------------------------------------------
```

APPENDIX B

MATLAB CODE FOR ALGORITHMS ANALYZING ULTRASOUND MOVIES OF MEDIAN NERVE MOVEMENT AND DEFORMATION

```
function main
clear;  clc;  close all;
cd('S:\Protocols\Boninger\Ultrasound');
[filename,dir_path]=uigetfile('*.*', 'Select file in batch directory');
cd(dir_path);  file_list=dir;  num_files=length(file_list)-2-0;
imagelevel=menu('Please select image level:','Radius','Pisiform');
videoid=strtok(filename, '.');
videoid=videoid(1:end-3);
%crop images down to region of interest - i.e. only the part with actual
anatomy in it
tempimage=imread(file_list(3).name);  imshow(tempimage);
title('Please select upper left point of
image');[start_col,start_row]=ginput(1);
title('Please select lower right point of
image');[end_col,end_row]=ginput(1);
close;
start_col=floor(start_col); start_row=floor(start_row);
end_col=floor(end_col); end_row=floor(end_row);
save('start_col.mat','start_col');save('start_row.mat','start_row');
save('end_col.mat','end_col');save('end_row.mat','end_row');
%find distance moved by bony landmark to account for sliding of probe then
%find distance moved by nerve relative to the bony landmark

%first, have user specify initial bony landmark
tempimagecropped=tempimage(start_row:end_row,start_col:end_col,1);
imshow(tempimagecropped);
title('Please select upper left point of bony
landmark');[bonylandmark_start_col,bonylandmark_start_row]=ginput(1);
title('Please select lower right point of bony
landmark');[bonylandmark_end_col,bonylandmark_end_row]=ginput(1);
bonylandmark_start_col=floor(bonylandmark_start_col);
bonylandmark_start_row=floor(bonylandmark_start_row);
bonylandmark_end_col=floor(bonylandmark_end_col);
bonylandmark_end_row=floor(bonylandmark_end_row);
```

```
bonylandmark=tempimagecropped(bonylandmark_start_row:bonylandmark_end_row,bon
ylandmark_start_col:bonylandmark_end_col,1);
close;
if imagelevel == 1 %check only the bottom half of image for radius
    bonystart_row=start_row+floor((end_row-start_row)/2);
    bonystart_col=start_col;
elseif imagelevel ==2 %check only the right half of image for pisiform
    bonystart_row=start_row;
    bonystart_col=start_col+floor((end_col-start_col)/2);
end
bonyvertexoriginal_col=[bonylandmark_start_col+start_col;bonylandmark_end_col
+start_col];
bonyvertexoriginal_row=[bonylandmark_start_row+start_row;bonylandmark_end_row
+start_row];
%second, have user specify initial median nerve template by tracing the nerve
mntempimage=tempimagecropped(1:ceil(0.67*size(tempimagecropped,1)),1:end);
imshow(mntempimage
title('Please trace the median nerve. Press any key when ready');pause;
%using roipoly we create a logical which specifies which pixels are part of
the median nerve.
figure;[mnroi,vertex_col,vertex_row]=roipoly(mntempimage);close all;
mnroioriginal=mnroi;
mnvertexoriginal_col=vertex_col+start_col;
mnvertexoriginal_row=vertex_row+start_row;
imshow(mntempimage);title('Please guess where the bottom right point of the
median nerve template is');
[mncolguess,mnrowguess]=ginput(1);close;
%we must then assign the actual grayscale values from the image to the
template using this logical
[r,c]=find(mnroi==1);
for a=min(r):max(r)
    for b=min(c):max(c)
        if mnroi(a,b)==1
            mntemplate(a-min(r)+1,b-min(c)+1)=mntempimage(a,b);
        end
    end
end
clear mnroi
for a=1:size(mntemplate,1)
    for b=1:size(mntemplate,2)
        if mntemplate(a,b)>0
            mnroi(a,b)=1;
        end
    end
end
%create a label matrix for use in regionprops
mnroi=bwlabel(mnroi);
stats(1,1) = regionprops (mnroi,mntemplate,'Area','Centroid','Orientation',
'MajorAxisLength','MinorAxisLength','MeanIntensity','Eccentricity','Extent','
ConvexHull');
stats_temp = regionprops(mnroi,mntemplate,'Extent');
mncorr_adjustment=.75*(1-stats_temp.Extent);
left_focus_row=floor((vertex_row(2)+vertex_row(12))/2);
left_focus_col=floor((vertex_col(2)+vertex_col(12))/2);
right_focus_row=floor((vertex_row(6)+vertex_row(8))/2);
right_focus_col=floor((vertex_col(6)+vertex_col(8))/2);
left_quarter_row=floor((vertex_row(3)+vertex_row(11))/2);
```

```
left_quarter_col=floor((vertex_col(3)+vertex_col(11))/2);
center_row=floor((vertex_row(4)+vertex_row(10))/2);
center_col=floor((vertex_col(4)+vertex_col(10))/2);
right_quarter_row=floor((vertex_row(5)+vertex_row(9))/2);
right_quarter_col=floor((vertex_col(5)+vertex_col(9))/2);
%now use cross correlation to track movement of bony landmark and median
%nerve
corrections=[];
vertex_archive=[];
mn_coordinates=[];
for i=1:130%num_files%floor(num_files/5)-1
    clear *corr
    tempimage=imread(file_list(3+(i-1)).name);
    tempimagecropped=tempimage(start_row:end_row,start_col:end_col,1);
    bonytempimage=tempimage(bonystart_row:end_row,bonystart_col:end_col);
mntempimage=tempimagecropped(1:ceil(0.67*size(tempimagecropped,1)),1:end);
    %track movement of bony landmark using cross correlation
    bonycorr=normxcorr2(bonylandmark,bonytempimage);
    maxbonycorr=max(max(bonycorr));
    %check to see if bonylandmark template needs to be updated
    if maxbonycorr<0.9
        imshow(tempimagecropped);
        title('Please select upper left point of bony
landmark');[bonylandmark_start_col,bonylandmark_start_row]=ginput(1);
        title('Please select lower right point of bony
landmark');[bonylandmark_end_col,bonylandmark_end_row]=ginput(1);
        close;
        bonylandmark_start_col=floor(bonylandmark_start_col);
bonylandmark_start_row=floor(bonylandmark_start_row);
        bonylandmark_end_col=floor(bonylandmark_end_col);
bonylandmark_end_row=floor(bonylandmark_end_row);
bonylandmark=tempimagecropped(bonylandmark_start_row:bonylandmark_end_row,bon
ylandmark_start_col:bonylandmark_end_col,1);
        bonycorr=normxcorr2(bonylandmark,bonytempimage);
        maxbonycorr=max(max(bonycorr));
    end
    [bonyrow(i),bonycol(i)]=find(bonycorr==maxbonycorr);
    %if landmark moves too far then find the next max of corr
    while i>1 && (abs(bonyrow(i)-bonyrow(i-1))>15 || abs(bonycol(i)-
bonycol(i-1))>15) %if the bony landmark moves more than 25 pixels in two
consecutive frames, then look at next highest peak in corr
        %         disp('bone moved too far. recalculating');
        bonycorr(bonyrow(i),bonycol(i))=0;
        maxbonycorr=max(max(bonycorr)); %maybe find top 5 values
        [bonyrow(i),bonycol(i)]=find(bonycorr==maxbonycorr);
    end
    %calculate distance bony landmark moved
    %     dist_bonylandmark_vert(i)=bonycol(i)-bonycol(1); %vertical movement
from original location
    %     dist_bonylandmark_hor(i)=bonyrow(i)-bonyrow(1); %horizontal
movement from original location
bony_coordinates(:,i)=[bonyrow(i);bonycol(i)];
    %define new bony landmark
    bonylandmark=bonytempimage( 1+bonyrow(i)-size(bonylandmark,1) :
bonyrow(i) , 1+bonycol(i)-size(bonylandmark,2) : bonycol(i) );
    bonyvertex_col=[1+bonycol(i)-
size(bonylandmark,2)+start_col;bonycol(i)+start_col];
```

```
    bonyvertex_row=[1+bonyrow(i)-
size(bonylandmark,1)+bonystart_row;bonyrow(i)+bonystart_row];
    %track movement of median nerve using cross correlation
    mncorr=normxcorr2(mntemplate,mntempimage);
    mncorr=mncorr+mncorr_adjustment;
    maxmncorr=max(max(mncorr));
    %check to see if mn template needs to be updated
    if maxmncorr<0.6 || rem(i,10)==0
        save('vertex_archive.mat','vertex_archive');
        save('mn_coordinates.mat','mn_coordinates');
        save('bony_coordinates.mat','bony_coordinates');
        i
        figure;imshow(mntempimage);figure;imshow(mntemplate);
        retracenerve=menu('Does the template need to be
updated','Yes','No');close all;
        if retracenerve==1
            corrections=[corrections i];
            save('corrections.mat','corrections');
            imshow(mntempimage);title('Please trace the median nerve. Press
any key when ready');pause;
            figure;[mnroi,vertex_col,vertex_row]=roipoly(mntempimage);close
all;
            [r,c]=find(mnroi==1);
            for a=min(r):max(r)
                for b=min(c):max(c)
                    if mnroi(a,b)==1
                        mntemplate(a-min(r)+1,b-min(c)+1)=mntempimage(a,b);
                    end
                end
            end
            mncorr=normxcorr2(mntemplate,mntempimage);
            maxmncorr=max(max(mncorr));
        end
    end
    [mnrow(i),mncol(i)]=find(mncorr==maxmncorr);
    if i==1
        dist_mn_vert_temp=mnrow(i)-mnrowguess; %vertical movement from
previous frame without accounting for bony landmark movement
        dist_mn_hor_temp=mncol(i)-mncolguess; %horizontal movement from
previous frame without accounting for bony landmark movement
    else
        dist_mn_vert_temp=mnrow(i)-mnrow(i-1); %vertical movement from
previous frame without accounting for bony landmark movement
        dist_mn_hor_temp=mncol(i)-mncol(i-1); %horizontal movement from
previous frame without accounting for bony landmark movement
    end
    %if mn moves too far then find the next max of corr
    while (abs(dist_mn_vert_temp)>5 || abs(dist_mn_hor_temp)>10)%if the mn
moves more than x pixels in two consecutive frames, then look at next highest
peak in corr
        %         disp('median nerve moved too far. recalculating');
        mncorr(mnrow(i),mncol(i))=0;
        maxmncorr=max(max(mncorr));
        [mnrow(i),mncol(i)]=find(mncorr==maxmncorr);
        if i==1
            dist_mn_vert_temp=mnrow(i)-mnrowguess; %vertical movement from
previous frame without accounting for bony landmark movement
```

```
            dist_mn_hor_temp=mncol(i)-mncolguess; %horizontal movement from
previous frame without accounting for bony landmark movement
        else
            dist_mn_vert_temp=mnrow(i)-mnrow(i-1); %vertical movement from
previous frame without accounting for bony landmark movement
            dist_mn_hor_temp=mncol(i)-mncol(i-1); %horizontal movement from
previous frame without accounting for bony landmark movement
        end
    end
    %calculate distance mn moved
    %     dist_mn_vert(i)=mnrow(i)-mnrow(1)-dist_bonylandmark_vert(i);
%vertical movement from original location with respect to bony landmark
    %     dist_mn_hor(i)=mncol(i)-mncol(1)-dist_bonylandmark_hor(i);
%horizontal movement from original location with respect to bony landmark
    mn_coordinates(:,i)=[mnrow(i);mncol(i)];%;dist_mn_vert;dist_mn_hor];
    %define new median nerve template using edge detection
[mntemplate,mnroi,vertex_col,vertex_row]=edge_detection(vertex_col,vertex_row
,mnroi,mntemplate,mntempimage,mnrow(i),mncol(i),dist_mn_vert_temp,dist_mn_hor
_temp,mnroioriginal);
    vertex_col=vertex_col+start_col;
    vertex_row=vertex_row+start_row;
    vertex_archive(:,1,i)=vertex_row;
    vertex_archive(:,2,i)=vertex_col;
    vertex_col=vertex_col-start_col;
    vertex_row=vertex_row-start_row;
    stats_temp = regionprops(mnroi,mntemplate,'Extent');
    close;
    mncorr_adjustment=1*(1-stats_temp.Extent);
end
save('vertex_archive.mat','vertex_archive');
save('corrections.mat','corrections');
%call weighting and smoothing filter for mntemplate vertices and coordinates
of mn and bony landmark
[vertex_archive_smoothed,mn_coordinates_smoothed,bony_coordinates_smoothed,ve
rtex_archive_weighted,mn_coordinates_weighted,bony_coordinates_weighted]=weig
hted_smoothing_filter(vertex_archive,mnrow,mncol,bonyrow,bonycol);
%save weighted and smoothed results
save('vertex_archive_smoothed.mat','vertex_archive_smoothed');
save('vertex_archive_weighted.mat','vertex_archive_weighted');
save('mn_coordinates_smoothed.mat','mn_coordinates_smoothed');
save('mn_coordinates_weighted.mat','mn_coordinates_weighted');
save('bony_coordinates_smoothed.mat','bony_coordinates_smoothed');
save('bony_coordinates_weighted.mat','bony_coordinates_weighted');
%calculate stats using regionprops for smoothed vertices
for i=1:size(vertex_archive_smoothed,3)
    tempimage=imread(file_list(3+(i-1)).name);
    clear mnroi mntemplate
mnroi=roipoly(tempimage,vertex_archive_smoothed(:,2,i),vertex_archive_smoothe
d(:,1,i));
    [r,c]=find(mnroi==1);
    for a=min(r):max(r)
        for b=min(c):max(c)
            if mnroi(a,b)==1
                mntemplate(a-min(r)+1,b-min(c)+1)=tempimage(a,b);
            end
        end
    end
```

```
    clear mnroi
    for a=1:size(mntemplate,1)
        for b=1:size(mntemplate,2)
            if mntemplate(a,b)>0
                mnroi(a,b)=1;
            end
        end
    end
    %create a label matrix for use in regionprops
    mnroi=bwlabel(mnroi);
    stats_smoothed(1,i) =
regionprops(mnroi,mntemplate,'Area','Centroid','Orientation','MajorAxisLength
','MinorAxisLength','MeanIntensity');
    centroidcol(1,i)=stats_smoothed(1,i).Centroid(1);
    centroidrow(1,i)=stats_smoothed(1,i).Centroid(2);
end
centroid_coordinates=[centroidrow;centroidcol];
save('stats_smoothed.mat','stats_smoothed');
save('centroid_coordinates.mat','centroid_coordinates');
%calculate key variables (mn max & min hor and vert displacement from
original location, max & min FR, max & min echointensity...)
[displacementfulldata,displacementkeymeasures,deformationfulldata,deformation
keymeasures,echointensityfulldata,echointensitykeymeasures]=keyvariables(stat
s_smoothed,mn_coordinates_smoothed,bony_coordinates_smoothed,centroid_coordin
ates);
%save key variables
save('displacementfulldata.mat','displacementfulldata');
save('displacementkeymeasures.mat','displacementkeymeasures');
save('deformationfulldata.mat','deformationfulldata');
save('deformationkeymeasures.mat','deformationkeymeasures');
save('echointensityfulldata.mat','echointensityfulldata');
save('echointensitykeymeasures.mat','echointensitykeymeasures');
%write output to txt file
cd('S:\Protocols\Boninger\Ultrasound');
fid=fopen('nervemovementkeyvariables.txt','a');
num_frames=size(vertex_archive_smoothed,3);
fprintf(fid,'%s\t%f\t%f\t%f\t%f\t%f\t%f\t%f\t%f\t%f\t%f\t%f\t%f\t%f\t%f\t%f\t%f\t
%f\t%f\t%f\t%f\t%f\t%f\t%f\t%f\t%f\t%f\t%f\t%f\t%f\t%f\t%f\t%f\t%f\t%f\t%f\t%f\t%
f\t%f\t%f\t%f\t%f\t%f\t%f\t%f\t%f\n',...
videoid,length(corrections),num_frames,displacementkeymeasures,deformationkey
measures,echointensitykeymeasures);
fclose(fid);
figure;hold on;plot(mn_coordinates(2,:));plot(displacementfulldata(2,:));
figure;plot(displacementfulldata(4,:));
end
%-----------------------------------------------------------------
function
[mntemplate,mnroi,vertex_col,vertex_row]=edge_detection(vertex_col,vertex_row
,mnroi,mntemplate,mntempimage,mnrow,mncol,dist_mn_vert_temp,dist_mn_hor_temp,
mnroioriginal)
%find the approximate foci of the ellipse. use these points as starting
%points when searching for the left 3 and right 3 points
% right_focus_col=floor(mncol-size(mntemplate,2)/2+stats.MajorAxisLength
/2*.75*cos(stats.Orientation*pi/180));
% left_focus_row=floor((vertex_row(2)+vertex_row(12))/2);
% right_focus_row=floor((vertex_row(6)+vertex_row(8))/2);
```

```
% right_focus_col=floor(mncol-size(mntemplate,2)/2+stats.MajorAxisLength
/2*.75*cos(stats.Orientation*pi/180));
% left_focus_row=floor(mnrow-size(mntemplate,1)/2+stats.MajorAxisLength
/2*.75*sin(stats.Orientation*pi/180));
% left_focus_col=floor(mncol+dist_mn_hor_temp-size(mntemplate,2)/2-
stats.MajorAxisLength/2*.75*cos(stats.Orientation*pi/180));
%left_focus_col=floor(mncol-size(mntemplate,2)/2-stats.MajorAxisLength
/2*.75*cos(stats.Orientation*pi/180));
left_focus_row=floor((vertex_row(2)+vertex_row(12))/2);
left_focus_col=floor((vertex_col(2)+vertex_col(12))/2+.5*dist_mn_hor_temp);
% right_focus_row=floor(mnrow-size(mntemplate,1)/2-
stats.MajorAxisLength/2*.75*sin(stats.Orientation*pi/180));
% right_focus_col=floor(mncol+dist_mn_hor_temp-size(mntemplate,2)
/2+stats.MajorAxisLength/2*.75*cos(stats.Orientation*pi/180));
%right_focus_col=floor(mncol-size(mntemplate,2)/2+stats.MajorAxisLength
/2*.75*cos(stats.Orientation*pi/180));
right_focus_row=floor((vertex_row(6)+vertex_row(8))/2);
right_focus_col=floor((vertex_col(6)+vertex_col(8))/2+.5*dist_mn_hor_temp);
% left_quarter_col=floor(mncol+dist_mn_hor_temp-size(mntemplate,2)/2-
stats.MajorAxisLength/4*.75*cos(stats.Orientation*pi/180));
%left_quarter_col=floor(mncol-size(mntemplate,2)/2-
stats.MajorAxisLength/4*.75*cos(stats.Orientation*pi/180));
left_quarter_row=floor((vertex_row(3)+vertex_row(11))/2);
left_quarter_col=floor((vertex_col(3)+vertex_col(11))/2+.5*dist_mn_hor_temp);
% center_col=floor(mncol+dist_mn_hor_temp-size(mntemplate,2)/2);
%center_col=floor(mncol-size(mntemplate,2)/2);
center_row=floor((vertex_row(4)+vertex_row(10))/2);
center_col=floor((vertex_col(4)+vertex_col(10))/2+.5*dist_mn_hor_temp);
% right_quarter_col=floor(mncol+dist_mn_hor_temp-size(mntemplate,2)
/2+stats.MajorAxisLength/4*.75*cos(stats.Orientation*pi/180));
%right_quarter_col=floor(mncol-size(mntemplate,2)
/2+stats.MajorAxisLength/4*.75*cos(stats.Orientation*pi/180));
right_quarter_row=floor((vertex_row(5)+vertex_row(9))/2);
right_quarter_col=floor((vertex_col(5)+vertex_col(9))/2+.5*dist_mn_hor_temp);
% left_focus_height=vertex_row(12)-vertex_row(2);
% right_focus_height=vertex_row(8)-vertex_row(6);
% left_quarter_height=vertex_row(11)-vertex_row(3);
% right_quarter_height=vertex_row(9)-vertex_row(5);
% center_height=vertex_row(10)-vertex_row(4);
% figure;imshow(mntempimage);hold on;plot(left_focus_col, left_focus_row,
'b*');plot(right_focus_col, right_focus_row, 'b*');
% plot(left_quarter_col, left_quarter_row, 'b*');plot(right_quarter_col,
right_quarter_row, 'b*');plot(center_col, center_row, 'b*');
% plot(vertex_col,vertex_row,'b*');plot(mncol,mnrow,'b*');pause;close;
% Find new left triad (left edge - point 1, far top left - point 2, far
bottom left - point 12)
% 1 -------------------------------------------------------------
clear edgevalues* *indices  c d e modecount *searchrange %slopeedgevalues
slope3edgevalues mean3edgevalues cmaxindices dmaxindices emaxindices
% if (left_focus_col-5:-1:vertex_col(1)-5) < 5
%     searchrange=left_focus_col-5:-1:vertex_col(1)-10;
% else
%     searchrange=left_focus_col-5:-1:vertex_col(1)-5;
% end
searchrange=mncol-size(mntemplate,2)+5+dist_mn_hor_temp:-1:mncol-
size(mntemplate,2)-5+dist_mn_hor_temp;
searchrange=int8(searchrange);
```

```
edgevalues=mntempimage(left_focus_row-5:left_focus_row+5, searchrange);
edgevalues=double(edgevalues);
for i=1:size(edgevalues,1)
    for j=1:size(edgevalues,2)-3
        edgevaluesmean3(i,j)=mean(edgevalues(i,j:j+2));
    end
end
% edgevaluesmean3slope=diff(edgevaluesmean3);
figure;plot(edgevalues');figure;plot(edgevaluesmean3');figure;plot(edgevalues
mean3slope');
% figure;imshow(uint8(edgevalues));pause;close all;
[d,dmaxindices]=max(edgevaluesmean3);
modecount=histc(dmaxindices,1:1:size(edgevaluesmean3,1));
count=0;
while count<2
    newvertexoffset=mode(dmaxindices);
    if newvertexoffset == 1
        modesearchrange=newvertexoffset:newvertexoffset+1;
    elseif newvertexoffset == length(modecount)
        modesearchrange=newvertexoffset-1:newvertexoffset;
    else
        modesearchrange=newvertexoffset-1:1:newvertexoffset+1;
    end
    if sum(modecount(modesearchrange))>=6
        x=find(dmaxindices == newvertexoffset);
        meanintensityatmode = mean(d(x));
        if meanintensityatmode>100
            vertex_col(1)=left_focus_col-newvertexoffset;
            count=2;
        end
    else
        modecount(newvertexoffset)=0;
    end
    count=count+1;
end
vertex_row(1)=left_focus_row;
vertex_col(13)=vertex_col(1);
vertex_row(13)=vertex_row(1);
% 2 ------------------------------------------------------------
clear edgevalues* *indices  c d e modecount *searchrange %slopeedgevalues
slope3edgevalues mean3edgevalues cmaxindices dmaxindices emaxindices
if (left_focus_row:-1:vertex_row(2)-5) < 5
    searchrange=left_focus_row:-1:vertex_row(2)-10;
else
    searchrange=left_focus_row:-1:vertex_row(2)-5;
end
searchrange=int8(searchrange);
edgevalues=mntempimage(searchrange, left_focus_col-5:left_focus_col+5);%-
floor(.167*left_focus_height)
edgevalues=double(edgevalues);
for i=1:size(edgevalues,1)-3
    for j=1:size(edgevalues,2)
        edgevaluesmean3(i,j)=mean(edgevalues(i:i+2,j));
    end
end
% edgevaluesmean3slope=diff(edgevaluesmean3);
```

```
figure;plot(edgevalues);figure;plot(edgevaluesmean3);figure;plot(edgevaluesme
an3slope);
% figure;imshow(uint8(edgevalues));pause;close all;
[d,dmaxindices]=max(edgevaluesmean3);
modecount=histc(dmaxindices,1:1:size(edgevaluesmean3,1));
count=0;
while count<2
    newvertexoffset=mode(dmaxindices);
    if newvertexoffset == 1
        modesearchrange=newvertexoffset:newvertexoffset+1;
    elseif newvertexoffset == length(modecount)
        modesearchrange=newvertexoffset-1:newvertexoffset;
    else
        modesearchrange=newvertexoffset-1:1:newvertexoffset+1;
    end
    if sum(modecount(modesearchrange))>=6
        x=find(dmaxindices == newvertexoffset);
        meanintensityatmode = mean(d(x));
        if meanintensityatmode>100
            vertex_row(2)=left_focus_row-newvertexoffset;
            count=2;
        end
    else
        modecount(newvertexoffset)=0;
    end
    count=count+1;
end
vertex_col(2)=left_focus_col;
% 12 ------------------------------------------------------------
clear edgevalues* *indices  c d e modecount *searchrange %slopeedgevalues
slope3edgevalues mean3edgevalues cmaxindices dmaxindices emaxindices
if (left_focus_row:vertex_row(12)+5) < 5
    searchrange=left_focus_row:vertex_row(12)+10;
else
    searchrange=left_focus_row:vertex_row(12)+5;
end
searchrange=int8(searchrange);
edgevalues=mntempimage(searchrange, left_focus_col-
5:left_focus_col+5);%+floor(.167*left_focus_height)
edgevalues=double(edgevalues);
for i=1:size(edgevalues,1)-3
    for j=1:size(edgevalues,2)
        edgevaluesmean3(i,j)=mean(edgevalues(i:i+2,j));
    end
end
% edgevaluesmean3slope=diff(edgevaluesmean3);
figure;plot(edgevalues);figure;plot(edgevaluesmean3);figure;plot(edgevaluesme
an3slope);
% figure;imshow(uint8(edgevalues));pause;close all;
[d,dmaxindices]=max(edgevaluesmean3);
modecount=histc(dmaxindices,1:1:size(edgevaluesmean3,1));
count=0;
while count<2
    newvertexoffset=mode(dmaxindices);
    if newvertexoffset == 1
        modesearchrange=newvertexoffset:newvertexoffset+1;
    elseif newvertexoffset == length(modecount)
```

```
        modesearchrange=newvertexoffset-1:newvertexoffset;
    else
        modesearchrange=newvertexoffset-1:1:newvertexoffset+1;
    end
    if sum(modecount(modesearchrange))>=6
        x=find(dmaxindices == newvertexoffset);
        meanintensityatmode = mean(d(x));
        if meanintensityatmode>100
            vertex_row(12)=left_focus_row+newvertexoffset;
            count=2;
        end
    else
        modecount(newvertexoffset)=0;
    end
    count=count+1;
end
vertex_col(12)=left_focus_col;
% Find new right triad (right edge - point 6, far top right - point 7, far
bottom right - point 8)
% 7 ----------------------------------------------------------------
clear edgevalues* *indices  c d e modecount modesearchrange %slopeedgevalues
slope3edgevalues mean3edgevalues cmaxindices dmaxindices emaxindices
% if (right_focus_col+5:mncol+10) < 5
%     searchrange=right_focus_col+5:mncol+15;
% else
%     searchrange=right_focus_col+5:mncol+10;
% end
searchrange=mncol-5+dist_mn_hor_temp:mncol+5+dist_mn_hor_temp;
searchrange=int8(searchrange);
edgevalues=mntempimage(right_focus_row-5:right_focus_row+5, searchrange);
edgevalues=double(edgevalues);
for i=1:size(edgevalues,1)
    for j=1:size(edgevalues,2)-3
        edgevaluesmean3(i,j)=mean(edgevalues(i,j:j+2));
    end
end
% edgevaluesmean3slope=diff(edgevaluesmean3);
figure;plot(edgevalues');figure;plot(edgevaluesmean3');figure;plot(edgevalues
mean3slope');
% figure;imshow(uint8(edgevalues));pause;close all;
[d,dmaxindices]=max(edgevaluesmean3);
modecount=histc(dmaxindices,1:1:size(edgevaluesmean3,1));
count=0;
while count<2
    newvertexoffset=mode(dmaxindices);
    if newvertexoffset == 1
        modesearchrange=newvertexoffset:newvertexoffset+1;
    elseif newvertexoffset == length(modecount)
        modesearchrange=newvertexoffset-1:newvertexoffset;
    else
        modesearchrange=newvertexoffset-1:1:newvertexoffset+1;
    end
    if sum(modecount(modesearchrange))>=6
        x=find(dmaxindices == newvertexoffset);
        meanintensityatmode = mean(d(x));
        if meanintensityatmode>100
            vertex_col(7)=right_focus_col+newvertexoffset;
```

```
            count=2;
        end
    else
        modecount(newvertexoffset)=0;
    end
    count=count+1;
end
vertex_row(7)=right_focus_row;
% 6 ------------------------------------------------------------
clear edgevalues* *indices  c d e modecount modesearchrange %slopeedgevalues
slope3edgevalues mean3edgevalues cmaxindices dmaxindices emaxindices
if (right_focus_row:-1:vertex_row(6)-5) < 5
    searchrange=right_focus_row:-1:vertex_row(6)-10;
else
    searchrange=right_focus_row:-1:vertex_row(6)-5;
end
searchrange=int8(searchrange);
edgevalues=mntempimage(searchrange, right_focus_col-5:right_focus_col+5);%-
floor(.167*right_focus_height)
edgevalues=double(edgevalues);
for i=1:size(edgevalues,1)-3
    for j=1:size(edgevalues,2)
        edgevaluesmean3(i,j)=mean(edgevalues(i:i+2,j));
    end
end
% edgevaluesmean3slope=diff(edgevaluesmean3);
figure;plot(edgevalues);figure;plot(edgevaluesmean3);figure;plot(edgevaluesme
an3slope);
% figure;imshow(uint8(edgevalues));pause;close all;
[d,dmaxindices]=max(edgevaluesmean3);
modecount=histc(dmaxindices,1:1:size(edgevaluesmean3,1));
count=0;
while count<2
    newvertexoffset=mode(dmaxindices);
    if newvertexoffset == 1
        modesearchrange=newvertexoffset:newvertexoffset+1;
    elseif newvertexoffset == length(modecount)
        modesearchrange=newvertexoffset-1:newvertexoffset;
    else
        modesearchrange=newvertexoffset-1:1:newvertexoffset+1;
    end
    if sum(modecount(modesearchrange))>=6
        x=find(dmaxindices == newvertexoffset);
        meanintensityatmode = mean(d(x));
        if meanintensityatmode>100
            vertex_row(6)=right_focus_row-newvertexoffset;
            count=2;
        end
    else
        modecount(newvertexoffset)=0;
    end
    count=count+1;
end
vertex_col(6)=right_focus_col;
% 8 ------------------------------------------------------------
clear edgevalues* *indices  c d e modecount modesearchrange %slopeedgevalues
slope3edgevalues mean3edgevalues cmaxindices dmaxindices emaxindices
```

```
if (right_focus_row:vertex_row(8)+5) < 5
    searchrange=right_focus_row:vertex_row(8)+10;
else
    searchrange=right_focus_row:vertex_row(8)+5;
end
searchrange=int8(searchrange);
edgevalues=mntempimage(searchrange, right_focus_col-
5:right_focus_col+5);%+floor(.167*right_focus_height)
edgevalues=double(edgevalues);
for i=1:size(edgevalues,1)-3
    for j=1:size(edgevalues,2)
        edgevaluesmean3(i,j)=mean(edgevalues(i:i+2,j));
    end
end
% edgevaluesmean3slope=diff(edgevaluesmean3);
figure;plot(edgevalues);figure;plot(edgevaluesmean3);figure;plot(edgevaluesme
an3slope);
% figure;imshow(uint8(edgevalues));pause;close all;
[d,dmaxindices]=max(edgevaluesmean3);
modecount=histc(dmaxindices,1:1:size(edgevaluesmean3,1));
count=0;
while count<2
    newvertexoffset=mode(dmaxindices);
    if newvertexoffset == 1
        modesearchrange=newvertexoffset:newvertexoffset+1;
    elseif newvertexoffset == length(modecount)
        modesearchrange=newvertexoffset-1:newvertexoffset;
    else
        modesearchrange=newvertexoffset-1:1:newvertexoffset+1;
    end
    if sum(modecount(modesearchrange))>=6
        x=find(dmaxindices == newvertexoffset);
        meanintensityatmode = mean(d(x));
        if meanintensityatmode>100
            vertex_row(8)=right_focus_row+newvertexoffset;
            count=2;
        end
    else
        modecount(newvertexoffset)=0;
    end
    count=count+1;
end
vertex_col(8)=right_focus_col;
% top of nerve -- only look for a horizontal edge (plot the vertical pixels)
for vertices 3-5
% 3 ------------------------------------------------------------
clear edgevalues* *indices  c d e modecount modesearchrange %slopeedgevalues
slope3edgevalues mean3edgevalues cmaxindices dmaxindices emaxindices
if (left_quarter_row:-1:vertex_row(3)-5) < 5
    searchrange=left_quarter_row:-1:vertex_row(3)-10;
else
    searchrange=left_quarter_row:-1:vertex_row(3)-5;
end
searchrange=int8(searchrange);
edgevalues=mntempimage(searchrange, left_quarter_col-5:left_quarter_col+5);%-
floor(.167*left_quarter_height)
edgevalues=double(edgevalues);
```

```
for i=1:size(edgevalues,1)-3
    for j=1:size(edgevalues,2)
        edgevaluesmean3(i,j)=mean(edgevalues(i:i+2,j));
    end
end
% edgevaluesmean3slope=diff(edgevaluesmean3);
figure;plot(edgevalues);figure;plot(edgevaluesmean3);figure;plot(edgevaluesme
an3slope);
% figure;imshow(uint8(edgevalues));pause;close all;
[d,dmaxindices]=max(edgevaluesmean3);
modecount=histc(dmaxindices,1:1:size(edgevaluesmean3,1));
count=0;
while count<2
    newvertexoffset=mode(dmaxindices);
    if newvertexoffset == 1
        modesearchrange=newvertexoffset:newvertexoffset+1;
    elseif newvertexoffset == length(modecount)
        modesearchrange=newvertexoffset-1:newvertexoffset;
    else
        modesearchrange=newvertexoffset-1:1:newvertexoffset+1;
    end
    if sum(modecount(modesearchrange))>=6
        x=find(dmaxindices == newvertexoffset);
        meanintensityatmode = mean(d(x));
        if meanintensityatmode>100
            vertex_row(3)=left_quarter_row-newvertexoffset;
            count=2;
        end
    else
        modecount(newvertexoffset)=0;
    end
    count=count+1;
end
vertex_col(3)=left_quarter_col;
% 4 ------------------------------------------------------------
clear edgevalues* *indices  c d e modecount modesearchrange %slopeedgevalues
slope3edgevalues mean3edgevalues cmaxindices dmaxindices emaxindices
if (center_row:-1:vertex_row(4)-5) < 5
    searchrange=center_row:-1:vertex_row(4)-10;
else
    searchrange=center_row:-1:vertex_row(4)-5;
end
searchrange=int8(searchrange);
edgevalues=mntempimage(searchrange, center_col-5:center_col+5);%-
floor(.167*center_height)
edgevalues=double(edgevalues);
for i=1:size(edgevalues,1)-3
    for j=1:size(edgevalues,2)
        edgevaluesmean3(i,j)=mean(edgevalues(i:i+2,j));
    end
end
% edgevaluesmean3slope=diff(edgevaluesmean3);
figure;plot(edgevalues);figure;plot(edgevaluesmean3);figure;plot(edgevaluesme
an3slope);
% figure;imshow(uint8(edgevalues));pause;close all;
[d,dmaxindices]=max(edgevaluesmean3);
modecount=histc(dmaxindices,1:1:size(edgevaluesmean3,1));
```

```
count=0;
while count<2
    newvertexoffset=mode(dmaxindices);
    if newvertexoffset == 1
        modesearchrange=newvertexoffset:newvertexoffset+1;
    elseif newvertexoffset == length(modecount)
        modesearchrange=newvertexoffset-1:newvertexoffset;
    else
        modesearchrange=newvertexoffset-1:1:newvertexoffset+1;
    end
    if sum(modecount(modesearchrange))>=6
        x=find(dmaxindices == newvertexoffset);
        meanintensityatmode = mean(d(x));
        if meanintensityatmode>100
            vertex_row(4)=center_row-newvertexoffset;
            count=2;
        end
    else
        modecount(newvertexoffset)=0;
    end
    count=count+1;
end
vertex_col(4)=center_col;
% 5 ----------------------------------------------------------------
clear edgevalues* *indices  c d e modecount modesearchrange %slopeedgevalues
slope3edgevalues mean3edgevalues cmaxindices dmaxindices emaxindices
if (right_quarter_row:-1:vertex_row(5)-5) < 5
    searchrange=right_quarter_row:-1:vertex_row(5)-10;
else
    searchrange=right_quarter_row:-1:vertex_row(5)-5;
end
searchrange=int8(searchrange);
edgevalues=mntempimage(searchrange, right_quarter_col-
5:right_quarter_col+5);%-floor(.167*right_quarter_height)
edgevalues=double(edgevalues);
for i=1:size(edgevalues,1)-3
    for j=1:size(edgevalues,2)
        edgevaluesmean3(i,j)=mean(edgevalues(i:i+2,j));
    end
end
% edgevaluesmean3slope=diff(edgevaluesmean3);
figure;plot(edgevalues);figure;plot(edgevaluesmean3);figure;plot(edgevaluesme
an3slope);
% figure;imshow(uint8(edgevalues));pause;close all;
[d,dmaxindices]=max(edgevaluesmean3);
modecount=histc(dmaxindices,1:1:size(edgevaluesmean3,1));
count=0;
while count<2
    newvertexoffset=mode(dmaxindices);
    if newvertexoffset == 1
        modesearchrange=newvertexoffset:newvertexoffset+1;
    elseif newvertexoffset == length(modecount)
        modesearchrange=newvertexoffset-1:newvertexoffset;
    else
        modesearchrange=newvertexoffset-1:1:newvertexoffset+1;
    end
    if sum(modecount(modesearchrange))>=6
```

```
        x=find(dmaxindices == newvertexoffset);
        meanintensityatmode = mean(d(x));
        if meanintensityatmode>100
            vertex_row(5)=right_quarter_row-newvertexoffset;
            count=2;
        end
    else
        modecount(newvertexoffset)=0;
    end
    count=count+1;
end
vertex_col(5)=right_quarter_col;
% % bottom of nerve -- only look for a horizontal edge (plot the vertical
pixels) for vertices 9-11
% 9 ------------------------------------------------------------
clear edgevalues* *indices  c d e modecount modesearchrange %slopeedgevalues
slope3edgevalues mean3edgevalues cmaxindices dmaxindices emaxindices
if (right_quarter_row:vertex_row(9)+5) < 5
    searchrange=right_quarter_row:vertex_row(9)+10;
else
    searchrange=right_quarter_row:vertex_row(9)+5;
end
searchrange=int8(searchrange);
edgevalues=mntempimage(searchrange, right_quarter_col-
5:right_quarter_col+5);%-floor(.167*right_quarter_height)
edgevalues=double(edgevalues);
for i=1:size(edgevalues,1)-3
    for j=1:size(edgevalues,2)
        edgevaluesmean3(i,j)=mean(edgevalues(i:i+2,j));
    end
end
% edgevaluesmean3slope=diff(edgevaluesmean3);
figure;plot(edgevalues);figure;plot(edgevaluesmean3);figure;plot(edgevaluesme
an3slope);
% figure;imshow(uint8(edgevalues));pause;close all;
[d,dmaxindices]=max(edgevaluesmean3);
modecount=histc(dmaxindices,1:1:size(edgevaluesmean3,1));
count=0;
while count<2
    newvertexoffset=mode(dmaxindices);
    if newvertexoffset == 1
        modesearchrange=newvertexoffset:newvertexoffset+1;
    elseif newvertexoffset == length(modecount)
        modesearchrange=newvertexoffset-1:newvertexoffset;
    else
        modesearchrange=newvertexoffset-1:1:newvertexoffset+1;
    end
    if sum(modecount(modesearchrange))>=6
        x=find(dmaxindices == newvertexoffset);
        meanintensityatmode = mean(d(x));
        if meanintensityatmode>100
            vertex_row(9)=right_quarter_row+newvertexoffset;
            count=2;
        end
    else
        modecount(newvertexoffset)=0;
    end
```

```
    count=count+1;
end
vertex_col(9)=right_quarter_col;
% 10 ------------------------------------------------------------
clear edgevalues* *indices  c d e modecount modesearchrange %slopeedgevalues
slope3edgevalues mean3edgevalues cmaxindices dmaxindices emaxindices
if (center_row:vertex_row(10)+5) < 5
    searchrange=center_row:vertex_row(10)+10;
else
    searchrange=center_row:vertex_row(10)+5;
end
searchrange=int8(searchrange);
edgevalues=mntempimage(searchrange, center_col-5:center_col+5);%-
floor(.167*center_height)
edgevalues=double(edgevalues);
for i=1:size(edgevalues,1)-3
    for j=1:size(edgevalues,2)
        edgevaluesmean3(i,j)=mean(edgevalues(i:i+2,j));
    end
end
% edgevaluesmean3slope=diff(edgevaluesmean3);
figure;plot(edgevalues);figure;plot(edgevaluesmean3);figure;plot(edgevaluesme
an3slope);
% figure;imshow(uint8(edgevalues));pause;close all;
[d,dmaxindices]=max(edgevaluesmean3);
modecount=histc(dmaxindices,1:1:size(edgevaluesmean3,1));
count=0;
while count<2
    newvertexoffset=mode(dmaxindices);
    if newvertexoffset == 1
        modesearchrange=newvertexoffset:newvertexoffset+1;
    elseif newvertexoffset == length(modecount)
        modesearchrange=newvertexoffset-1:newvertexoffset;
    else
        modesearchrange=newvertexoffset-1:1:newvertexoffset+1;
    end
    if sum(modecount(modesearchrange))>=6
        x=find(dmaxindices == newvertexoffset);
        meanintensityatmode = mean(d(x));
        if meanintensityatmode>100
            vertex_row(10)=center_row+newvertexoffset;
            count=2;
        end
    else
        modecount(newvertexoffset)=0;
    end
    count=count+1;
end
vertex_col(10)=center_col;
% 11 ------------------------------------------------------------
clear edgevalues* *indices  c d e modecount modesearchrange %slopeedgevalues
slope3edgevalues mean3edgevalues cmaxindices dmaxindices emaxindices
if (left_quarter_row:vertex_row(11)+5) < 5
    searchrange=left_quarter_row:vertex_row(11)+10;
else
    searchrange=left_quarter_row:vertex_row(11)+5;
end
```

```
searchrange=int8(searchrange);
edgevalues=mntempimage(searchrange, left_quarter_col-
5:left_quarter_col+5);%+floor(.167*left_quarter_height)
edgevalues=double(edgevalues);
for i=1:size(edgevalues,1)-3
    for j=1:size(edgevalues,2)
        edgevaluesmean3(i,j)=mean(edgevalues(i:i+2,j));
    end
end
% edgevaluesmean3slope=diff(edgevaluesmean3);
figure;plot(edgevalues);figure;plot(edgevaluesmean3);figure;plot(edgevaluesme
an3slope);
% figure;imshow(uint8(edgevalues));pause;close all;
[d,dmaxindices]=max(edgevaluesmean3);
modecount=histc(dmaxindices,1:1:size(edgevaluesmean3,1));
count=0;
while count<2
    newvertexoffset=mode(dmaxindices);
    if newvertexoffset == 1
        modesearchrange=newvertexoffset:newvertexoffset+1;
    elseif newvertexoffset == length(modecount)
        modesearchrange=newvertexoffset-1:newvertexoffset;
    else
        modesearchrange=newvertexoffset-1:1:newvertexoffset+1;
    end
    if sum(modecount(modesearchrange))>=6
        x=find(dmaxindices == newvertexoffset);
        meanintensityatmode = mean(d(x));
        if meanintensityatmode>100
            vertex_row(11)=left_quarter_row+newvertexoffset;
            count=2;
        end
    else
        modecount(newvertexoffset)=0;
    end
    count=count+1;
end
vertex_col(11)=left_quarter_col;
%create new template
clear mnroi mntemplate
[mnroi,vertex_col,vertex_row]=roipoly(mntempimage,vertex_col,vertex_row);
% figure;imshow(mnroioriginal); figure;imshow(mnroi);
[r,c]=find(mnroi==1);
for a=min(r):max(r)
    for b=min(c):max(c)
        if mnroi(a,b)==1
            mntemplate(a-min(r)+1,b-min(c)+1)=mntempimage(a,b);
        end
    end
end
clear mnroi
for a=1:size(mntemplate,1)
    for b=1:size(mntemplate,2)
        if mntemplate(a,b)>0
            mnroi(a,b)=1;
        end
    end
```

```
end
%figure;imshow(mntemplate)
%create a label matrix for use in regionprops
mnroi=bwlabel(mnroi);
% figure;imshow(mntempimage);hold on;plot(left_focus_col, left_focus_row,
'b*');plot(right_focus_col, right_focus_row, 'b*');
% plot(left_quarter_col, left_quarter_row, 'b*');plot(right_quarter_col,
right_quarter_row, 'b*');plot(center_col, center_row, 'b*');
% plot(vertex_col,vertex_row,'b*');plot(mncol,mnrow,'b*');pause;close;
end
%-----------------------------------------------------------------

%-----------------------------------------------------------------
function
[vertex_archive_smoothed,mn_coordinates_smoothed,bony_coordinates_smoothed,ve
rtex_archive_weighted,mn_coordinates_weighted,bony_coordinates_weighted]=weig
hted_smoothing_filter(vertex_archive,mnrow,mncol,bonyrow,bonycol)
% mnrow=mn_coordinates(1,:);mncol=mn_coordinates(2,:);
% bonyrow=bony_coordinates(1,:);bonycol=bony_coordinates(2,:);
vertex_archive_weighted=floor(vertex_archive);
for vk=1:size(vertex_archive,3)
    for vi=1:size(vertex_archive,1)
        for vj=1:size(vertex_archive,2)
            if vk==5
vertex_archive_weighted(vi,vj,vk)=floor(.5*vertex_archive(vi,vj,1)+.5*vertex_
archive(vi,vj,10));
            end
            if vk>=10 && vk<size(vertex_archive,3)-5
                if rem(vk,10)==5
vertex_archive_weighted(vi,vj,vk)=floor(.5*vertex_archive(vi,vj,vk-
5)+.5*vertex_archive(vi,vj,vk+5));
                end
            end
        end
    end
end
for vk=2:size(vertex_archive,3)
    for vi=1:size(vertex_archive,1)
        for vj=1:size(vertex_archive,2)
            if vk>5 && vk<size(vertex_archive,3)-5
                if rem(vk,10)==0
                    %do nothing
                elseif rem(vk,10)<5
vertex_archive_weighted(vi,vj,vk)=floor(mean([vertex_archive(vi,vj,vk),vertex
_archive(vi,vj,vk-rem(vk,10)),vertex_archive_weighted(vi,vj,vk+5-
rem(vk,10))]));
                elseif rem(vk,10)>5
vertex_archive_weighted(vi,vj,vk)=floor(mean([vertex_archive(vi,vj,vk),vertex
_archive_weighted(vi,vj,vk+5-rem(vk,10)),vertex_archive_weighted(vi,vj,vk+10-
rem(vk,10))]));
                end
            elseif vk<5
vertex_archive_weighted(vi,vj,vk)=floor(mean([vertex_archive(vi,vj,vk),vertex
_archive(vi,vj,1),vertex_archive_weighted(vi,vj,5)]));
            elseif vk>size(vertex_archive,3)-5
vertex_archive_weighted(vi,vj,vk)=floor(mean([vertex_archive(vi,vj,vk),vertex
_archive_weighted(vi,vj,size(vertex_archive,3))]));
```

```
            end
        end
    end
end
for vi=1:size(vertex_archive,1)
    for vj=1:size(vertex_archive,2)
vertex_archive_smoothed(vi,vj,:)=smooth(vertex_archive_weighted(vi,vj,:),5,'m
oving');
    end
end
% mnrow and mncol and bony
mnrow_weighted=mnrow;
mncol_weighted=mncol;
bonyrow_weighted=bonyrow;
bonycol_weighted=bonycol;
for vk=1:size(mnrow,2)
    if vk==5
        mnrow_weighted(vk)=floor(.5*mnrow(1)+.5*mnrow(10));
        mncol_weighted(vk)=floor(.5*mncol(1)+.5*mncol(10));
        bonyrow_weighted(vk)=floor(.5*bonyrow(1)+.5*bonyrow(10));
        bonycol_weighted(vk)=floor(.5*bonycol(1)+.5*bonycol(10));
    end
    if vk>=10 && vk<size(mnrow,2)-5
        if rem(vk,10)==5
            mnrow_weighted(vk)=floor(.5*mnrow(vk-5)+.5*mnrow(vk+5));
            mncol_weighted(vk)=floor(.5*mncol(vk-5)+.5*mncol(vk+5));
            bonyrow_weighted(vk)=floor(.5*bonyrow(vk-5)+.5*bonyrow(vk+5));
            bonycol_weighted(vk)=floor(.5*bonycol(vk-5)+.5*bonycol(vk+5));
        end
    end
end
for vk=1:size(mnrow,2)
    if vk>5 && vk<size(mnrow,2)-5
        if rem(vk,10)==0
            %do nothing
        elseif rem(vk,10)<5
            mnrow_weighted(vk)=floor(mean([mnrow(vk),mnrow(vk-
rem(vk,10)),mnrow_weighted(vk+5-rem(vk,10))]));
            mncol_weighted(vk)=floor(mean([mncol(vk),mncol(vk-
rem(vk,10)),mncol_weighted(vk+5-rem(vk,10))]));
            bonyrow_weighted(vk)=floor(mean([bonyrow(vk),bonyrow(vk-
rem(vk,10)),bonyrow_weighted(vk+5-rem(vk,10))]));
            bonycol_weighted(vk)=floor(mean([bonycol(vk),bonycol(vk-
rem(vk,10)),bonycol_weighted(vk+5-rem(vk,10))]));
        elseif rem(vk,10)>5
            mnrow_weighted(vk)=floor(mean([mnrow(vk),mnrow_weighted(vk+5-
rem(vk,10)),mnrow_weighted(vk+10-rem(vk,10))]));
            mncol_weighted(vk)=floor(mean([mncol(vk),mncol_weighted(vk+5-
rem(vk,10)),mncol_weighted(vk+10-rem(vk,10))]));
bonyrow_weighted(vk)=floor(mean([bonyrow(vk),bonyrow_weighted(vk+5-
rem(vk,10)),bonyrow_weighted(vk+10-rem(vk,10))]));
bonycol_weighted(vk)=floor(mean([bonycol(vk),bonycol_weighted(vk+5-
rem(vk,10)),bonycol_weighted(vk+10-rem(vk,10))]));
        end
    elseif vk<5
mnrow_weighted(vk)=floor(mean([mnrow(vk),mnrow(1),mnrow_weighted(5)]));
mncol_weighted(vk)=floor(mean([mncol(vk),mncol(1),mncol_weighted(5)]));
```

```
bonyrow_weighted(vk)=floor(mean([bonyrow(vk),bonyrow(1),bonyrow_weighted(5)])
);
bonycol_weighted(vk)=floor(mean([bonycol(vk),bonycol(1),bonycol_weighted(5)])
);
    elseif vk>size(mnrow,2)-5
mnrow_weighted(vk)=floor(mean([mnrow(1,vk),mnrow_weighted(size(mnrow,2))]));
mncol_weighted(vk)=floor(mean([mncol(1,vk),mncol_weighted(size(mncol,2))]));
bonyrow_weighted(vk)=floor(mean([bonyrow(1,vk),bonyrow_weighted(size(bonyrow,
2))]));
bonycol_weighted(vk)=floor(mean([bonycol(1,vk),bonycol_weighted(size(bonycol,
2))]));
    end
end
mnrow_smoothed=smooth(mnrow_weighted,5,'moving')';
mncol_smoothed=smooth(mncol_weighted,5,'moving')';
bonyrow_smoothed=smooth(bonyrow_weighted,5,'moving')';
bonycol_smoothed=smooth(bonycol_weighted,5,'moving')';
mn_coordinates_weighted=[mnrow_weighted; mncol_weighted];
mn_coordinates_smoothed=[mnrow_smoothed; mncol_smoothed];
bony_coordinates_weighted=[bonyrow_weighted; bonycol_weighted];
bony_coordinates_smoothed=[bonyrow_smoothed; bonycol_smoothed];
end
%-----------------------------------------------------------------

%-----------------------------------------------------------------
function
[displacementfulldata,displacementkeymeasures,deformationfulldata,deformation
keymeasures,echointensityfulldata,echointensitykeymeasures]=keyvariables(stat
s_smoothed,mn_coordinates_smoothed,bony_coordinates_smoothed,centroid_coordin
ates)
for i = 1:length(mn_coordinates_smoothed)
    centroidprofilerow(1,i)=mn_coordinates_smoothed(1,i)-
centroid_coordinates(1,i);
    centroidprofilecol(1,i)=mn_coordinates_smoothed(2,i)-
centroid_coordinates(2,i);
    centroiddisplacementvert(1,i)=((centroidprofilerow(i)-
centroidprofilerow(1))-(bony_coordinates_smoothed(1,i)-
bony_coordinates_smoothed(1,1)))*(1/13.5);
    centroiddisplacementhor(1,i)=((centroidprofilecol(i)-
centroidprofilecol(1))-(bony_coordinates_smoothed(2,i)-
bony_coordinates_smoothed(2,1)))*(1/13.5);
end
%calculate distance traveled per frame and convert from pixels to mm - 1
pixel = 1/13.5 mm
centroiddistancevert=(diff(centroidprofilerow)-
diff(bony_coordinates_smoothed(1,1:end)))*(1/13.5);
centroiddistancehor=(diff(centroidprofilecol)-
diff(bony_coordinates_smoothed(2,1:end)))*(1/13.5);
for i = 1:length(centroiddistancehor)
centroiddistanceresultant(i)=sqrt(centroiddistancehor(i)^2+centroiddistanceve
rt(i)^2);
end
for i = 1:length(centroiddisplacementhor)
centroiddisplacementresultant(i)=sqrt(centroiddisplacementhor(i)^2+centroiddi
splacementvert(i)^2);
end
centroiddistancevert=smooth(centroiddistancevert,3,'moving')';
```

```
centroiddistancehor=smooth(centroiddistancehor,3,'moving')';
centroiddistanceresultant=smooth(centroiddistanceresultant,3,'moving')';
centroiddisplacementresultant=smooth(centroiddisplacementresultant,3,'moving'
)';
centroidtotaldistancetraveledvert=sum(abs(centroiddistancevert));
centroidtotaldistancetraveledhor=sum(abs(centroiddistancehor));
centroidtotaldistancetraveledresultant=sum(abs(centroiddistanceresultant));
maxcentroiddisplacementvert=max(centroiddisplacementvert);
maxcentroiddisplacementhor=max(centroiddisplacementhor);
maxcentroiddisplacementresultant=max(centroiddisplacementresultant);
mincentroiddisplacementvert=min(centroiddisplacementvert);
mincentroiddisplacementhor=min(centroiddisplacementhor);
mincentroiddisplacementresultant=min(centroiddisplacementresultant);
meancentroiddisplacementvert=mean(centroiddisplacementvert);
meancentroiddisplacementhor=mean(centroiddisplacementhor);
meancentroiddisplacementresultant=mean(centroiddisplacementresultant);
totalcentroiddisplacementvert=maxcentroiddisplacementvert-
mincentroiddisplacementvert;
totalcentroiddisplacementhor=maxcentroiddisplacementhor-
mincentroiddisplacementhor;
totalcentroiddisplacementresultant=maxcentroiddisplacementresultant-
mincentroiddisplacementresultant;
%convert mm/frame to mm/s - 1 frame = 1/33 s given video captured at 33 Hz
centroidvelocityvert=centroiddistancevert/(1/33);
centroidvelocityhor=centroiddistancehor/(1/33);
centroidvelocityresultant=centroiddistanceresultant/(1/33);
maxcentroidvelocityvert=max(centroidvelocityvert);
mincentroidvelocityvert=min(centroidvelocityvert);
meancentroidvelocityvert=mean(abs(centroidvelocityvert));
maxcentroidvelocityhor=max(centroidvelocityhor);
mincentroidvelocityhor=min(centroidvelocityhor);
meancentroidvelocityhor=mean(abs(centroidvelocityhor));
maxcentroidvelocityresultant=max(centroidvelocityresultant);
mincentroidvelocityresultant=min(centroidvelocityresultant);
meancentroidvelocityresultant=mean(abs(centroidvelocityresultant));
for i = 1:length(stats_smoothed)
flatteningratio(i)=stats_smoothed(1,i).MajorAxisLength/stats_smoothed(1,i).Mi
norAxisLength;
    flatteningratiochange(i)=flatteningratio(i)-flatteningratio(1);
    area(i)=stats_smoothed(1,i).Area*(1/13.5)^2;
    areachange(i)=area(i)-area(1);
    intensity(i)=stats_smoothed(1,i).MeanIntensity;
    intensitychange(i)=intensity(i)-intensity(1);
end
maxflatteningratio=max(flatteningratio);
minflatteningratio=min(flatteningratio);
meanflatteningratio=mean(flatteningratio);
maxarea=max(area);
minarea=min(area);
meanarea=mean(area);
maxintensity=max(intensity);
minintensity=min(intensity);
meanintensity=mean(intensity);
maxflatteningratiochange=max(flatteningratiochange);
minflatteningratiochange=min(flatteningratiochange);
meanfalltteningratiochange=mean(flatteningratiochange);
maxareachange=max(areachange);
```

```
minareachange=min(areachange);
meanareachange=mean(areachange);
maxintensitychange=max(intensitychange);
minintensitychange=min(intensitychange);
meanintensitychange=mean(intensitychange);
%add filler so variables are same size
centroiddistancevert=[0 centroiddistancevert];
centroiddistancehor=[0 centroiddistancehor];
centroiddistanceresultant=[0 centroiddistanceresultant];
centroidvelocityvert=[0 centroidvelocityvert];
centroidvelocityhor=[0 centroidvelocityhor];
centroidvelocityresultant=[0 centroidvelocityresultant];
displacementfulldata=[centroidprofilerow; centroidprofilecol;...
    centroiddisplacementvert; centroiddisplacementhor;
centroiddisplacementresultant;...
    centroiddistancevert; centroiddistancehor; centroiddistanceresultant;...
    centroidvelocityvert; centroidvelocityhor; centroidvelocityresultant;];
displacementkeymeasures=[totalcentroiddisplacementvert
totalcentroiddisplacementhor totalcentroiddisplacementresultant...
    centroidtotaldistancetraveledvert centroidtotaldistancetraveledhor
centroidtotaldistancetraveledresultant...
    maxcentroiddisplacementvert maxcentroiddisplacementhor
maxcentroiddisplacementresultant...
    mincentroiddisplacementvert mincentroiddisplacementhor
mincentroiddisplacementresultant...
    meancentroiddisplacementvert meancentroiddisplacementhor
meancentroiddisplacementresultant...
    maxcentroidvelocityvert maxcentroidvelocityhor
maxcentroidvelocityresultant...
    mincentroidvelocityvert mincentroidvelocityhor
mincentroidvelocityresultant...
    meancentroidvelocityvert meancentroidvelocityhor
meancentroidvelocityresultant];
deformationfulldata=[flatteningratio; flatteningratiochange; area;
areachange];
deformationkeymeasures=[maxflatteningratio minflatteningratio
meanflatteningratio maxarea minarea meanarea...
    maxflatteningratiochange minflatteningratiochange
meanfaltteningratiochange maxareachange minareachange meanareachange];
echointensityfulldata=[intensity; intensitychange];
echointensitykeymeasures=[maxintensity minintensity meanintensity
maxintensitychange minintensitychange meanintensitychange];
end
%-----------------------------------------------------------------
clear;  clc;  close all;
cd('S:\Protocols\Boninger\Ultrasound
[filename,dir_path]=uigetfile('*.*', 'Select file in batch directory');
cd(dir_path);  file_list=dir;
videoid=strtok(filename, '.');
videoid=videoid(1:end-3);
load('bony_coordinates_smoothed');bony_coordinates_auto=bony_coordinates_smoo
thed; clear bony_coordinates_smoothed
load('mn_coordinates_smoothed');mn_coordinates_auto=mn_coordinates_smoothed;
clear mn_coordinates_smoothed
load('stats_smoothed.mat');stats_auto=stats_smoothed; clear stats_smoothed
save('stats_auto.mat','stats_auto');
```

```
load('vertex_archive.mat');vertex_archive_auto=vertex_archive; clear
vertex_archive
load('start_col');
load('start_row');
bony_coordinates_auto(2,:)=bony_coordinates_auto(2,:)+start_col;
bony_coordinates_auto(1,:)=bony_coordinates_auto(1,:)+2*start_row;
mn_coordinates_auto(2,:)=mn_coordinates_auto(2,:)+start_col;
mn_coordinates_auto(1,:)=mn_coordinates_auto(1,:)+start_row;
for i=1:10
    i
    tempimage=imread(file_list(21+10*(i-1)).name);
    imshow(tempimage);hold on;
    plot(vertex_archive_auto(:,2,1+10*(i-1)),vertex_archive_auto(:,1,1+10*(i-
1)),'r*');
    plot(bony_coordinates_auto(2,1+10*(i-1)),bony_coordinates_auto(1,1+10*(i-
1)),'b*');plot(mn_coordinates_auto(2,1+10*(i-
1)),mn_coordinates_auto(1,1+10*(i-1)),'r*');
    title('Please select lower right point of bony
landmark');[bonylandmark_end_col,bonylandmark_end_row]=ginput(1);
    bony_coordinates(:,i)=[bonylandmark_end_row;bonylandmark_end_col];
    title('Please trace the median nerve. Press any key when
ready');pause;close;
    %using roipoly we create a logical which specifies which pixels are part
of the median nerve.
    figure;[mnroi,vertex_col,vertex_row]=roipoly(tempimage);close all;
    vertex_archive(:,1,i)=vertex_row;
    vertex_archive(:,2,i)=vertex_col;
    imshow(tempimage);title('Please guess where the bottom right point of the
median nerve template is');
    [mncolguess,mnrowguess]=ginput(1);close;
    mn_coordinates(:,i)=[mnrowguess;mncolguess];
end
x1=1:10:100;x1new=1:1:100;
x2=1:20:100;x2new=1:1:100;
bony_coordinates_interp_10(1,:)=interp1(x1,bony_coordinates(1,:),x1new,'splin
e');
bony_coordinates_interp_10(2,:)=interp1(x1,bony_coordinates(2,:),x1new,'splin
e');
bony_coordinates_interp_20(1,:)=interp1(x2,bony_coordinates(1,1:2:end),x2new,
'spline');
bony_coordinates_interp_20(2,:)=interp1(x2,bony_coordinates(2,1:2:end),x2new,
'spline');
mn_coordinates_interp_10(1,:)=interp1(x1,mn_coordinates(1,:),x1new,'spline');
mn_coordinates_interp_10(2,:)=interp1(x1,mn_coordinates(2,:),x1new,'spline');
mn_coordinates_interp_20(1,:)=interp1(x2,mn_coordinates(1,1:2:end),x2new,'spl
ine');
mn_coordinates_interp_20(2,:)=interp1(x2,mn_coordinates(2,1:2:end),x2new,'spl
ine');
% figure;plot(x2,bony_coordinates(1,1:2:end),'o',x2new,
bony_coordinates_interp_20(1,:));
% hold
on;plot(x2,bony_coordinates(2,1:2:end),'o',x2new,bony_coordinates_interp_20(2
,:));
% figure;plot(bony_coordinates_interp_10(1,:),'b');hold
on;plot(bony_coordinates_interp_20(1,:),'r');
% figure;plot(bony_coordinates_interp_10(2,:),'b');hold
on;plot(bony_coordinates_interp_20(2,:),'r');
```

```
save('bony_coordinates_interp_10.mat','bony_coordinates_interp_10');
save('bony_coordinates_interp_20.mat','bony_coordinates_interp_20');
save('mn_coordinates_interp_10.mat','mn_coordinates_interp_10');
save('mn_coordinates_interp_20.mat','mn_coordinates_interp_20');
%interpolate rows using every 10th point
clear vertex_temp
vertex_temp(1,:)=vertex_archive(1,1,1:end);
vertex_archive_interp_10(1,1,:)=interp1(x1,vertex_temp,x1new,'spline');
vertex_temp(1,:)=vertex_archive(2,1,1:end);
vertex_archive_interp_10(2,1,:)=interp1(x1,vertex_temp,x1new,'spline');
vertex_temp(1,:)=vertex_archive(3,1,1:end);
vertex_archive_interp_10(3,1,:)=interp1(x1,vertex_temp,x1new,'spline');
vertex_temp(1,:)=vertex_archive(4,1,1:end);
vertex_archive_interp_10(4,1,:)=interp1(x1,vertex_temp,x1new,'spline');
vertex_temp(1,:)=vertex_archive(5,1,1:end);
vertex_archive_interp_10(5,1,:)=interp1(x1,vertex_temp,x1new,'spline');
vertex_temp(1,:)=vertex_archive(6,1,1:end);
vertex_archive_interp_10(6,1,:)=interp1(x1,vertex_temp,x1new,'spline');
vertex_temp(1,:)=vertex_archive(7,1,1:end);
vertex_archive_interp_10(7,1,:)=interp1(x1,vertex_temp,x1new,'spline');
vertex_temp(1,:)=vertex_archive(8,1,1:end);
vertex_archive_interp_10(8,1,:)=interp1(x1,vertex_temp,x1new,'spline');
vertex_temp(1,:)=vertex_archive(9,1,1:end);
vertex_archive_interp_10(9,1,:)=interp1(x1,vertex_temp,x1new,'spline');
vertex_temp(1,:)=vertex_archive(10,1,1:end);
vertex_archive_interp_10(10,1,:)=interp1(x1,vertex_temp,x1new,'spline');
vertex_temp(1,:)=vertex_archive(11,1,1:end);
vertex_archive_interp_10(11,1,:)=interp1(x1,vertex_temp,x1new,'spline');
vertex_temp(1,:)=vertex_archive(12,1,1:end);
vertex_archive_interp_10(12,1,:)=interp1(x1,vertex_temp,x1new,'spline');
vertex_archive_interp_10(13,1,:)=vertex_archive_interp_10(1,1,:);
%interpolate cols using every 10th point
clear vertex_temp
vertex_temp(1,:)=vertex_archive(1,2,1:end);
vertex_archive_interp_10(1,2,:)=interp1(x1,vertex_temp,x1new,'spline');
vertex_temp(1,:)=vertex_archive(2,2,1:end);
vertex_archive_interp_10(2,2,:)=interp1(x1,vertex_temp,x1new,'spline');
vertex_temp(1,:)=vertex_archive(3,2,1:end);
vertex_archive_interp_10(3,2,:)=interp1(x1,vertex_temp,x1new,'spline');
vertex_temp(1,:)=vertex_archive(4,2,1:end);
vertex_archive_interp_10(4,2,:)=interp1(x1,vertex_temp,x1new,'spline');
vertex_temp(1,:)=vertex_archive(5,2,1:end);
vertex_archive_interp_10(5,2,:)=interp1(x1,vertex_temp,x1new,'spline');
vertex_temp(1,:)=vertex_archive(6,2,1:end);
vertex_archive_interp_10(6,2,:)=interp1(x1,vertex_temp,x1new,'spline');
vertex_temp(1,:)=vertex_archive(7,2,1:end);
vertex_archive_interp_10(7,2,:)=interp1(x1,vertex_temp,x1new,'spline');
vertex_temp(1,:)=vertex_archive(8,2,1:end);
vertex_archive_interp_10(8,2,:)=interp1(x1,vertex_temp,x1new,'spline');
vertex_temp(1,:)=vertex_archive(9,2,1:end);
vertex_archive_interp_10(9,2,:)=interp1(x1,vertex_temp,x1new,'spline');
vertex_temp(1,:)=vertex_archive(10,2,1:end);
vertex_archive_interp_10(10,2,:)=interp1(x1,vertex_temp,x1new,'spline');
vertex_temp(1,:)=vertex_archive(11,2,1:end);
vertex_archive_interp_10(11,2,:)=interp1(x1,vertex_temp,x1new,'spline');
vertex_temp(1,:)=vertex_archive(12,2,1:end);
vertex_archive_interp_10(12,2,:)=interp1(x1,vertex_temp,x1new,'spline');
```

```
vertex_archive_interp_10(13,2,:)=vertex_archive_interp_10(1,2,:);
%interpolate rows using every 20th point
clear vertex_temp
vertex_temp(1,:)=vertex_archive(1,1,1:2:end);
vertex_archive_interp_20(1,1,:)=interp1(x2,vertex_temp,x2new,'spline');
vertex_temp(1,:)=vertex_archive(2,1,1:2:end);
vertex_archive_interp_20(2,1,:)=interp1(x2,vertex_temp,x2new,'spline');
vertex_temp(1,:)=vertex_archive(3,1,1:2:end);
vertex_archive_interp_20(3,1,:)=interp1(x2,vertex_temp,x2new,'spline');
vertex_temp(1,:)=vertex_archive(4,1,1:2:end);
vertex_archive_interp_20(4,1,:)=interp1(x2,vertex_temp,x2new,'spline');
vertex_temp(1,:)=vertex_archive(5,1,1:2:end);
vertex_archive_interp_20(5,1,:)=interp1(x2,vertex_temp,x2new,'spline');
vertex_temp(1,:)=vertex_archive(6,1,1:2:end);
vertex_archive_interp_20(6,1,:)=interp1(x2,vertex_temp,x2new,'spline');
vertex_temp(1,:)=vertex_archive(7,1,1:2:end);
vertex_archive_interp_20(7,1,:)=interp1(x2,vertex_temp,x2new,'spline');
vertex_temp(1,:)=vertex_archive(8,1,1:2:end);
vertex_archive_interp_20(8,1,:)=interp1(x2,vertex_temp,x2new,'spline');
vertex_temp(1,:)=vertex_archive(9,1,1:2:end);
vertex_archive_interp_20(9,1,:)=interp1(x2,vertex_temp,x2new,'spline');
vertex_temp(1,:)=vertex_archive(10,1,1:2:end);
vertex_archive_interp_20(10,1,:)=interp1(x2,vertex_temp,x2new,'spline');
vertex_temp(1,:)=vertex_archive(11,1,1:2:end);
vertex_archive_interp_20(11,1,:)=interp1(x2,vertex_temp,x2new,'spline');
vertex_temp(1,:)=vertex_archive(12,1,1:2:end);
vertex_archive_interp_20(12,1,:)=interp1(x2,vertex_temp,x2new,'spline');
vertex_archive_interp_20(13,1,:)=vertex_archive_interp_20(1,1,:);
%interpolate cols using every 20th point
clear vertex_temp
vertex_temp(1,:)=vertex_archive(1,2,1:2:end);
vertex_archive_interp_20(1,2,:)=interp1(x2,vertex_temp,x2new,'spline');
vertex_temp(1,:)=vertex_archive(2,2,1:2:end);
vertex_archive_interp_20(2,2,:)=interp1(x2,vertex_temp,x2new,'spline');
vertex_temp(1,:)=vertex_archive(3,2,1:2:end);
vertex_archive_interp_20(3,2,:)=interp1(x2,vertex_temp,x2new,'spline');
vertex_temp(1,:)=vertex_archive(4,2,1:2:end);
vertex_archive_interp_20(4,2,:)=interp1(x2,vertex_temp,x2new,'spline');
vertex_temp(1,:)=vertex_archive(5,2,1:2:end);
vertex_archive_interp_20(5,2,:)=interp1(x2,vertex_temp,x2new,'spline');
vertex_temp(1,:)=vertex_archive(6,2,1:2:end);
vertex_archive_interp_20(6,2,:)=interp1(x2,vertex_temp,x2new,'spline');
vertex_temp(1,:)=vertex_archive(7,2,1:2:end);
vertex_archive_interp_20(7,2,:)=interp1(x2,vertex_temp,x2new,'spline');
vertex_temp(1,:)=vertex_archive(8,2,1:2:end);
vertex_archive_interp_20(8,2,:)=interp1(x2,vertex_temp,x2new,'spline');
vertex_temp(1,:)=vertex_archive(9,2,1:2:end);
vertex_archive_interp_20(9,2,:)=interp1(x2,vertex_temp,x2new,'spline');
vertex_temp(1,:)=vertex_archive(10,2,1:2:end);
vertex_archive_interp_20(10,2,:)=interp1(x2,vertex_temp,x2new,'spline');
vertex_temp(1,:)=vertex_archive(11,2,1:2:end);
vertex_archive_interp_20(11,2,:)=interp1(x2,vertex_temp,x2new,'spline');
vertex_temp(1,:)=vertex_archive(12,2,1:2:end);
vertex_archive_interp_20(12,2,:)=interp1(x2,vertex_temp,x2new,'spline');
vertex_archive_interp_20(13,2,:)=vertex_archive_interp_20(1,2,:);
save('vertex_archive_interp_10.mat','vertex_archive_interp_10');
save('vertex_archive_interp_20.mat','vertex_archive_interp_20');
```

```
%manually select every 10th point starting with the 6th frame. this will
%ensure that we are between the points used for the automated and
%interpolation algorithms.
%also select every 10th point starting with the 6th frame of the
%interpolated and auto data.
for i=1:10
    i
    tempimage=imread(file_list(21+10*(i-1)).name);%34+10*(i-1)).name);
    imshow(tempimage);hold on;
    plot(vertex_archive_auto(:,2,5+10*(i-1)),vertex_archive_auto(:,1,5+10*(i-
1)),'r*');
    plot(bony_coordinates_auto(2,5+10*(i-1)),bony_coordinates_auto(1,5+10*(i-
1)),'b*');plot(mn_coordinates_auto(2,5+10*(i-
1)),mn_coordinates_auto(1,5+10*(i-1)),'r*');
    title('Please select lower right point of the median nerve');
    [mnautocol,mnautorow]=ginput(1);
    mn_coordinates_compare_auto(:,i)=[mnautorow;mnautocol];
    title('Please select lower right point of bony
landmark');[bonylandmark_end_col,bonylandmark_end_row]=ginput(1);
bony_coordinates_compare_manual(:,i)=[bonylandmark_end_row;bonylandmark_end_c
ol];
    title('Please trace the median nerve. Press any key when
ready');pause;close;
    %using roipoly we create a logical which specifies which pixels are part
of the median nerve.
    figure;[mnroi,vertex_col,vertex_row]=roipoly(tempimage);close all;
    vertex_archive_compare_manual(:,1,i)=vertex_row;
    vertex_archive_compare_manual(:,2,i)=vertex_col;
    imshow(tempimage);title('Please guess where the bottom right point of the
median nerve template is');
    [mncolguess,mnrowguess]=ginput(1);close;
    mn_coordinates_compare_manual(:,i)=[mnrowguess;mncolguess];
    [r,c]=find(mnroi==1);
    for a=min(r):max(r)
        for b=min(c):max(c)
            if mnroi(a,b)==1
                mntemplate(a-min(r)+1,b-min(c)+1)=tempimage(a,b);
            end
        end
    end
    clear mnroi
    for a=1:size(mntemplate,1)
        for b=1:size(mntemplate,2)
            if mntemplate(a,b)>0
                mnroi(a,b)=1;
            end
        end
    end
    % figure;imshow(mntemplate);pause;close;
    mnroi=bwlabel(mnroi);
    stats_compare_manual(1,i) =
regionprops(mnroi,mntemplate,'Area','Centroid','Orientation','MajorAxisLength
','MinorAxisLength','MeanIntensity');
    mn_coordinates_compare_interp_10(:,i)=mn_coordinates_interp_10(:,5+10*(i-
1));
    mn_coordinates_compare_interp_20(:,i)=mn_coordinates_interp_20(:,5+10*(i-
1));
```

```
bony_coordinates_compare_interp_10(:,i)=bony_coordinates_interp_10(:,5+10*(i-
1));
bony_coordinates_compare_interp_20(:,i)=bony_coordinates_interp_20(:,5+10*(i-
1));
    bony_coordinates_compare_auto(:,i)=bony_coordinates_auto(:,5+10*(i-1));
    stats_compare_auto(1,i)=stats_auto(1,5+10*(i-1));
end
save('vertex_archive_compare_manual.mat','vertex_archive_compare_manual');
save('bony_coordinates_compare_manual.mat','bony_coordinates_compare_manual')
;
save('mn_coordinates_compare_manual.mat','mn_coordinates_compare_manual');
save('stats_compare_manual.mat','stats_compare_manual');
save('stats_compare_auto.mat','stats_compare_auto');
save('bony_coordinates_compare_interp_10.mat','bony_coordinates_compare_inter
p_10');
save('mn_coordinates_compare_interp_10.mat','mn_coordinates_compare_interp_10
');
save('bony_coordinates_compare_interp_20.mat','bony_coordinates_compare_inter
p_20');
save('mn_coordinates_compare_interp_20.mat','mn_coordinates_compare_interp_20
');
save('bony_coordinates_compare_auto.mat','bony_coordinates_compare_auto');
save('mn_coordinates_compare_auto.mat','mn_coordinates_compare_auto');
%DETERMINE THE THE AREA AND FR FOR EACH AT EVERY 10TH POINT STARTING WITH THE
6TH
for i=1:10
    tempimage=imread(file_list(21+10*(i-1)).name);%34+10*(i-1)).name);
    clear mnroi mntemplate
    mnroi=roipoly(tempimage,vertex_archive_interp_10(:,2,5+10*(i-
1)),vertex_archive_interp_10(:,1,5+10*(i-1)));
    [r,c]=find(mnroi==1);
    for a=min(r):max(r)
        for b=min(c):max(c)
            if mnroi(a,b)==1
                mntemplate(a-min(r)+1,b-min(c)+1)=tempimage(a,b);
            end
        end
    end
    clear mnroi
    for a=1:size(mntemplate,1)
        for b=1:size(mntemplate,2)
            if mntemplate(a,b)>0
                mnroi(a,b)=1;
            end
        end
    end
    % figure;imshow(mntemplate);pause;close;
    mnroi=bwlabel(mnroi);
    stats_compare_interp_10(1,i) =
regionprops(mnroi,mntemplate,'Area','Centroid','Orientation','MajorAxisLength
','MinorAxisLength','MeanIntensity');
    clear mnroi mntemplate
    mnroi=roipoly(tempimage,vertex_archive_interp_20(:,2,5+10*(i-
1)),vertex_archive_interp_20(:,1,5+10*(i-1)));
    [r,c]=find(mnroi==1);
    for a=min(r):max(r)
        for b=min(c):max(c)
```

```
            if mnroi(a,b)==1
                mntemplate(a-min(r)+1,b-min(c)+1)=tempimage(a,b);
            end
        end
    end
    clear mnroi
    for a=1:size(mntemplate,1)
        for b=1:size(mntemplate,2)
            if mntemplate(a,b)>0
                mnroi(a,b)=1;
            end
        end
    end
    % figure;imshow(mntemplate);pause;close;
    mnroi=bwlabel(mnroi);
    if i<10
    stats_compare_interp_20(1,i) =
regionprops(mnroi,mntemplate,'Area','Centroid','Orientation','MajorAxisLength
','MinorAxisLength','MeanIntensity');
    end
end
% stats_compare_interp_20(i)=stats_compare_interp_20(i-1)
save('stats_compare_interp_10.mat','stats_compare_interp_10');
save('stats_compare_interp_20.mat','stats_compare_interp_20');
%plot results
% for i=1:10
% imshow(tempimage);hold on;
%
plot(vertex_archive_auto(:,2,i),vertex_archive_auto(:,1,i),'b*');plot(mn_coor
dinates_auto(2,1)+start_col,mn_coordinates_auto(1,1)+start_row,'b*');
%
plot(vertex_archive_compare_manual(:,2,i),vertex_archive_compare_manual(:,1,i
),'r*');plot(mn_coordinates_compare_manual(2,i),mn_coordinates_compare_manual
(1,i),'r*');
%
plot(vertex_archive_interp_10(:,2,i),vertex_archive_interp_10(:,1,i),'g*');pl
ot(mn_coordinates_interp_10(2,i),mn_coordinates_interp_10(1,i),'g*');
%
plot(vertex_archive_interp_20(:,2,i),vertex_archive_interp_20(:,1,i),'y*');pl
ot(mn_coordinates_interp_20(2,i),mn_coordinates_interp_20(1,i),'y*');
% end
%calculate the mean percent error comparing each method to manual
for i=1:10
    disterror_mncoord_auto(i)=sqrt((mn_coordinates_compare_manual(1,i)-
mn_coordinates_compare_auto(1,i))^2+(mn_coordinates_compare_manual(2,i)-
mn_coordinates_compare_auto(2,i))^2);
    disterror_mncoord_interp_10(i)=sqrt((mn_coordinates_compare_manual(1,i)-
mn_coordinates_compare_interp_10(1,i))^2+(mn_coordinates_compare_manual(2,i)-
mn_coordinates_compare_interp_10(2,i))^2);
    disterror_bonycoord_auto(i)=sqrt((bony_coordinates_compare_manual(1,i)-
bony_coordinates_compare_auto(1,i))^2+(bony_coordinates_compare_manual(2,i)-
bony_coordinates_compare_auto(2,i))^2);
disterror_bonycoord_interp_10(i)=sqrt((bony_coordinates_compare_manual(1,i)-
bony_coordinates_compare_interp_10(1,i))^2+(bony_coordinates_compare_manual(2
,i)-bony_coordinates_compare_interp_10(2,i))^2);
flattening_manual(i)=stats_compare_manual(1,i).MajorAxisLength/stats_compare_
manual(1,i).MinorAxisLength;
```

```
flattening_auto(i)=stats_compare_auto(1,i).MajorAxisLength/stats_compare_auto
(1,i).MinorAxisLength;
flattening_interp_10(i)=stats_compare_interp_10(1,i).MajorAxisLength/stats_co
mpare_interp_10(1,i).MinorAxisLength;
    percerror_area_auto(i)=(stats_compare_auto(1,i).Area-
stats_compare_manual(1,i).Area)/stats_compare_manual(1,i).Area*100;
    percerror_flat_auto(i)=(flattening_auto(i)-
flattening_manual(i))/flattening_manual(i)*100;
    percerror_area_interp_10(i)=(stats_compare_interp_10(1,i).Area-
stats_compare_manual(1,i).Area)/stats_compare_manual(1,i).Area*100;
    percerror_flat_interp_10(i)=(flattening_interp_10(i)-
flattening_manual(i))/flattening_manual(i)*100;
    if i<10
    disterror_mncoord_interp_20(i)=sqrt((mn_coordinates_compare_manual(1,i)-
mn_coordinates_compare_interp_20(1,i))^2+(mn_coordinates_compare_manual(2,i)-
mn_coordinates_compare_interp_20(2,i))^2);
disterror_bonycoord_interp_20(i)=sqrt((bony_coordinates_compare_manual(1,i)-
bony_coordinates_compare_interp_20(1,i))^2+(bony_coordinates_compare_manual(2
,i)-bony_coordinates_compare_interp_20(2,i))^2);
flattening_interp_20(i)=stats_compare_interp_20(1,i).MajorAxisLength/stats_co
mpare_interp_20(1,i).MinorAxisLength;
    percerror_area_interp_20(i)=(stats_compare_interp_20(1,i).Area-
stats_compare_manual(1,i).Area)/stats_compare_manual(1,i).Area*100;
    percerror_flat_interp_20(i)=(flattening_interp_20(i)-
flattening_manual(i))/flattening_manual(i)*100;
    end
end
    mean_disterror_mncoord_auto=mean(disterror_mncoord_auto);
    mean_disterror_mncoord_interp_10=mean(disterror_mncoord_interp_10);
    mean_disterror_mncoord_interp_20=mean(disterror_mncoord_interp_20);
    mean_disterror_bonycoord_auto=mean(disterror_bonycoord_auto);
    mean_disterror_bonycoord_interp_10=mean(disterror_bonycoord_interp_10);
    mean_disterror_bonycoord_interp_20=mean(disterror_bonycoord_interp_20);
    mean_percerror_area_auto=mean(abs(percerror_area_auto));
    mean_percerror_flat_auto=mean(abs(percerror_flat_auto));
    mean_percerror_area_interp_10=mean(abs(percerror_area_interp_10));
    mean_percerror_flat_interp_10=mean(abs(percerror_flat_interp_10));
    mean_percerror_area_interp_20=mean(abs(percerror_area_interp_20));
    mean_percerror_flat_interp_20=mean(abs(percerror_flat_interp_20));
%save results
cd('S:\Protocols\Boninger\Ultrasound');
fid=fopen('nervemovementvalidationerrorvariables.txt','a');
fprintf(fid,'%s\t%s\t%s\t%s\t%s\t%s\t%s\t%s\t%s\t%s\t%s\t%s\t%s\n',...
'videoid','mean_disterror_mncoord_auto','mean_disterror_mncoord_interp_10','m
ean_disterror_mncoord_interp_20',...
'mean_disterror_bonycoord_auto','mean_disterror_bonycoord_interp_10','mean_di
sterror_bonycoord_interp_20',...
'mean_percerror_flat_auto','mean_percerror_flat_interp_10','mean_percerror_fl
at_interp_20',...
'mean_percerror_area_auto','mean_percerror_area_interp_10','mean_percerror_ar
ea_interp_20');
fprintf(fid,'%s\t%f\t%f\t%f\t%f\t%f\t%f\t%f\t%f\t%f\t%f\t%f\t%f\n',...
    videoid, mean_disterror_mncoord_auto, mean_disterror_mncoord_interp_10,
mean_disterror_mncoord_interp_20,...
    mean_disterror_bonycoord_auto, mean_disterror_bonycoord_interp_10,
mean_disterror_bonycoord_interp_20,...
```

```
    mean_percerror_flat_auto, mean_percerror_flat_interp_10,
mean_percerror_flat_interp_20,...
    mean_percerror_area_auto, mean_percerror_area_interp_10,
mean_percerror_area_interp_20);
fclose(fid);
```

BIBLIOGRAPHY

1. Falkenburg SA, Schultz DJ. Ergonomics for the upper extremity. Hand Clin 1993 May;9(2):263-71.

2. NIOSH. Musculoskeletal Disorders and Workplace Factors: A critical review of epidemiology for work related musculoskeletal disorders of the neck, upper extremity, and low back. Cincinnati, OH: National Institute for Occupational Safety and Health, Publications Dissemination; 1997.

3. Silverstein BA, Fine LJ, Armstrong TJ. Occupational factors and carpal tunnel syndrome. Am J Ind Med 1987;11(3):343-58.

4. Masear VR, Hayes JM, Hyde AG. An industrial cause of carpal tunnel syndrome. J Hand Surg [Am] 1986 Mar;11(2):222-7.

5. Armstrong TJ, Chaffin DB. Carpal tunnel syndrome and selected personal attributes. J Occup Med 1979 Jul;21(7):481-6.

6. Tanaka S, Wild DK, Seligman PJ, Behrens V, Cameron L, Putz-Anderson V. The US prevalence of self-reported carpal tunnel syndrome: 1988 National Health Interview Survey data. Am J Public Health 1994 Nov;84(11):1846-8.

7. Atroshi I, Gummesson C, Johnsson R, Ornstein E, Ranstam J, Rosen I. Prevalence of carpal tunnel syndrome in a general population. JAMA 1999 Jul;282(2):153-8.

8. Bland JD, Rudolfer SM. Clinical surveillance of carpal tunnel syndrome in two areas of the United Kingdom, 1991-2001. J Neurol Neurosurg Psychiatry 2003 Dec;74(12):1674-9.

9. Mondelli M, Giannini F, Giacchi M. Carpal tunnel syndrome incidence in a general population. Neurology 2002 Jan;58(2):289-94.

10. [Anonymous]. Diagnosis of the carpal tunnel syndrome. Lancet 1985 Apr;1(8433):854-5.

11. Palmer DH, Hanrahan LP. Social and economic costs of carpal tunnel surgery. Instr Course Lect 1995;44:167-72.

12. Burnham RS, Steadward RD. Upper extremity peripheral nerve entrapments among wheelchair athletes: prevalence, location, and risk factors. Arch Phys Med Rehabil 1994 May;75(5):519-24.

13. Davidoff G, Werner R, Waring W. Compressive mononeuropathies of the upper extremity in chronic paraplegia. Paraplegia 1991 Jan;29(1):17-24.

14. Subbarao JV, Klopfstein J, Turpin R. Prevalence and impact of wrist and shoulder pain in patients with spinal cord injury. J Spinal Cord Med 1995 Jan;18(1):9-13.

15. Sie IH, Waters RL, Adkins RH, Gellman H. Upper extremity pain in the postrehabilitation spinal cord injured patient. Arch Phys Med Rehabil 1992 Jan;73(1):44-8.

16. Tun CG, Upton J. The paraplegic hand: electrodiagnostic studies and clinical findings. J Hand Surg [Am] 1988 Sep;13(5):716-9.

17. Gellman H, Chandler DR, Petrasek J, Sie I, Adkins R, Waters RL. Carpal tunnel syndrome in paraplegic patients. J Bone Joint Surg Am 1988 Apr;70(4):517-9.

18. Aljure J, Eltorai I, Bradley WE, Lin JE, Johnson B. Carpal tunnel syndrome in paraplegic patients. Paraplegia 1985 Jun;23(3):182-6.

19. Yang J, Boninger ML, Leath JD, Fitzgerald SG, Dyson-Hudson TA, Chang MW. Carpal tunnel syndrome in manual wheelchair users with spinal cord injury: a cross-sectional multicenter study. Am J Phys Med Rehabil 2009 Dec;88(12):1007-16.

20. Boninger ML, Impink BG, Cooper RA, Koontz AM. Relation between median and ulnar nerve function and wrist kinematics during wheelchair propulsion. Arch Phys Med Rehabil 2004 Jul;85(7):1141-5.

21. Boninger ML, Cooper RA, Baldwin MA, Shimada SD, Koontz A. Wheelchair pushrim kinetics: body weight and median nerve function. Arch Phys Med Rehabil 1999 Aug;80(8):910-5.

22. Buchberger W, Judmaier W, Birbamer G, Lener M, Schmidauer C. Carpal tunnel syndrome: diagnosis with high-resolution sonography. AJR Am J Roentgenol 1992 Oct;159(4):793-8.

23. Buchberger W, Schon G, Strasser K, Jungwirth W. High-resolution ultrasonography of the carpal tunnel. J Ultrasound Med 1991 Oct;10(10):531-7.

24. Lee CH, Kim TK, Yoon ES, Dhong ES. Correlation of high-resolution ultrasonographic findings with the clinical symptoms and electrodiagnostic data in carpal tunnel syndrome. Ann Plast Surg 2005 Jan;54(1):20-3.

25. Keles I, Karagulle Kendi AT, Aydin G, Zog SG, Orkun S. Diagnostic precision of ultrasonography in patients with carpal tunnel syndrome. Am J Phys Med Rehabil 2005 Jun;84(6):443-50.

26. Lee D, van Holsbeeck MT, Janevski PK, Ganos DL, Ditmars DM, Darian VB. Diagnosis of carpal tunnel syndrome. Ultrasound versus electromyography. Radiol Clin North Am 1999 Jul;37(4):859-72, x.

27. Swen WA, Jacobs JW, Bussemaker FE, de Waard JW, Bijlsma JW. Carpal tunnel sonography by the rheumatologist versus nerve conduction study by the neurologist. J Rheumatol 2001 Jan;28(1):62-9.

28. Yesildag A, Kutluhan S, Sengul N, Koyuncuoglu HR, Oyar O, Guler K, Gulsoy UK. The role of ultrasonographic measurements of the median nerve in the diagnosis of carpal tunnel syndrome. Clin Radiol 2004 Oct;59(10):910-5.

29. El Miedany YM, Aty SA, Ashour S. Ultrasonography versus nerve conduction study in patients with carpal tunnel syndrome: substantive or complementary tests? Rheumatology (Oxford) 2004 Jul;43(7):887-95.

30. Kele H, Verheggen R, Bittermann HJ, Reimers CD. The potential value of ultrasonography in the evaluation of carpal tunnel syndrome. Neurology 2003 Aug;61(3):389-91.

31. Nakamichi K, Tachibana S. Ultrasonographic measurement of median nerve cross-sectional area in idiopathic carpal tunnel syndrome: Diagnostic accuracy. Muscle Nerve 2002 Dec;26(6):798-803.

32. Kamolz LP, Schrogendorfer KF, Rab M, Girsch W, Gruber H, Frey M. The precision of ultrasound imaging and its relevance for carpal tunnel syndrome. Surg Radiol Anat 2001;23(2):117-21.

33. Nakamichi KI, Tachibana S. Enlarged median nerve in idiopathic carpal tunnel syndrome. Muscle Nerve 2000 Nov;23(11):1713-8.

34. Sarria L, Cabada T, Cozcolluela R, Martinez-Berganza T, Garcia S. Carpal tunnel syndrome: usefulness of sonography. Eur Radiol 2000;10(12):1920-5.

35. Duncan I, Sullivan P, Lomas F. Sonography in the diagnosis of carpal tunnel syndrome. AJR Am J Roentgenol 1999 Sep;173(3):681-4.

36. Chen P, Maklad N, Redwine M, Zelitt D. Dynamic high-resolution sonography of the carpal tunnel. AJR Am J Roentgenol 1997 Feb;168(2):533-7.

37. Beekman R, Visser LH. Sonography in the diagnosis of carpal tunnel syndrome: a critical review of the literature. Muscle Nerve 2003 Jan;27(1):26-33.

38. Seror P. Sonography and electrodiagnosis in carpal tunnel syndrome diagnosis, an analysis of the literature. Eur J Radiol 2008 Jul;67(1):146-52.

39. Keberle M, Jenett M, Kenn W, Reiners K, Peter M, Haerten R, Hahn D. Technical advances in ultrasound and MR imaging of carpal tunnel syndrome. Eur Radiol 2000;10(7):1043-50.

40. Altinok MT, Baysal O, Karakas HM, Firat AK. Sonographic evaluation of the carpal tunnel after provocative exercises. J Ultrasound Med 2004 Oct;23(10):1301-6.

41. Massy-Westropp N, Grimmer K, Bain G. The effect of a standard activity on the size of the median nerve as determined by ultrasound visualization. J Hand Surg [Am] 2001 Jul;26(4):649-54.

42. Impink BG, Boninger ML, Walker H, Collinger JL, Niyonkuru C. Ultrasonographic median nerve changes after a wheelchair sporting event. Arch Phys Med Rehabil 2009 Sep;90(9):1489-94.

43. Brown R, Pedowitz R, Rydevik B, Woo S, Hargens A, Massie J, Kwan M, Garfin SR. Effects of acute graded strain on efferent conduction properties in the rabbit tibial nerve. Clin Orthop Relat Res 1993 Nov;(296):288-94.

44. Rydevik BL, Kwan MK, Myers RR, Brown RA, Triggs KJ, Woo SL, Garfin SR. An in vitro mechanical and histological study of acute stretching on rabbit tibial nerve. J Orthop Res 1990 Sep;8(5):694-701.

45. Sunderland S. Stretch-compression neuropathy. Clin Exp Neurol 1981;18:1-13.

46. Wall EJ, Massie JB, Kwan MK, Rydevik BL, Myers RR, Garfin SR. Experimental stretch neuropathy. Changes in nerve conduction under tension. J Bone Joint Surg Br 1992 Jan;74(1):126-9.

47. Kwan MK, Wall EJ, Massie J, Garfin SR. Strain, stress and stretch of peripheral nerve. Rabbit experiments in vitro and in vivo. Acta Orthop Scand 1992 Jun;63(3):267-72.

48. Erel E, Dilley A, Greening J, Morris V, Cohen B, Lynn B. Longitudinal sliding of the median nerve in patients with carpal tunnel syndrome. J Hand Surg [Br] 2003 Oct;28(5):439-43.

49. Nakamichi K, Tachibana S. Restricted motion of the median nerve in carpal tunnel syndrome. J Hand Surg [Br] 1995 Aug;20(4):460-4.

50. Nakamichi K, Tachibana S. Transverse sliding of the median nerve beneath the flexor retinaculum. J Hand Surg [Br] 1992 Apr;17(2):213-6.

51. Yoshii Y, Villarraga HR, Henderson J, Zhao C, An KN, Amadio PC. Ultrasound assessment of the displacement and deformation of the median nerve in the human carpal tunnel with active finger motion. J Bone Joint Surg Am 2009 Dec;91(12):2922-30.

52. Levine DW, Simmons BP, Koris MJ, Daltroy LH, Hohl GG, Fossel AH, Katz JN. A self-administered questionnaire for the assessment of severity of symptoms and functional status in carpal tunnel syndrome. J Bone Joint Surg Am 1993 Nov;75(11):1585-92.

53. Michelsen H, Posner MA. Medical history of carpal tunnel syndrome. Hand Clin 2002 May;18(2):257-68.

54. Werner RA, Jacobson JA, Jamadar DA. Influence of body mass index on median nerve function, carpal canal pressure, and cross-sectional area of the median nerve. Muscle Nerve 2004 Oct;30(4):481-5.

55. Werner RA, Andary M. Carpal tunnel syndrome: pathophysiology and clinical neurophysiology. Clin Neurophysiol 2002 Sep;113(9):1373-81.

56. Werner RA, Armstrong TJ. Carpal tunnel syndrome: ergonomic risk factors and intra carpal canal pressure. Phys Med Rehabil Clin N Am 1997;8(3):555-69.

57. Moore JS. Carpal tunnel syndrome. Occup Med 1992 Oct;7(4):741-63.

58. Kerwin G, Williams CS, Seiler JG, III. The pathophysiology of carpal tunnel syndrome. Hand Clin 1996 May;12(2):243-51.

59. Brain WR, Wright AD, Wilkinson M. Spontaneous compression of both median nerves in the carpal tunnel; six cases treated surgically. Lancet 1947 Mar;1(8):277-82.

60. Gelberman RH, Hergenroeder PT, Hargens AR, Lundborg GN, Akeson WH. The carpal tunnel syndrome. A study of carpal canal pressures. J Bone Joint Surg Am 1981 Mar;63(3):380-3.

61. Werner CO, Elmqvist D, Ohlin P. Pressure and nerve lesion in the carpal tunnel. Acta Orthop Scand 1983 Apr;54(2):312-6.

62. Szabo RM, Chidgey LK. Stress carpal tunnel pressures in patients with carpal tunnel syndrome and normal patients. J Hand Surg Am 1989 Jul;14(4):624-7.

63. Werner RA, Albers JW, Franzblau A, Armstrong TJ. The relationship between body mass index and the diagnosis of carpal tunnel syndrome. Muscle Nerve 1994 Jun;17(6):632-6.

64. Gelberman RH, Rydevik BL, Pess GM, Szabo RM, Lundborg G. Carpal tunnel syndrome. A scientific basis for clinical care. Orthop Clin North Am 1988 Jan;19(1):115-24.

65. Werner R, Armstrong TJ, Bir C, Aylard MK. Intracarpal canal pressures: the role of finger, hand, wrist and forearm position. Clin Biomech (Bristol , Avon) 1997 Jan;12(1):44-51.

66. Okutsu I, Ninomiya S, Yoshida A, Hamanaka I, Kitajima I. Measurement of carpal canal and median nerve pressure in patients with carpal tunnel syndrome. Tech Hand Up Extrem Surg 2004 Jun;8(2):124-8.

67. Goss BC, Agee JM. Dynamics of intracarpal tunnel pressure in patients with carpal tunnel syndrome. J Hand Surg Am 2010 Feb;35(2):197-206.

68. Seradge H, Jia YC, Owens W. In vivo measurement of carpal tunnel pressure in the functioning hand. J Hand Surg Am 1995 Sep;20(5):855-9.

69. Luchetti R, Schoenhuber R, Nathan P. Correlation of segmental carpal tunnel pressures with changes in hand and wrist positions in patients with carpal tunnel syndrome and controls. J Hand Surg Br 1998 Oct;23(5):598-602.

70. Armstrong TJ, Castelli WA, Evans FG, Diaz-Perez R. Some histological changes in carpal tunnel contents and their biomechanical implications. J Occup Med 1984 Mar;26(3):197-201.

71. Lundborg G. Nerve Injury and Repair. Edinburgh: Churchill Livingstone; 1988.

72. Driscoll PJ, Glasby MA, Lawson GM. An in vivo study of peripheral nerves in continuity: biomechanical and physiological responses to elongation. J Orthop Res 2002 Mar;20(2):370-5.

73. Mackinnon SE, Dellon AL. Experimental study of chronic nerve compression. Clinical implications. Hand Clin 1986 Nov;2(4):639-50.

74. Suzuki Y, Shirai Y. Motor nerve conduction analysis of double crush syndrome in a rabbit model. J Orthop Sci 2003;8(1):69-74.

75. Bland JD. Carpal tunnel syndrome. Curr Opin Neurol 2005 Oct;18(5):581-5.

76. Szabo RM. Carpal tunnel syndrome as a repetitive motion disorder. Clin Orthop Relat Res 1998 Jun;(351):78-89.

77. Boninger ML, Cooper RA, Robertson RN, Shimada SD. Three-dimensional pushrim forces during two speeds of wheelchair propulsion. Am J Phys Med Rehabil 1997 Sep;76(5):420-6.

78. Cobb TK, An KN, Cooney WP. Externally applied forces to the palm increase carpal tunnel pressure. J Hand Surg [Am] 1995 Mar;20(2):181-5.

79. Goodman CM, Steadman AK, Meade RA, Bodenheimer C, Thornby J, Netscher DT. Comparison of carpal canal pressure in paraplegic and nonparaplegic subjects: clinical implications. Plast Reconstr Surg 2001 May;107(6):1464-71.

80. Dalyan M, Cardenas DD, Gerard B. Upper extremity pain after spinal cord injury. Spinal Cord 1999 Mar;37(3):191-5.

81. Pentland WE, Twomey LT. Upper limb function in persons with long term paraplegia and implications for independence: Part I. Paraplegia 1994 Apr;32(4):211-8.

82. Gellman H, Sie I, Waters RL. Late complications of the weight-bearing upper extremity in the paraplegic patient. Clin Orthop Relat Res 1988 Aug;(233):132-5.

83. Baldwin MA, Boninger ML, Shimada SD, Cooper RA, O'Connor TJ. A Relationship Between Pushrim Kinetics and Median Nerve Dysfunction. Proceedings 21st Annual RESNA Conference 1998.

84. Shimada SD, Boninger ML, Cooper RA, Baldwin MA. Relationship between wrist biomechanics during wheelchiar propulsion and median nerve dysfunction. Proceedings 21st Annual RESNA Conference 1998;128-30.

85. Cooper RA, Robertson RN, VanSickle DP, Boninger ML, Shimada SD. Projection of the point of force application onto a palmar plane of the hand during wheelchair propulsion. IEEE Trans Rehabil Eng 1996 Sep;4(3):133-42.

86. VanSickle DP, Cooper RA, Boninger ML, Robertson RN, Shimada SD. A unified method for calculating the center of pressure during wheelchair propulsion. Ann Biomed Eng 1998 Mar;26(2):328-36.

87. Koontz AM, Cooper RA, Boninger ML. An autoregressive modeling approach to analyzing wheelchair propulsion forces. Med Eng Phys 2001 May;23(4):285-91.

88. Boninger ML, Koontz AM, Sisto SA, Dyson-Hudson TA, Chang M, Price R, Cooper RA. Pushrim biomechanics and injury prevention in spinal cord injury: recommendations based on CULP-SCI investigations. J Rehabil Res Dev 2005 May;42(3 Suppl 1):9-19.

89. Bay BK, Sharkey NA, Szabo RM. Displacement and strain of the median nerve at the wrist. J Hand Surg [Am] 1997 Jul;22(4):621-7.

90. Ugbolue UC, Hsu WH, Goitz RJ, Li ZM. Tendon and nerve displacement at the wrist during finger movements. Clin Biomech (Bristol , Avon) 2005 Jan;20(1):50-6.

91. van Doesburg MH, Yoshii Y, Villarraga HR, Henderson J, Cha SS, An KN, Amadio PC. Median nerve deformation and displacement in the carpal tunnel during index finger and thumb motion. J Orthop Res 2010 Mar.

92. Wilkinson M, Grimmer K, Massy-Westropp N. Ultrasound of the Carpal Tunnel and Median Nerve: A Reproducibility Study. Journal of Diagnostic Medical Sonography 2001 Nov;17:323-8.

93. Aleman L, Berna JD, Reus M, Martinez F, Domenech-Ratto G, Campos M. Reproducibility of sonographic measurements of the median nerve. J Ultrasound Med 2008 Feb;27(2):193-7.

94. Altinok T, Baysal O, Karakas HM, Sigirci A, Alkan A, Kayhan A, Yologlu S. Ultrasonographic assessment of mild and moderate idiopathic carpal tunnel syndrome. Clin Radiol 2004 Oct;59(10):916-25.

95. Shavelson R, Webb N. Generalizability Theory: A Primer. Newbury Park, CA: Sage; 1991.

96. Portney L, Watkins M. Foundation of Clincal Research: Applications to Practice. Second Edition ed. Upper Saddle River, NJ: Prentice-Hall, Inc.; 2000.

97. Alshami AM, Cairns CW, Wylie BK, Souvlis T, Coppieters MW. Reliability and size of the measurement error when determining the cross-sectional area of the tibial nerve at the tarsal tunnel with ultrasonography. Ultrasound Med Biol 2009 Jul;35(7):1098-102.

98. Impink BG, Gagnon D, Collinger JL, Boninger ML. Repeatability of Ultrasonographic Median Nerve Measures. Muscle Nerve 2010;in press.

99. Werner RA, Franzblau A, Albers JW, Armstrong TJ. Influence of body mass index and work activity on the prevalence of median mononeuropathy at the wrist. Occup Environ Med 1997 Apr;54(4):268-71.

100. Sambandam SN, Priyanka P, Gul A, Ilango B. Critical analysis of outcome measures used in the assessment of carpal tunnel syndrome. Int Orthop 2008 Aug;32(4):497-504.

101. Kaymak B, Ozcakar L, Cetin A, Candan CM, Akinci A, Hascelik Z. A comparison of the benefits of sonography and electrophysiologic measurements as predictors of symptom severity and functional status in patients with carpal tunnel syndrome. Arch Phys Med Rehabil 2008 Apr;89(4):743-8.

102. Collinger JL, Fullerton B, Impink BG, Koontz AM, Boninger ML. Validation of Greyscale Based Quantitative Ultrasound: Relationship to Established Clinical Measures of Shoulder Pathology. American Journal of Physical Medicine and Rehabilitation 2010;(in press).

103. Wu G, van der Helm FC, Veeger HE, Makhsous M, Van Roy P, Anglin C, Nagels J, Karduna AR, McQuade K, Wang X, Werner FW, Buchholz B. ISB recommendation on definitions of joint coordinate systems of various joints for the reporting of human joint motion--Part II: shoulder, elbow, wrist and hand. J Biomech 2005 May;38(5):981-92.

104. Cooper RA, Boninger ML, Shimada SD, Lawrence BM. Glenohumeral joint kinematics and kinetics for three coordinate system representations during wheelchair propulsion. Am J Phys Med Rehabil 1999 Sep;78(5):435-46.

105. Boninger ML, Cooper RA, Robertson RN, Rudy TE. Wrist biomechanics during two speeds of wheelchair propulsion: an analysis using a local coordinate system. Arch Phys Med Rehabil 1997 Apr;78(4):364-72.

106. Boninger ML, Baldwin M, Cooper RA, Koontz A, Chan L. Manual wheelchair pushrim biomechanics and axle position. Arch Phys Med Rehabil 2000 May;81(5):608-13.

107. Dilley A, Greening J, Lynn B, Leary R, Morris V. The use of cross-correlation analysis between high-frequency ultrasound images to measure longitudinal median nerve movement. Ultrasound Med Biol 2001 Sep;27(9):1211-8.

108. Chhaya S, Hall-Craggs J, Greening J, Morris V. Carpal tunnel syndrome: ultrasound observations of median nerve movement and its relationship to symptoms in patients andnormal volunteers. Rheumatology (Oxford) 2001;40(Supplement 1):130-1 (Abstract 370).

109. Hough AD, Moore AP, Jones MP. Reduced longitudinal excursion of the median nerve in carpal tunnel syndrome. Arch Phys Med Rehabil 2007 May;88(5):569-76.

110. Hobson-Webb LD, Massey JM, Juel VC, Sanders DB. The ultrasonographic wrist-to-forearm median nerve area ratio in carpal tunnel syndrome. Clin Neurophysiol 2008 Jun;119(6):1353-7.

111. Klauser AS, Halpern EJ, De Zordo T, Feuchtner GM, Arora R, Gruber J, Martinoli C, Loscher WN. Carpal tunnel syndrome assessment with US: value of additional cross-sectional area measurements of the median nerve in patients versus healthy volunteers. Radiology 2009 Jan;250(1):171-7.